



---

**Universidad de Valladolid**

**PROGRAMA DE DOCTORADO EN  
TECNOLOGÍAS DE LA INFORMACIÓN Y LAS TELECOMUNICACIONES**

**TESIS DOCTORAL:**  
**Optimization Techniques for  
Planning and Operation of the  
Next Generation of  
Elastic Optical Networks**

Presentada por **Soheil Hosseini**  
para optar al grado de  
Doctor/a por la Universidad de Valladolid

Dirigida por:  
Prof. Ramón J. Durán Barroso  
Dr. Ignacio de Miguel Jiménez



تقدیم به پدر و مادر عزیزم، خواهر و برادرهایم





## Abstract

The attraction of new services and applications over the Internet makes it critical for the network operators to increase the capacity of the current elastic optical networks (EONs). Two promising technologies have been proposed for the next generation of EONs to enhance their bandwidth: Space Division Multiplexing (SDM) and Multiband elastic optical networks (MB-EONs). SDM with multi-core fibers (MCFs) is considered as a promising technology to increase the capacity of optical networks. The realization of SDM networks transforms the traditional routing, modulation level, and spectrum assignment (RMLSA) problem in EONs into a more complex problem involving routing, modulation level, space, and spectrum assignment (RMLSSA) algorithms. To enhance the network performance while employing the SDM technology, in this thesis, we introduce a novel dynamic multipath RMLSSA algorithm for SDM-EON with the aim of minimizing the blocking ratio and the energy consumed by bandwidth variable transponders (BVTs).

Despite the potential advantages that SDM technology offers, it also introduces significant challenges, including the progressive shortage of available dark fibers and the immaturity of multicore and multimode fibers for multichannel transmission. Therefore, network operators postpone the process of capacity enhancement through SDM networks. Accordingly, currently, MB-EONs are at the forefront of this capacity improvement in the short and medium term. These networks employ additional spectral bands from the optical fiber other than the C (conventional) band. Due to the current availability of L-band erbium doped fiber amplifiers (EDFAs), lighting up the L-band of already installed fibers is considered as a pragmatic approach. However, network operators envision a soft migration from current C-band to fully upgraded C+L-bands networks to distribute the high cost of equipping all fibers and nodes of a network with multi-band devices over several years. Therefore, it is essential to propose network planning strategies to achieve a partially upgraded EON in which only a subset of links of the network operate over C+L bands. To this end, in this thesis, we propose several planning strategies to determine which links should be migrated from the C to the C+L bands. In the process of migration, the deployment of the appropriate type of transceivers is important for the network operators. Therefore, the thesis also provides insights into the matter of choosing the most efficient transceivers, i.e., single band transceivers or multi-band transceivers.

As C+L band systems increase the capacity of optical networks, survivability against network failures must get more emphasis. Therefore, equipping a partially/fully upgraded C+L band network with different protection methods is another focus of the thesis. Despite the importance of designing different survivability methods, it should be taken into account that the level of protection needed against network failures varies across different users/services. To address this issue, this thesis also proposes an SLA-

differentiated protection mechanism for C+L multiband networks, ensuring each service receives the appropriate protection level based on its specific requirements.

---

## Acknowledgments

The research developed in this thesis is sponsored by the IoTalentum project, which has received funding from the EU H2020 Research and Innovation Programme under the MSCA grant agreement no. 953442. It is also supported by Ministerio de Ciencia, Innovación y Universidades / Agencia Estatal de Investigación (Grants PID2020-112675RB-C42 and PID2023-148104OB-C41, funded by MICIU/AEI/10.13039/501100011033 and the later also by ERFD/EU), and by Consejería de Educación de la Junta de Castilla y León and the European Regional Development Fund (Grant VA231P20).

During the preparation of this work the author used DeepL and ChatGPT in order to improve the grammar and readability of some sentences. After using these tools/services, the author reviewed and edited the content as needed and take full responsibility for the content of the publication.

This thesis is the result of years of hard work, but it would not have been possible without the love, support, and encouragement of the people who mean the most to me.

To my mother and father, your daily video calls were the highlights of my days. Every call was filled with warmth, love, and the kind words that kept me going. No matter how difficult things got, hearing your voices always gave me the comfort and strength I needed. I cannot express how grateful I am for your endless love and support throughout this journey.

To my sister and brothers, our video calls brought so much light into my life. Whether we were talking about everything and nothing at once —discussing football matches, sharing funny stories, debating random topics, or just catching up on the little details of our lives— those moments with you were truly precious. Thank you for the endless conversations; even after two hours, you always wanted to keep chatting while I was ready to say, “Okay, folks, I love you, but I need a break!”. Your love and encouragement have been the perfect recipe for me throughout this journey.

I am deeply grateful to my supervisors, Ramón and Ignacio. Your expertise, guidance, encouragement, and patience have been invaluable. You have not only shaped my work but also helped me grow as a researcher and a person. Your belief in my potential has inspired me throughout this journey, and I am truly thankful for your mentorship.

Thank you Óscar, for your invaluable support during my time at Telefónica. Our engaging discussions and your insightful feedback were crucial in enhancing the quality of the works that I have done. I also want to thank Noemí, Juan Carlos, Ruben, and Patricia for your kindness, unwavering support, and most importantly, always being there when I needed help.

TO ALL OF YOU, I offer my heartfelt thanks for the encouragement, guidance, and support that has made this achievement possible.

# Contents

Chapter 1. Introduction .....	1
1.1 Contributions of the Ph.D. Thesis .....	2
1.2 Thesis Structure .....	3
Chapter 2. Next Generation of Optical Networks .....	5
2.1 Elastic Optical Networks (EONs) .....	5
2.1.1 Resource Allocation in EONs .....	5
2.1.2 Survivability in EONs .....	6
2.1.3 Admission Control Mechanisms in EONs .....	6
2.2 Space Division Multiplexed Elastic Optical Networks (SDM-EON) .....	7
2.3 Multi-band Elastic Optical Networks (MB-EON) .....	8
Chapter 3. Energy Efficient Multipath Routing in SDM-EON .....	13
3.1 Problem Definitions .....	13
3.2 Dynamic Energy Efficient Multipath Routing, Modulation Level, Core, and Spectrum Assignment Algorithm (EEMPR) .....	15
3.3 Simulation Setup and Results .....	21
3.3.1 Analysis for Different Numbers of $K$ -shortest Paths .....	22
3.3.2 Comparison of EEMPR and MPIRA for $K=5$ Shortest Paths .....	24
3.3.3 Analysis for Other Topologies .....	26
3.4 Conclusions .....	34
Chapter 4. Efficient Migration from the C-band to C+L bands .....	37
4.1 A Heuristic for the Partial Migration of EONs to C+L Bands .....	37
4.1.1 Simulation Setup .....	39
4.1.2 Simulation Results .....	40
4.1.3 Conclusions .....	43
4.2 An ILP Formulation for the Partial Migration of EON to C+L Bands .....	43
4.2.1 Objective of the ILP Formulation .....	43
4.2.2 Inputs for the ILP Formulation .....	44
4.2.3 Decision Variables .....	44
4.2.4 ILP Formulation .....	45
4.2.5 Simulation Setup and Results .....	46

4.2.6 Conclusions .....	49
4.3 Partial Migration Subject to a Partial Upgrade of the Number of EDFAs .....	50
4.3.1 Description of the Problem and Proposed Solution Strategies .....	50
4.3.2 The MostUsed Method .....	51
4.3.3 The MaxPaths Method .....	52
4.3.4 The MaxFibers Method .....	55
4.3.5 Simulation Results .....	55
4.3.5.1 Uniform Traffic .....	57
4.3.5.2 Non-uniform Traffic .....	62
4.3.6 Conclusions .....	68
4.4 Cost-effective Transceivers in the Process of Partial Migration .....	68
4.4.1 Simulation Setup and Results .....	69
4.4.2 Conclusions .....	72
<b>Chapter 5. Survivability Against Network Failures in MB-EON .....</b>	<b>73</b>
5.1 Survivability in a Fully Upgraded C+L band Network .....	73
5.1.1 Simulation Setup and Results .....	75
5.1.2 Conclusions .....	77
5.2 Survivability in a Partially Upgraded C+L-band Network .....	77
5.2.1 Simulation Setup and Results .....	78
5.2.2 Conclusions .....	80
5.3 Dynamic Restoration in a Partially Upgraded C+L-band Network .....	81
5.3.1 Failure Scenarios and Survivability Strategies .....	81
5.3.2 Simulation Setup and Results .....	81
5.3.3 Conclusions .....	86
<b>Chapter 6. SLA-Differentiated Protection in MB-EONs .....</b>	<b>87</b>
6.1 SLA Differentiation Protection Techniques .....	89
6.2 Admission Control (AC) .....	91
6.3 Enhanced SLA-Differentiated Protection .....	92
6.4 Simulation Setup and Results .....	92
6.4.1 Analysis of the SLA Categories .....	92
6.4.2 Analysis of SLA-Differentiated Protection Techniques under Uniform Traffic: “Gold (DPP)” and “Silver” or “Silver Plus” .....	94
6.4.3 Analysis of SLA-Differentiated Protection Techniques under Non-Uniform Traffic: “Gold (DPP)” and “Silver Plus” .....	99

---

6.4.4 Analysis of SLA-Differentiated Protection Techniques under Uniform Traffic: “Gold (DPP)” or “Gold (SBPP)” and “Silver Plus” .....	100
6.4.5 Analysis of Admission Control Mechanism under Uniform Traffic: “Gold (DPP)” and “Silver Plus” .....	102
6.4.6 Analysis of Enhanced SLA-Differentiation Protection .....	104
6.5 Conclusions .....	111
 Chapter 7. Conclusions and Future Plans.....	 113
 Chapter 8. List of Publications .....	 117
8.1 Journals .....	117
8.2 Conferences .....	117
 References .....	 119





## List of Figures

Figure 1. Spectral bands over a single mode fiber. ....	9
Figure 2. Architecture with separate amplifiers for the implementation of C+L line systems [54]. .....	9
Figure 3. (a) Example network topology (distances are given in km), (b) Core and spectrum availability through the selected path (s-A-B-d), (c) Allocation of resources to request R with multipath routing. ....	20
Figure 4. The NSFNET topology [77] (distances are given in km). ....	21
Figure 5. The even-wide hexagonal structure for a seven-core fiber. ....	21
Figure 6. Request blocking rate of EEMPR in NSFNet at K=1, 3, 5, 7 .....	23
Figure 7. Request blocking rate of MPIRA in NSFNet at K=1, 3, 5, 7 .....	23
Figure 8. Bandwidth blocking rate of EEMPR in NSFNet at K=1, 3, 5, 7 .....	23
Figure 9. Bandwidth blocking rate of MPIRA in NSFNet at K=1, 3, 5, 7 .....	23
Figure 10. Energy consumption per transmitted bit of EEMPR in NSFNet at K=1, 3, 5, 7 .....	24
Figure 11. Energy consumption per transmitted bit of MPIRA in NSFNet at K=1, 3, 5, 7 .....	24
Figure 12. Delay relative to shortest path of EEMPR in NSFNet at K=1, 3, 5, 7 .....	24
Figure 13. Delay relative to shortest path of MPIRA in NSFNet at K=1, 3, 5, 7 .....	24
Figure 14. Request blocking ratio comparison in NSFNet topology at K=5. ....	25
Figure 15. Bandwidth blocking ratio comparison in NSFNet topology at K=5. ....	25
Figure 16. Energy consumption per transmitted bit comparison in NSFNet topology at K=5....	25
Figure 17. Reduction in energy per bit in NSFNet topology at K=5. ....	25
Figure 18. Reduction in number of sublightpaths in NSFNet topology at K=5. ....	26
Figure 19. Delay in relation to shortest path comparison in NSFNet topology at K=5 .....	26
Figure 20. Network topologies (a) SmallNet [80], (b) USNet [80], (c) JPN12 [38], (d) DT [81] (distances in km). ....	28
Figure 21. Analysis in the SmallNet (left column) and USNet (right column) topologies in terms of BBR (a and b), energy consumption (c and d) and delay in relation to shortest path (e and f). .....	30
Figure 22. Analysis in the JPN12 (left column) and DT (right column) topologies in terms of BBR (a and b), energy consumption (c and d) and delay in relation to shortest path (e and f). ....	31
Figure 23. Histograms of the 5-shortest paths lengths for the NSFNet. ....	32
Figure 24. Histograms of the 5-shortest paths lengths for (a) SmallNet, (b) USNet, (c) JPN12 and (d) DT. ....	33
Figure 25. Reduction in the number of sublightpaths for (a) SmallNet, (b) USNet, (c) JPN12 and (d) DT. ....	34

Figure 26. Bandwidth blocking ratio depending on the network load. Shortest path ( $K=1$ ) is used as routing strategy. ....	41
Figure 27. Bandwidth blocking ratio of length-based RBMLSA depending on the network load. $K$ in $K$ shortest paths algorithm is set to 3.....	42
Figure 28. Supported load with different number of upgraded fibers respect to employing only C-band. ....	42
Figure 29. Bandwidth blocking ratio depending on the network traffic load in (a) NSFNet, (b) JPN12, and (c) DT-network topologies.....	48
Figure 30. Bandwidth blocking ratio depending on the network traffic load considering uniform traffic in (a) NSFNet, (b) JPN12, and (c) DT-network topologies.....	58
Figure 31. Maximum supported traffic load in a partially upgraded network with blocking probability $\leq 10^{-3}$ , considering uniform traffic. ....	59
Figure 32. Bandwidth blocking ratio depending on the network traffic load considering non-uniform traffic in (a) NSFNet, (b) JPN12, and (c) DT-network topologies, for MaxPaths when different policies to set the $\alpha_{sd1}$ weights are used. ....	64
Figure 33. Bandwidth blocking ratio depending on the network traffic load considering non-uniform traffic in (a) NSFNet, (b) JPN12, and (c) DT-network topologies, for MostUsed and MaxPaths.....	66
Figure 34. Bandwidth blocking ratio for different number of links upgraded.....	70
Figure 35. Number of transceivers to be acquired (if traffic load increases to 0.6). ....	71
Figure 36. The implementation of C+L band networks through (a) separate amplifiers architecture and (b) wideband amplifier architecture [54]. ....	74
Figure 37. Request blocking ratio depending on the network load.....	76
Figure 38. Bandwidth blocking ratio depending on the network load. ....	77
Figure 39. Example of the use of disjoint paths in classical path protection and the use of separate amplifiers (i.e., a different EDFA to amplify each band). ....	78
Figure 40. Request blocking ratio depending on the network traffic load in the (a) NSFNet topology, (b) JPN12 topology, and (c) DT network under different upgrade scenarios. ....	79
Figure 41. Comparison of the hybrid approaches (L-band for primary connections vs. L+C bands for primary connections) in (a) 50% upgraded and (b) fully upgraded NSFNet, JPN12, and DT topologies.....	80
Figure 42. BBR depending on network load considering partial migration and dynamic restoration in the (a) NSFNet, (b) JPN12, and (c) DT topologies.....	83
Figure 43. Supported traffic load with different levels of partial migration using the dynamic restoration with respect to the dedicated protection (failure rate = every 500 connections). .	84
Figure 44. Supported traffic load with different levels of partial migration using the dynamic restoration with respect to the dedicated protection (fiber-cut failure is not introduced to the network).....	85
Figure 45. Supported traffic load with different levels of partial migration using the dynamic restoration with respect to the dedicated protection (failure rate = every 1000 connections).	86
Figure 46. Hybrid protection method. ....	90

Figure 47. Request blocking ratio of different SLA categories depending on network traffic load.	93
Figure 48. Average computing time per request of different SLA categories depending on network traffic load.	94
Figure 49. Global request blocking ratio with respect to the network load and the percentage of “gold” connections, when considering “gold (DPP)” and “silver” clients	95
Figure 50. Request blocking ratio of each SLA category with respect to the network load and the percentage of “gold” connections, when considering “gold (DPP)” and “silver” clients.	96
Figure 51. Global request blocking ratio with respect to the network load and the percentage of “gold” connections, when considering “gold” and “silver plus” clients.	96
Figure 52. Request blocking ratio of each SLA with respect to the network load and the percentage of “gold” connections, when considering “gold (DPP)” and “silver plus” clients.	97
Figure 53. Comparison in terms of global request ratio when EDFA protection (“silver”) and hybrid protection (“silver plus”) is used for the low priority category.	98
Figure 54. Request blocking ratio of “silver” and “silver plus” SLA categories depending on network traffic load and the percentage of “gold” connections.	98
Figure 55. Request blocking ratio of “gold (DPP)” SLA in the presence of “silver” or “silver plus” SLA categories.	99
Figure 56. Request blocking ratio of each SLA with respect to the network load and the percentage of “gold” connections, when considering “gold (DPP)” and “silver plus” clients.	100
Figure 57. Request blocking ratio of each SLA with respect to the network load and the percentage of “gold” connections, when considering “gold (DPP)” and “silver plus” clients.	100
Figure 58. Comparison in terms of global request ratio when DPP and SBPP are used for the high priority category.	101
Figure 59. Request blocking ratio of “silver plus” SLA category depending on the percentage of “gold” connections when DPP or SBPP is used for the “gold” SLA.	101
Figure 60. Request blocking ratio of “gold” SLA category depending on the percentage of “gold” connections when DPP or SBPP is used for the “gold” SLA.	102
Figure 61. Global request blocking ratio depending on different thresholds for the AC.	103
Figure 62. “Gold (DPP)” request blocking ratio depending on different thresholds for the AC.	104
Figure 63. “Silver Plus” request blocking ratio depending on different thresholds for the AC.	104
Figure 64. Impact of the AC procedure on request blocking ratio.	104
Figure 65. Comparison of the global request blocking ratios for cases A1 to A3, when DPP is used for “gold” traffic.	107
Figure 66. Comparison of the request blocking ratios for each client type in the case A3, when DPP is used for “gold” traffic.	108
Figure 67. Comparison of the global request blocking ratios for cases B1 to B3, when DPP is used for “gold” traffic.	108
Figure 68. Comparison of the request blocking ratios for each client type in the case B3, when DPP is used for “gold” traffic.	109

Figure 69. Comparison of the global request blocking ratios for cases A1 to A3, when SBPP is used for “gold” traffic..... 109

Figure 70. Comparison of the global request blocking ratios for cases A1 to A3, when SBPP is used for “gold” traffic..... 110

Figure 71. Comparison of the global request blocking ratios for cases A1 to A3, when SBPP is used for “gold” traffic..... 110

Figure 72. Comparison of the global request blocking ratios for cases A1 to A3, when SBPP is used for “gold” traffic..... 110

## List of Tables

Table 1. Transmission reach and XT-threshold for each modulation level for a MCF with seven cores with hexagonal arrangement (based on [45]).	14
Table 2. Crosstalk parameters for a MCF with seven cores with hexagonal arrangement [76].	15
Table 3. Characteristics of the five network topologies.	29
Table 4. Maximum Optical Reach for Each Spectral Band in C+L Line Systems [86].	40
Table 5. Characteristics of the evaluated network topologies.	56
Table 6. Metrics of the upgrade solutions for the NSFNet (uniform traffic).	61
Table 7. Metrics of the upgrade solutions for the JPN12 (uniform traffic).	61
Table 8. Metrics of the upgrade solutions for the DT (uniform traffic).	62
Table 9. Metrics of the upgrade solutions for the NSFNet (non-uniform traffic, $\alpha_{sd1} = PsPd$ ).	67
Table 10. Metrics of the upgrade solutions for the JPN12 (non-uniform traffic, $\alpha_{sd1} = PsPd$ ).	67
Table 11. Metrics of the upgrade solutions for the DT (non-uniform traffic, $\alpha_{sd1} = PsPd$ ).	67
Table 12. Number of elements and cost to upgrade the network with the two alternatives considering $BBR < 10^{-3}$ .	72
Table 13. Specifications of different SLA categories <sup>1</sup> .	91
Table 14. Specification of the analyzed client types.	105
Table 15. The analyzed network cases.	106



## List of Abbreviations

Abbreviation	Explanation
5G	Fifth Generation
AC	Admission Control
ASE	Amplified Spontaneous Emission
BBR	Bandwidth Blocking Ratio
BDM	Band Division Multiplexing
BPSK	Binary Phase Shift Keying
BVT	Bandwidth Variable Transponder
CAPEX	Capital Expenditure
DPP	Dedicated Path Protection
DSP	Digital Signal Processing
DT	Deutsche Telekom
EDFA	Erbium Doped Fiber Amplifier
FS	Frequency Slot
GGN	Generalized Gaussian Noise
GSNR	Generalized Signal-to-Noise Ratio
ILP	Integer Linear programming
IoT	Internet of Things
ISRS	Inter-band Stimulated Raman Scattering
MB-EON	Multiband Elastic Optical Network
MCF	Multicore Fiber
MFT	Multifiber Transmission
MILP	Mixed Integer Linear Programming
MMF	Multimode Fiber
NSFNet	National Science Foundation Network

---

OFDM	Orthogonal Frequency Division Multiplexing
OSNR	Optical Signal-to-Noise Ratio
QAM	Quadrature Amplitude Modulation
QoS	Quality of Service
QoT	Quality of Transmission
QPSK	Quadrature Phase Shift Keying
RBMLSA	Routing, Band, Modulation Level, and Spectrum Assignment
RBR	Request Blocking Ratio
RMLSA	Routing, Modulation Level and Spectrum Assignment
RMLSSA	Routing, Modulation Level, Space, and Spectrum Assignment
ROADM	Reconfigurable Optical Add-Drop Multiplexer
RSA	Routing and Spectrum Assignment
RSSA	Routing, Space, and Spectrum Assignment
SBPP	Shared Backup Path Protection
SDM	Space Division Multiplexing
SDM-EON	Space Division Multiplexed Elastic Optical Network
SLA	Service Level Agreement
SNR	Signal-to-Noise Ratio
WDM	Wavelength Division Multiplexing
XT	Crosstalk

---



# Chapter 1.

## Introduction

Optical networks play a crucial role in modern telecommunications, offering high data transmission speeds, low signal attenuation, flexibility of configuration, and energy efficiency, which are essential for meeting the ever-growing demands of high-speed internet, cloud computing, and emerging technologies like fifth generation (5G) networks and the Internet of Things (IoT). However, the traditional wavelength division multiplexing (WDM) networks face inefficiency as a result of assigning an entire wavelength, even when the requested bandwidth is significantly less than the wavelength's full capacity [1]. Therefore, over the last decade, elastic optical networks (EON) have been proposed as a promising approach to overcome the aforementioned inefficiency, and to pave the way for the emerging demands. The deployment of EON in backbone networks results in an improved utilization of system resources owing to just-enough bandwidth allocation. Just-enough bandwidth allocation is achieved through the aggregation of fine-grained frequency slots (FSs) with a capacity of, typically, 6.25 GHz or 12.5 GHz into super-channels to meet the bandwidth required by the incoming connection requests [2], [3]. In summary, the flexible bit rate lightpaths are the main advantages of EON compared to the fixed-grid WDM networks, and they require the use of components such as bandwidth variable transponders (BVTs) and reconfigurable optical add-drop multiplexers (ROADMs). The provided flexibility by EONs along with the introduction of advanced technologies like digital signal processing (DSP) and coherent transceivers employing multi-level modulation formats [4] improve the optical transmission capacity. However, this type of capacity scaling is not enough to cope with the growth rate in bandwidth demand [5].

Two solutions that are currently receiving a great deal of attention from the research community are space division multiplexing (SDM) [6], [7] and band division multiplexing (BDM) [8], [9]. By benefitting from parallel signal transmission, the deployment of SDM technology yields dramatic capacity improvement compared to EONs [6]. SDM-enabled EONs can be realized through several strategies, including multifiber transmission (MFT), the use of multicore fibers (MCFs) or the use of multimode fibers (MMFs) [10], [11]. Although the utilization of MCFs or MMFs increases the transmission capacity to the range of petabit/s/fiber [12], their implementation relies on installing new optical fiber infrastructures, which imposes a substantial capital expenditure (CAPEX). Furthermore, MCF and MMF technologies have not yet been commercialized and are still in the research phase. Regarding the use of MF transmission, it is a practical solution if unused optical fibers are available (although it requires enabling C-band line systems in those fibers). Nevertheless, in the event of shortage or lack of available dark fibers, leasing and rolling out new cables may cause huge CAPEX cost and delays [13].

As it is mentioned, an attractive and practical solution to increase the capacity of optical fibers is known as multiband elastic optical networks (MB-EONs). In MB-EONs, the goal of increasing network capacity is ensured by using other spectral bands in addition to the conventional C-band [14]. The main motivation behind promoting the MB-EON technology is that scaling the network capacity can be done through the efficient utilization of the available spectrum at already installed fibers, thus maximizing the return on investment of the existing optical fibers [15]. The implementation of MB-EONs requires the deployment of new amplifiers, transceivers, and ROADMs able to operate in spectral bands beyond the C-band (in the O-, E-, S-, L-, and/or U-bands). For instance, lighting up the L-band increases the available bandwidth of a network that initially uses only the C-band by more than two times, from  $\sim 5$  to  $\sim 11.5$  THz [13]. Also, thanks to the L-band-ready erbium doped fiber amplifiers (EDFAs), C+L band systems are commercially available, which is another main reason for deploying C+L multi-band optical networks.

### **1.1 Contributions of the Ph.D. Thesis**

The key contributions of the thesis are as follows:

- 1) Proposal of a new multipath routing algorithm with the aim of minimizing the blocking probability and the energy consumed by BVTs in SDM-EONs with MCFs.
- 2) Proposal of algorithms to partially upgrade C to C+L optical networks. To manage the costs imposed on the network operator by the extension of spectral bands beyond the C-band, network planning and design should be done carefully. The high cost of the components required to upgrade a network to C+L-band optical line systems leads network operators to postpone the deployment of a complete upgrade and to adopt a partial migration strategy instead.
- 3) Proposal of a techno-economic analysis to answer the question of which type of transceivers should the industry focus to help operators in the migration of their networks from the C-band to the C+L-bands. To manage the partial upgrade of a network, operators have two alternatives to acquire new transceivers: a) multi-band C+L transceivers, or b) separate single-band C and single-band L transceivers.
- 4) Proposal of different survivability methods for the C+L band systems. To manage a failure in any network component while moving from the C-band to the L-band, the incoming connection requests should be able to maintain a continuous transmission even in the occurrence of a failure.
- 5) Proposal of a service level agreement (SLA) differentiated protection mechanism to improve the quality of service (QoS) of MB-EONs. To manage network resources effectively and to enhance network performance, the provisioning of QoS-aware classification for data traffic should be performed.

---

## 1.2 Thesis Structure

The thesis is structured as follows:

- Chapter 2 introduces the next generation of optical networks, including EON, SDM, and MB-EON. Furthermore, a literature review on various design methods of these networks is conducted based on the previously mentioned contributions of the thesis.
- Chapter 3 proposes a multi-path routing algorithm for SDM-EON to reduce the blocking probability of the incoming connection requests. A simulation study comparing our proposed method with another similar proposal from the literature is presented for different types of topologies in terms of link distances.
- Chapter 4 presents different planning strategies to efficiently upgrade the C-band EON to C+L multi-band optical networks. The network performance in terms of bandwidth blocking ratio as a function of the traffic load and the number of links upgraded from the C-band to the C+L bands is investigated. Additionally, Chapter 4 introduces a techno-economic model to determine the most efficient transceivers that the network operators may acquire when migrating from the current C-band optical networks to C+L multi-band optical networks.
- Chapter 5 proposes and evaluates different protection techniques to provide resiliency against potential network failures in multi-band C+L optical networks.
- Chapter 6 proposes a mechanism for SLA differentiated protection in C+L multi-band networks, where each service receives the appropriate degree of protection based on its needs. Specifically, in this chapter, we aim to protect connection requests against a single fiber cut and/or failure in an EDFA based on their priority.
- Chapter 7 provides the conclusions of the present thesis and some future work directions.



## Chapter 2 .

### Next Generation of Optical Networks

#### 2.1 Elastic Optical Networks (EONs)

High-performance optical networks, which are flexible, cost-effective, and bandwidth efficient, are much needed as a result of the rise of high-speed and bandwidth-hungry applications on the Internet. The advent of elastic optical networks (EONs) is rooted from the limitations faced by the previous generation of optical networks based on wavelength division multiplexing (WDM), and allow to increase the efficiency of the network in a productive way [3]. It is not surprising that EONs based on orthogonal frequency division multiplexing (OFDM) are highly accepted as the next generation of optical networks, leveraging on flexible spectrum reservation and adaptive selection of the most suitable modulation format [16].

##### 2.1.1 Resource Allocation in EONs

Dealing with the resource allocation problem depends on the type of traffic that a network may face. Three different types of traffic can be defined: 1) static, 2) semi-static, and 3) dynamic traffic [17]. In a static traffic scenario, the specifications of the connections are known in advance. For the static traffic scenario, a constant matrix includes the traffic information, with the assumption that the established lightpaths remain in the network permanently. The key difference between the static and semi-static traffic scenarios is that in case of traffic variations, the established lightpaths in the semi-static traffic scenario could be adjusted. In a dynamic traffic scenario, that we consider in the thesis, there is no prior information regarding the incoming connection requests. Once a connection request arrives at the network, attempts are made to serve the connection by allocating the required bandwidth. Furthermore, connections remain in the network temporarily, which means that an established lightpath is released when the corresponding holding time ends.

Allocating resources for end-to-end dynamic connection requests, considering the restrictions of spectrum continuity and contiguity, is a fundamental problem in EONs, known as the routing and spectrum assignment (RSA) [18]. These constraints (i.e., contiguity and continuity) should be applied during the phase of resource allocation while serving an incoming connection request. The allocation of adjacent and sequential spectrum slots on each link refers to the contiguity constraint. On the other hand, the continuity constraint guarantees that the same range of spectrum slots should be assigned to the connection along the whole lightpath. The employment of spectrum converters by the network operators may lead the continuity constraint to be alleviated. However, using the spectrum converters results in an increase in the network cost [18], [19].

Moreover, greater scalability can be obtained by using more spectrally efficient modulation formats (in case that they meet quality of transmission (QoT) requirements), thus reducing the

number of FSs needed to support the demands, and resulting in more connection requests being accepted. Therefore, in EONs, the valuable concept of distance-adaptive modulation cannot be overlooked. Hence, the RSA problem transforms into the route, modulation level and spectrum assignment (RMLSA) problem [20], [21].

The spectrum allocation can be performed following different policies like First-Fit, Best-Fit, and so on. The First-Fit policy, which prioritizes a block of available slots with the lowest starting index is the most straightforward and cost-effective approach [22]. According to the Best-Fit policy, a block of FSs with the closest size to the requested slots is prioritized, if it satisfies the contiguity and continuity constraints. Although the employment of the Best-Fit policy incurs higher time-complexity, the network performance evaluation results confirm that this approach leads the network to be more efficient through a reduction in blocking ratio [23], [24].

### 2.1.2 Survivability in EONs

The flexibility provided by EONs over the standard C-band spectrum significantly increases the number of connections that might pass through an optical fiber compared to non-elastic networks. Therefore, as providing resiliency against any fault in network links is essential, the concept of survivability has been widely investigated in EONs [25], [26], [27].

In this regard, different survivability methods have been proposed to protect EONs against potential failures, such as dedicated path protection (DPP) [28] and shared backup path protection (SBPP) [29].

With DPP, two link-disjoint optical connections (lightpaths) are established for each connection request. Therefore, in this method, fast switching from the primary lightpath to the backup one is guaranteed if a single failure occurs. On the other hand, SBPP is an efficient approach in which the protection capacity can be shared among different protection lightpaths if the associated primary lightpaths are disjoint. This operational efficiency in terms of network resources of this approach makes SBPP an attractive option for enhancing network survivability [30], [31].

### 2.1.3 Admission Control Mechanisms in EONs

The employment of admission control (AC) mechanisms leads the overall network performance to be improved. This is due to the fact that AC mechanisms helps optimizing resource allocation. Regarding AC mechanisms, different approaches have been proposed. Wang *et al.* [32] have presented three different AC mechanisms. Among them, one which depends on spectrum partitioning generally leads to better results in terms of bandwidth blocking ratio and fragmentation ratio. Authors in [33] have introduced two different mixed integer linear programming (MILP) formulations for lightpath AC with the aim of maximizing the acceptance probability for the upcoming connection requests. In that paper, the proposed methods have been analyzed in both fixed-grid and flex-grid optical transport networks. The introduced AC strategy in [34] is aimed at maximizing a pre-determined reward. In this way, connections admission is performed based on the reward increase they can bring to the network.

## 2.2 Space Division Multiplexed Elastic Optical Networks (SDM-EON)

Despite the additional flexibility provided by EONs, the capacity limit of SMFs has become a critical concern. Therefore, the introduction of spectrally and spatially flexible optical networks applying the SDM technology looks an extremely promising solution to get around the capacity crunch in upcoming optical transmission networks [35], [36]. SDM networks provide an additional degree of freedom in the format of the spatial domain. In order to transport optical signals in SDM systems, every link holds various spatial paths, which can be a fiber (in a multi-fiber cable), a core (in a multi-core fiber, MCF), or even a mode (in a multi-mode fiber, MMF) [6]. In particular, enhanced capacity, appropriate spatial switching granularity, and similar features of attenuation with a typical single-core fibers are all strong incentives for utilizing MCFs. The new dimension (space) with the vertical direction relative to the frequency zone acts as an effective factor to grant a great deal of freedom in signal management [37]. Evidently, the higher the degree of freedom, the greater the complexity of network control, leading to the use of route, space, and spectrum assignment (RSSA) [38] or even route, modulation level, space and spectrum assignment (RMLSSA) algorithms [39].

A problem with MCFs is the leakage of a fraction of the signal power of a core to the neighbor ones, which triggers signal interference if the same spectral slots are used [40]. This phenomenon is known as inter-core crosstalk (XT), and causes a reduction in signal quality [41]. Taking some approaches such as trench-assisted multi-core fibers, emplacing certain distance among cores, and distributing optical signals in the contrary directions over the adjacent cores can contribute to the inter-core XT reduction. However, it does not mean that the impact of XT can be fully cleared. Therefore, XT-aware RSSA methods are required for lightpath allocation, to ensure that such an impairment does not exceedingly influence the lightpath quality [42], [43], [44].

Multipath routing has been studied in the context of EONs and, more recently, in the context of SDM-EON. Jafari-Beyrami *et al.* [45] have presented two fragmentation-aware heuristics with/without inter-core XT consideration in SDM-EON with MCFs. Whenever a connection is going to be blocked through the single path strategy; it will be divided upmost into two sub-demands across the cores. For alleviating the fragmentation rate of the path links, those sub-demands are assigned to two cores with the highest fragmentation level. However, because the provided algorithms consider the central core as the common core, they would only be able to work in the MCFs with central core structure. Another proposal to reduce fragmentation is that of [46], which sets a maximum number of paths and a minimum number of frequency slots for a connection to use multipath routing. In [47], authors introduced three heuristics to minimize the amount of fragmentation in SDM-EON. The aim of the introduced algorithms is to reduce the blocking probability. In that paper, the Spectrum Block Multipathing per Cores (SBMC) leads to better results in terms of blocking ratio compared to the other proposed algorithms. However, in SBMC, an incoming connection request might be divided into  $n$  sub-demands to be established over different cores of the fiber, which leads to the usage of more network resources.

Paira *et al.* [48] have proposed different survivable multipath routing algorithms and assessed their performance in terms of blocking probability, energy efficiency, fragmentation, and XT

awareness. The introduction of survivability is the main contribution of that paper, demonstrating improved blocking rate compared with the traditional p-cycle and shared protection methods. However, a single demand may be divided between three different paths, which increases the differential delay among those flows. Zhu *et al.* [49] have proposed a distance-adaptive energy-aware resource allocation (DERA) algorithm using a survival multipath scheme. In that work, the selection of the paths is done by taking into account the expected energy consumption rather than simply relying on shortest path considerations. Halder *et al.* [50] have proposed two route, core and spectrum allocation schemes for offline survivable SDM-EON using multipath-based protection, and consider two classes of incoming connection requests, those that have to be established immediately upon arrival and those which can tolerate some delay until being established. Oliveira *et al.* [51] have introduced an algorithm called Multi/singlepath rOuting For multiCore network (MOFIO). When a single path is employed to connect the source to the destination, SBPP is utilized to make the network resilient against a failure. When multipath routing is performed, the SBPP method is executed to protect each of the produced primary paths. For multipath routing, two different paths are considered in order to improve the ratio of accepted requests, which increases the level of differential delay.

In another study on multipath routing in SDM-EONs, by Moura and da Fonseca [52], two families of RMLSSA algorithms, named Connected Component Labeling (CCL) and Inscribed Rectangles Algorithm (IRA), are proposed and compared, with an algorithm called Multipath Inscribed Rectangles Algorithm Minimal Crosstalk (MPIRAXT) generally providing the best results in those tests. The algorithms are based on the use of image processing techniques with the objective of reducing the computational complexity. In that study, rectangles of different sizes show the available set of FSs. In each rectangle, the width multiplied by the length should fulfill the amount of slots requested by an incoming connection request. If a single path is not capable of satisfying the requested demand, the bandwidth can be divided between two to five shortest paths. Although the authors give priority to using the rectangles, which stretch across only one spatial path, the employment of multiple paths as well as the selection of the rectangles with more than one unit length as the block of available FSs increase the energy consumption associated with the optical transponders and the amount of differential delay.

In [53], it is shown that in networks with MCFs, using an architecture based on ROADMs without lane changes (therefore, imposing core continuity constraint in the routes of the connection) is much more economic (and reduces complexity), at the expense of a small reduction in performance. Accordingly, in Chapter 3, we propose a novel multipath RMLSSA algorithm with the aim of avoiding differential delay and reducing energy consumption, while keeping the blocking probability low enough, and considering continuity constraints in both spectrum and core location in order to use cost-effective SDM ROADMs without lane change support.



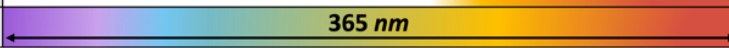
### 2.3 Multi-band Elastic Optical Networks (MB-EON)

As it is mentioned, SDM realization through MCFs or MMFs requires the installation of new optical fiber infrastructure and the deployment of advanced digital signal processing techniques, which impose a huge cost on network operators. On the other hand, as MFT is achieved through a bundle of existing SMFs, it is usually considered as a viable solution if those



unused optical fibers are available. However, network capacity enhancement through the employment of MFT is greatly affected by a shortage in optical fibers.

Due to the scarcity of dark fibers, network operators are increasingly turning their attention to band division multiplexing (BDM) as a promising technology. To keep the costs associated with capacity upgrade affordable, rather than rolling out new optical fiber infrastructure, it is considered essential to take advantage of the spectral bands of the fibers already installed. The BDM technology is realized through lighting up different spectral bands over the existing SMFs. Currently, the C-band window (1530 nm - 1565 nm, with a bandwidth of around 4 THz) is used as the conventional spectrum for the transmission of optical signals. The availability of EDFAs and a low value for the loss factor justify the selection of this range of spectrum as a standard window for the development of optical communication systems. The main goal of the BDM technology is to increase the capacity of optical fibers by using different spectral bands beyond the C-band, such as O, E, S, L, and/or U bands, providing a total bandwidth of around 50 THz [13]. Different potential spectral bands of a SMF to be lit up for capacity improvement are shown in Fig. 1 [13].

Band	O	E	S	C	L
Wavelength (nm)	1260-1360	1360-1460	1460-1530	1530-1565	1565-1625
C-band					
C+L bands					
All bands					

**Figure 1.** Spectral bands over a single mode fiber.

The implementation of C+L amplifiers for MB-EONs can be done by means of several architectures [54]. The most common architecture, shown in Fig. 2, is based on the use of a demultiplexer/multiplexer structure and a separate EDFAs to amplify each spectral band [54]. This architecture imposes a 400 GHz guard band between the C-band and the L-band. In our proposals in the domain of multi-band networks, we consider this architecture when an amplifier is migrated to a C+L band system.

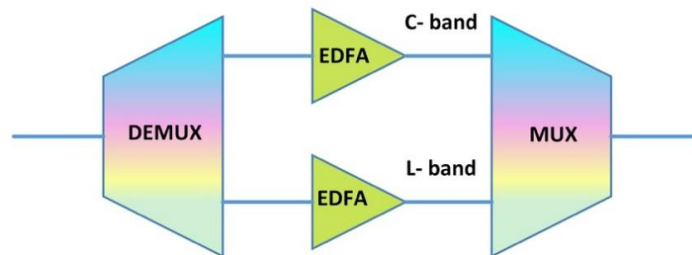


**Figure 2.** Architecture with separate amplifiers for the implementation of C+L line systems [54].

Once a network has been migrated to the other spectral bands from the C-band, the use of different spectral bands brings another dimension to the operation mechanisms of EONs, moving from the RMLSA problem to the routing, band, modulation level, and spectrum assignment (RBMLSA) problem in MB-EON [55], [56].

Several works have compared the replication of C-band line systems with the exploitation of different spectral bands to analyze the advantages of MB-EONs. Thus, Shariati *et al.* [57] have shown that the exploitation of the C + L + S-bands improves the network capacity by 8%–14% compared to the deployment of MFT with three C-band fibers. Ferrari *et al.* [58] have presented a comprehensive comparison between SDM and BDM technologies. They conclude that in case of availability of dark fibers, the employment of pure SDM technology is better, and if the availability of dark fibers is limited, the most practical solution relies on the mixed employment of BDM and SDM technologies. In [59], the network performance under three different methods, namely, C-band single-mode fiber transmission, SDM technology in which two fibers enable MFT, and a C+L band system, is analyzed. Simulation results demonstrate that the C+L band system doubles the network capacity while its application does not lead to severe physical penalties compared to MFT over two fibers. From a techno-economic perspective, Jana *et al.* [60] conclude that the application of SDM technology using available dark fibers enabled by MFT technique forces network operators to devote more expenditures compared to the C+L band systems for long-haul networks.

Other works have analyzed the impact of physical impairments in multiband networks. Multiband systems impose a nonlinear interference, known as inter-band stimulated Raman scattering (ISRS), which induces power transfer between spectral bands [61], [62]. D'Amico *et al.* [61] evaluated the QoT in C+L band systems and concluded that the degradation in generalized signal-to-noise ratio (GSNR) is related to SRS. Mitra *et al.* [63] employed an optical SNR (OSNR) model considering ISRS as well as amplified spontaneous emission (ASE) noise, which is generated by the amplifiers in the C+L-bands, and Cantono *et al.* [64] concluded that the application of the generalized Gaussian noise (GGN) model is the most appropriate solution for the prediction of QoT of wideband optical line systems.

Regarding the operation of MB-EONs, several works have focused on partially migrated networks, i.e., hybrid C/C+L networks, where just a subset of the links have been upgraded to exploit the C+L-bands. Bao *et al.* [65] proposed a technique called link-oriented resource balancing (LoRB) to select a block of slots for spectrum assignment such that the contiguous available resource separation degree (CARSD) for the transmission path is minimum. Yao *et al.* [56] proposed an RBMLSA algorithm for hybrid C/C+L networks, which is aware of the interactive effect of the ISRS impairment that new requests might have on the existing requests. Moreover, different policies for the spectrum assignment under a hybrid C/C+L network were introduced. However, [65] and [56] do not address how to plan the C/C+L network, i.e., how to determine which subset of links should provide C+L transmission capabilities.

Moving from a C-band only network to a fully upgraded network in which all the links can operate in the C+L-bands is a considerably costly process. Therefore, methods for partially or gradually migrating C-band networks toward C+L have been proposed, as it is of the utmost importance for operators. The work by Uzunidis *et al.* [66] combines and analyzes many of the

issues previously mentioned in this section. They first incorporate the main physical impairments of MB systems into an RBMLSA algorithm and use it to assess the performance advantages of MB-EONs (in terms of traffic blocking) compared with the replication of C-band fibers. Then, they demonstrate that upgrading a C-band network to a MB solution can be done in gradual phases in order to reduce the first-day CAPEX. This is because not all fibers and spectral bands have the same level of utilization. Therefore, they conclude that the network operator may plan the deployment of MB systems in specific links as they are needed due to traffic increases. A network planning framework to achieve a cost-effective network upgrade is presented in [67]. In that paper, Moniz *et al.* focus on upgrading a network by combining two strategies. On the one hand, by deploying line interfaces in some of the existing fibers to enable operation in the L-band. On the other hand, by deploying new optical fibers (and associated line interfaces) to operate in the C+L-bands. They combine those two strategies with the aim of minimizing the total cost of the required fibers and line interfaces for the upgrade. Ahmed *et al.* [68] propose several heuristics to gradually migrate a C-band network toward a fully upgraded C+L band network in a set of sequential steps. They take into account the traffic evolution and the impact of the physical layer and determine when to perform each migration step and which fibers should be upgraded in each of those steps. The aim is to minimize the total cost of the upgrade until the network is fully migrated to the C+L-bands through those sequential steps. Then, they extend their work in [69] by proposing and comparing several methods to reprovision (or reallocate) the existing lightpaths in the network when it is partially upgraded (in each of those sequential steps) to support the C+L-bands. In summary, to manage the imposed cost while leveraging the L-band spectrum, a network can be partially rather than fully migrated in a single/multiple step(s) by upgrading just a subset of the fibers to operate in the C+L-bands. Therefore, our proposals in Chapter 4 aim at achieving a partially upgraded network through prioritizing the optical fibers based on different metrics.

In the aforementioned studies, the transceivers that should be purchased in order to realize the C+L band systems were not considered, even though they have an important impact on the upgrade costs. Therefore, in Chapter 4, we also focus on transceivers, and analyze the question of whether it is worthwhile for network operators to invest in multi-band transceivers to accommodate increased network traffic loads, as opposed to using separate C-band and L-band transceivers for that aim.

As it is mentioned, moving from the C-band to the C+L-bands increases the capacity of optical networks by more than two times. Hence, the failure in any network component will lead to huge data loss, thus making the provisioning of the C+L band systems with survivability methods a critical issue. Therefore, lighting up the L-band has inspired researchers to design new survivability methods capable to operate in C+L band networks. In this regard, Luo *et al.* [70] have proposed a protection scheme for a C+L band line system considering multi-core fibers. They have assigned the primary and backup resources to the C-band and the L-band, respectively. In that paper, the main motivation behind considering different frequency bands for the assignment of working and protection lightpaths is to increase the signal to noise ratio (SNR) parameter associated to the C-band. This is because the usage of reserved slots on the L-band is limited to having a link failure so that the effect of ISRS is reduced.

Through the development of C+L band networks using the separate amplifiers architecture (see Fig. 2), Jana *et al.* [71] employ the same route for the establishment of primary and backup connections to provide the network with protection against amplifiers failures scenarios, using a different band for each connection, but they employ the C-band for the primary connection and the L-band for the backup one. The establishment of primary and backup connections is successful if there are enough available resources over the C-band and the L-band and a tolerable threshold level of the lightpath quality considering the fill margin is not exceeded. Otherwise, the backup lightpath for the connection request is served using a different route. It should be noted that this thesis proposes a method that is very similar to that of Jana. In fact, it was published in [72] before Jana's paper. The method will be described later in Chapter 5. Eira *et al.* [73] have analyzed the total number of optical interfaces required by a long-haul network (C+L band system versus C-band only network) while it is equipped with optical protection or shared restoration.

Given the critical importance of protection methods in C+L band networks, the thesis devotes Chapters 5 and 6 to an in-depth exploration of this subject. In Chapter 5, we propose and analyze different survivability methods in a fully/partially upgraded C+L band networks. Additionally, Chapter 6 combines the protection methods proposed in Chapter 5 with SLA differentiation. In Chapter 6, three different levels of protection based on the priority of the incoming connection requests are defined and we demonstrate an improvement on network performance when compared with only using the DPP strategy for all connections.

## Chapter 3 .

### Energy Efficient Multipath Routing in SDM-EON

In this chapter, we propose a novel energy efficient and XT-aware multipath routing algorithm to solve the dynamic RMLSSA problem in SDM-EONs with MCFs to serve dynamic traffic demands. In our approach, multipath routing, when required, is performed over a single path. In this way, a demand is divided into different smaller sub-demands, and the lightpaths associated to those sub-demands are called sublightpaths. Those sublightpath use different cores but are routed through the same set of fibers, so that the connection is not affected by the differential delay problem which typically arises when multipath solutions are adopted. Moreover, continuity constraints in both the spectrum and the core assigned to the lightpaths (or sublightpaths) are assumed in order to use the efficient ROADM architecture presented in [53]. In the proposed method, the use of distance adaptive modulation formats is considered, and the impact of inter-core XT is also incorporated. This new method is compared with an efficient multipath method proposed by Moura and Da Fonseca [52]. Through an in-depth simulation analysis, we demonstrate that our proposed method is as efficient as Moura and Da Fonseca's proposal in networks with short links (typically national networks), while it significantly outperforms in networks with long links (large countries, continental and inter-continental networks). This advantage manifests as a reduction in blocking ratio, energy consumption, the number of sublightpaths generated per demand, and average end-to-end delay.

In Section 3.1, the network model as well as key definitions and assumptions are presented. Then, we discuss the proposed algorithm in Section 3.2. Section 3.3 is dedicated to presenting a simulation study and analyzing the numerical results. Finally, the conclusion is outlined in Section 3.4.

It is worth mentioning that the proposals and results presented in this chapter have been published in [74].

#### 3.1 Problem Definitions

In this chapter, the network topology is represented by a connected graph,  $\mathcal{G} = (\mathcal{N}, \mathcal{E})$ , where  $\mathcal{N}$  is the set of switching nodes and  $\mathcal{E}$  the set of links. Moreover,  $N$  and  $E$  denote the number of nodes and links, respectively. Links are bidirectional, having an individual multicore fiber for each direction. Each multicore fiber has a set of  $C$  cores identified by  $\mathcal{C} = \{1, 2, \dots, C\}$ , and the spectrum of each core is divided into an ordered collection of  $F$  frequency slots,  $\mathcal{F} = \{1, 2, \dots, F\}$ . Regarding modulation formats, we assume the use of binary phase shift keying (BPSK), quadrature phase shift keying (QPSK), and 8 and 16 quadrature amplitude modulation (8QAM and 16QAM). A dynamic operation scheme is considered for forthcoming connection demands, so that the associated lightpaths are dynamically established and released. Every connection request  $R$  is characterized by  $R(s, d, \gamma, \tau)$ , where  $s$  and  $d$  are the source and

destination nodes, respectively,  $\gamma$  is the number of required FSs (assuming a BPSK modulation level), and  $\tau$  specifies the time span (or service time) of the connection. However, a more spectrally efficient (but less robust) modulation format than BPSK can be used if the route,  $r$ , employed for establishing that connection does not exceed the transmission reach for that modulation format (as shown in Table 1 [45]). If that is the case, the demanded bandwidth (number of FSs) of that specific request can be reduced to  $\gamma_{modified}$ , calculated by Equation. (1) [75] in accordance with the selected modulation level for that route. Thus,

$$\gamma_{modified} = \left\lceil \frac{\gamma}{L_{modulation}^r} \right\rceil, \quad (1)$$

where  $L_{modulation}^r$  is the number of bits per symbol associated to the topmost attainable modulation level of route  $r$  when taking into account the transmission reach (Table 1). Be aware that Equation. (1) may lead to a floating-point number for some connection requests; thus, the ceiling function is called for the sake of being rounded up to an integer number. Note that the data shown in Table 1, based on [45] correspond to the use of trench-assisted single-mode seven-core fibers, where the cores have an even-wide hexagonal structure, and considering that paths exceeding 4000 km must use BPSK modulation format, which are the conditions that we will also assume in the simulation studies in this chapter.

**Table 1.** Transmission reach and XT-threshold for each modulation level for a MCF with seven cores with hexagonal arrangement (based on [45]).

Modulation Level	BPSK	QPSK	8QAM	16QAM
Transmission Reach [km]	—	4000	2000	1000
$XT_{threshold}$ [dB]	-22.75	-25.76	-28.77	-31.79
$L_{modulation}$	1	2	3	4

Regarding spectrum, we assume spectrum continuity and contiguity constraints, i.e., identical slots indexes have to be employed by an end-to-end lightpath from the source to the destination node, and the entire set of allocated FSs to a lightpath should be spectrally adjacent. To prevent interference between spectrally adjacent connections, a guard-band of one slot is considered. Moreover, core continuity is also assumed along the routes to use the efficient ROADM architecture presented in [53].

As previously mentioned, transmission in SDM-EONs with MCFs is impaired by inter-core XT, which arises from the occupancy of similar spectrum ranges in neighbor cores, thereby leading to the signal quality reduction. Accordingly, it is crucial to estimate the accumulated XT in lightpaths established in MCFs to ensure they satisfy quality of transmission requirements.

The XT value for a signal propagating through a certain core of a MCF is computed by Equation. (2) (in natural units) [76],

$$XT = \frac{n \cdot \exp(-(n+1)hl)}{1 + \exp(-(n+1)hl)}, \quad (2)$$

where  $n$  represents the number of neighbor cores having at least one common used FS with the connection being evaluated, and  $l$  is the transmission length in meters. The mean value of increased XT per unit length, can be determined by Equation. (3) [76].

$$h = \frac{2\kappa^2 R_B}{\beta \Lambda}, \quad (3)$$

where  $R_B$ ,  $\beta$ ,  $\kappa$  and  $\Lambda$  are, respectively, the bending radius, propagation constant, coupling coefficient, and core pitch of the fiber. The required parameters (again, for a MCF with seven cores arranged in a hexagonal structure) are shown in Table 2 [76].

**Table 2.** Crosstalk parameters for a MCF with seven cores with hexagonal arrangement [76].

Parameter	Value
Bending Radius ( $R_B$ ) [m]	0.05
Propagation Constant ( $\beta$ ) [1/m]	$4 \times 10^6$
Coupling Coefficient ( $\kappa$ )	$4 \times 10^{-4}$
Core Pitch ( $\Lambda$ ) [m]	$4 \times 10^{-5}$

The summation of the value of inter-core XT over the links in the lightpath should be calculated as the accumulated XT to assure the lightpath quality. In particular, the maximum threshold of XT should be met by the accumulated XT when a connection demand is served. The maximum optical reach depending on the modulation format is taken into account as a reference of the inter-core XT threshold for every lightpath (Table 1).

### 3.2 Dynamic Energy Efficient Multipath Routing, Modulation Level, Core, and Spectrum Assignment Algorithm (EEMPR)

In this section, our objective is to propose a XT-aware multipath routing, modulation level, core, and spectrum assignment, which can effectively reduce the blocking probability and improve energy efficiency. Splitting the requested demand through different cores improves the chance of finding available slots and satisfying subdemands, thereby reducing the blocking ratio. On the other hand, we keep the number of generated sublightpaths as low as possible allowing to reduce the energy consumption of transponders compared to the MPIRAXT algorithm [52]. We provide a general description of the algorithm, accompanied by a simple example, as well as the pseudocode of the method (Algorithm 1).

The algorithm works as follows. First of all, the  $K$ -shortest distance paths for each source-destination pair must be precomputed. Then, for each request,  $R(s, d, \gamma, \tau)$ , the algorithm starts by considering the shortest of those paths between  $s$  and  $d$  (lines 1-2) and the most spectrally efficient modulation format that can be used according to the length of the path is selected. Thus, a set of  $\gamma_{modified}$  available frequency slots along that route must be searched (line 3). It should be noted that a FS of a core  $c$  is available for the connection, only if it is available in the

same core number  $c$  of all the links composing the path. Therefore, the intersection of the FSs' status of the correspondent cores of different links over the selected route must be computed (line 4).

In order to allocate resources, the algorithm searches iteratively for spectral availability (in the whole route) from core number 1 to  $C$ , and within each core from slot 1 to  $F$  (lines 9-30). However, for resource allocation (lines 32-65) it uses an Best-Fit strategy [23], [24], that is, it prioritizes the allocation of a set of contiguous FSs in a single core whose size exactly matches the demand, i.e., its size is equal to  $\gamma_{modified}$  plus the guardband slot if required (lines 36-44) and as long as XT requirements are also fulfilled (lines 38). If a set of available FSs of exact size is not found (or cannot be used due to XT), but at least one set of available consecutive slots has a larger size, then the set with the smallest size that satisfies the demand is used [23], [24] (lines 45-53). In contrast, if no set of available consecutive slots is equal to or greater than the required number (or does not comply with XT requirements), then multipath routing will be used (lines 54-62), and the demand will be split to be served through different spectral gaps (possibly in different cores) along the same path. In that case the biggest available set of consecutive slots found in any of the cores will be selected to serve the demand. For the allocation of the remaining required spectral slots (line 59), the procedure mentioned above will be repeated (i.e., an exact-fit strategy will be used), until the demand is fully satisfied. It should be noted that resources are only effectively allocated if the demand can be fully served by multipath routing (lines 40 and 49); otherwise, no resources will be allocated at all (line 65), i.e., a demand cannot be partially fulfilled. If no available resources are found in any of the  $K$ -shortest paths between the  $s$  and  $d$  nodes, the request will be blocked (line 68).

The time complexity of the algorithm (including XT computation) in the worst-case scenario is  $O(KC^3F^3E)$ . The main 'for' loop of the algorithm (lines 1-66) runs  $K$  times. For each candidate path, first, the intersection of the FSs' status in the cores of the links must be computed (line 4), which has a complexity of  $O(CFE)$ . Then, an inner loop (lines 10-30) runs  $C$  times, and has an additional loop running  $F$  times, where spectral gaps are identified and added to a sorted list according to the sizes of those gaps (measured in FSs) and core numbers. The complexity of lines 10-30 is thus  $O(C^2F^2)$ . Finally, in lines 33-63, there is a 'do-while' loop which is executed up to  $CF$  times. Internally, gaps are classified (line 35), with complexity  $O(CF)$ , and there are three sequential loops (lines 36-44, 45-53 and 54-62), each executed again up to  $CF$  times. In these loops, the most demanding task is the XT computation, which has complexity  $O(CFE)$ . Thus, the complexity of lines 33-63 is  $O(C^3F^3E)$ . Therefore, the complexity of the algorithm is  $O(K(CFE + C^2F^2 + C^3F^3E))$ , which is asymptotically equivalent to  $O(KC^3F^3E)$ .

Regarding space complexity, the algorithm needs to store the  $K$ -shortest paths of up to  $E-1$  links, for a set of  $N(N-1)$  different source-destination pairs, so the space complexity is  $O(KEN^2)$ . Additionally, the availability state of the spectral slots in each core of each fiber link needs also to be stored, which has space complexity  $O(FCE)$ . Although there are additional variables and data structures, their space complexity is equal or lower. Therefore, the space complexity of the algorithm is  $O(KEN^2 + FCE)$ .



---

**Algorithm 1: Energy Efficient Multipath Routing, Modulation Level, Core, and Spectrum Assignment Algorithm (EEMPR)**


---

**Given:** Physical network topology  $\mathcal{G} = (\mathcal{N}, \mathcal{E})$

Set of  $K$ -shortest distance paths for each  $s$ - $d$  pair (sorted with increasing length for each  $s$ - $d$  pair),  $\mathbf{p}_k$

Availability of each frequency slot ( $f$ ) in each core ( $c$ ) in each link ( $e$ )

$s_{ecf}, e \in \mathcal{E}, c \in \mathcal{C}, f \in \mathcal{F}$  (being TRUE if available and FALSE if unavailable)

**Input:** An incoming connection request  $\mathbf{R}(s, d, \gamma, \tau)$ ,

**Output:** Establishment of lightpath (or sublightpaths) for the arrived connection request, and updated spectral utilization of each core/link

**Auxiliary procedures:**

XT\_is\_OK(): checks XT requirements.

classify\_gaps(): classifies spectral gaps in three categories according to the comparison of their size with the required number of slots (shown below, lines 71-77).

```

0  procedure EEMPR( $R$ )
1    for  $k = 1$  to  $K$ :
2      Select path  $p_k$  between nodes  $s$  and  $d$ 
3      According to length of  $p_k$  and Table 1, determine modulation format,  $\gamma_{modified}$  and  $XT_{threshold}$ 
4       $S_{cf} = \bigcap_{e \in p_k} S_{f,c,e} \quad \forall c \in \mathcal{C}, f \in \mathcal{F}$ 
5
6       $gaps\_list = \emptyset$  # List with sets of consecutive available slots
7       $pending\_sublightpaths = \emptyset$  # List of sublightpaths to be established to satisfy a demand
8       $required\_slots = \gamma_{modified}$ 
9      # Search of available spectral gaps in all cores
10     for  $c = 1$  to  $C$ :
11        $f = 1$ 
12        $f_{initial} = 1$ 
13        $size = 0$ 
14       while  $f \leq F$ :
15         if  $S_{cf} = \text{TRUE}$  (i.e., slot  $f$  of core  $c$  is available along the route):
16            $size = size + 1$ 
17         else: # end of gap
18           if  $f \neq F$ :
19              $size = size - 1$  # Reduce the usable size of the for transmission due to the guardband slot.
20           end if
21           if  $size \geq 1$ : # Only consider gaps with at least 1 available slot for transmission
22              $gap = \text{tuple}(c, f_{initial}, size)$ 
23             Add  $gap$  tuple to  $gaps\_list$  sorted by descending  $size$  (then increasing  $c$  and increasing  $f_{initial}$ )
24           end if
25            $size = 0$ 
26            $f_{initial} = f + 1$ 
27         end if
28          $f = f + 1$ 
29       end while
30     end for
31
32     # Allocation of gaps to sublightpaths
33     do:
34        $gap\_assigned\_in\_this\_iteration = \text{FALSE}$ 
35        $exact\_fit\_gaps, big\_gaps, small\_gaps = \text{classify\_gaps}(required\_slots, gaps\_list)$ 
36       for  $gap$  in  $exact\_fit\_gaps$ :
37         # Gap which provides exactly the remaining  $required\_slots$ 

```

---

```

38     if XT_is_OK(gap):
39         prereserve gap (only required_slots and guardband) and add to pending_sublightpaths list
40         establish all pending_sublightpaths (reserve slots for transmission and required guardbands)
41         request is ACCEPTED
42         go to end procedure EEMPR
43     end if
44 end for
45 for gap in big_gaps:
46     # Gap big enough to provide the remaining required_slots
47     if XT_is_OK(gap):
48         prereserve gap and add to pending_sublightpaths list
49         establish all pending_sublightpaths (reserve slots for transmission and required guardbands)
50         request is ACCEPTED
51         go to end procedure EEMPR
52     end if
53 end for
54 for gap in small_gaps:
55     # Gap not big enough to provide the remaining required_slots (multipath routing required)
56     if XT_is_OK(gap):
57         prereserve gap and add to pending_sublightpaths list
58         delete gap from gaps_list
59         required_slots = required_slots - gap.size # remaining slots to provide
60         gap_assigned_in_this_iteration = TRUE
61     end if
62 end for
63 while(gap_assigned_in_this_iteration == TRUE)
64     # Not enough spectral resources in path k
65     release all prereserved resources
66 end for
67 #Not enough spectral resources in any path
68 request is REJECTED
69 end procedure EEMPR
70
71 procedure classify_gaps(required_slots, gaps_list):
72     # Remember that list (and thus sublists) are sorted by descending size (then increasing c and increasing finitial)
73     exact_fit_gaps = gaps in gaps_list with size = required_slots # sorted by increasing c and increasing finitial
74     big_gaps = gaps in gaps_list with size > required_slots # sorted by decreasing size, increasing c and finitial
75     small_gaps = gaps in gaps_list with size < required_slots # sorted by decreasing size, increasing c and finitial
76     return exact_fit_gaps, big_gaps, small_gaps
77 end procedure classify_gaps

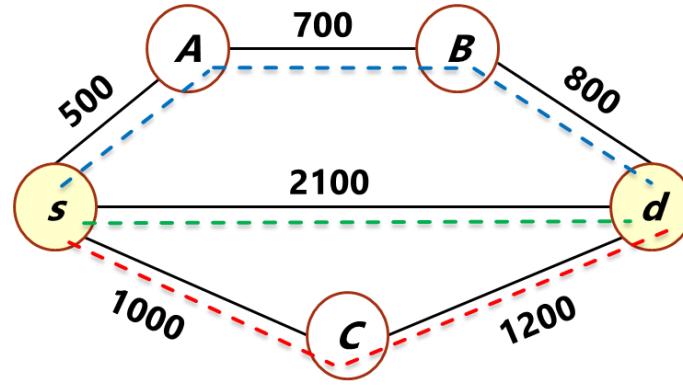
```

To show an example of the algorithm, let us assume an optical network comprising 5 nodes and 6 links (Fig. 3). Every fiber consists of seven cores, and the spectrum is divided into 15 frequency slots. For the sake of simplicity, we assume that there are no idle slots in the last two cores, and thus, only five cores (1 to 5) are represented in the figure. A request,  $R$ , to establish a connection between nodes  $s$  and  $d$ , requiring 19 slots (if BPSK were used), is received. A set of  $K$ -shortest distance paths (with  $K=3$ ) for each source-destination pair has been previously precomputed. Thus, Fig. 3(a) shows the 3-shortest distance paths between nodes  $s$  and  $d$ . The shortest of these paths,  $s$ -A-B- $d$  (represented in blue), has a length of 2000 km, is selected as the first option to serve the request. Then, based on Table 1, since the distance of the path is less than 4000 km and more than or equal to 2000 km, the QPSK modulation format is selected.

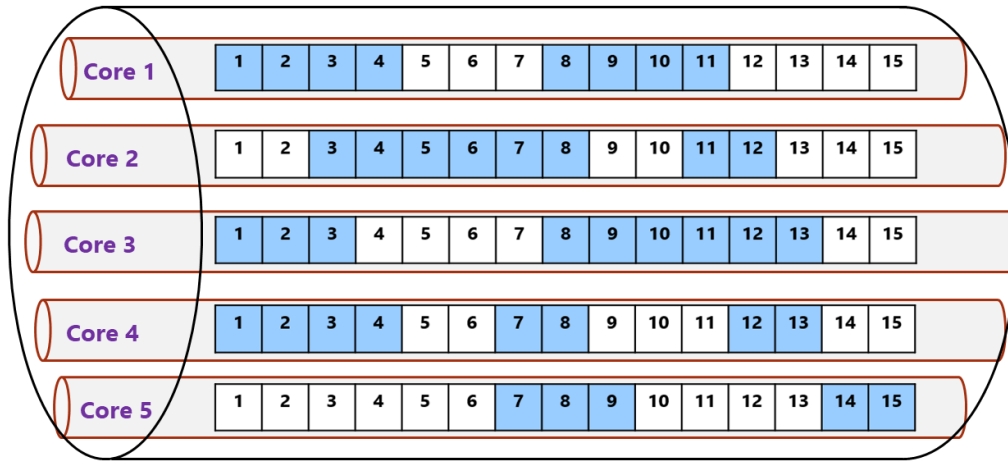
Therefore,  $\gamma_{modified} = \left\lceil \frac{19}{2} \right\rceil = 10$  slots as specified by Equation. (1).

Fig. 3(b) shows the spectral availability through the selected path ( $s-A-B-d$ ). Blue slots in the figure represent FSs that are used in each core by other connections in at least one of the links of the path (and thus cannot be used to serve the connection request,  $R$ ), and white slots represent available spectral slots through the whole path. Taking into account the core continuity and the spectrum continuity constraints, it is not feasible for  $R$  to be accommodated using a single lightpath through path  $s-A-B-d$ , as there are not 10 consecutive available slots in any single core. Therefore, the request must be served by means of several sublightpaths. Through first-fit core evaluation from the core with the smallest index to the one with the highest one, the largest number of successive empty FSs (6) is found in core number 5. As a result, slots 1 to 5 would be allocated for traffic transmission, and slot 6 would be reserved but used as a guard-band (sublightpath 1 in Fig. 3(c)). Therefore, 5 additional slots should still be provided to satisfy the demand. There is no such a big gap. The biggest available spectral available gap is then found in core 1, which has a size of 4 slots, and in fact does not require a guard-band, as it is at the end of the spectral range and, at the other side, slot 11 is already a guard-band. Those slots are then reserved (sublightpath 2 in Fig. 3(c)). For the final spectral slot to be provided to satisfy the demand, the first exact-fit gap is found in core 2, so that one would be selected and then the demand would be fully served (sublightpath 3 in Fig. 3(c)), assuming in this example, for the sake of simplicity, that XT requirements are also fulfilled.

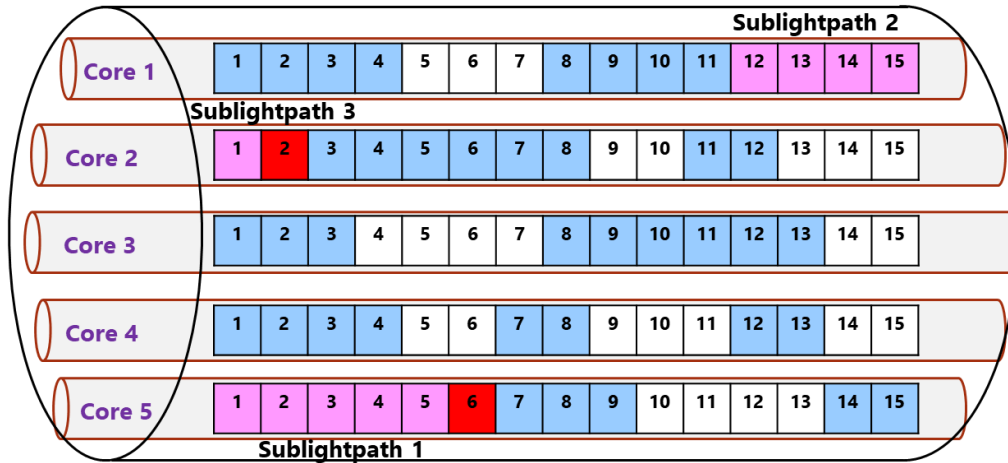
In the case that not enough spectral resources were available in path  $s-A-B-d$  (even exploiting multipath routing), the algorithm would then check with the second shortest available path, and then, if necessary, with the third one (as  $K=3$  in this example).



(a)



(b)



(c)

**Figure 3.** (a) Example network topology (distances are given in km), (b) Core and spectrum availability through the selected path (s-A-B-d), (c) Allocation of resources to request R with multipath routing.

### 3.3 Simulation Setup and Results

In this section, the performance of EEMPR is assessed and compared with MPIRAXT (from now on MPIRA) [52]. For that aim, an SDM-EON simulator has been developed in Python. The physical topology considered in the simulation is the National Science Foundation Network (NSFNET) topology, with 14 nodes and 21 links, as depicted in Fig. 4 [77]. Each link in the network is composed by two unidirectional single-mode multi-core fibers (one per direction), and each fiber has seven cores with even-wide hexagonal structure (Fig. 5). Optical transmission employs the C-band, and the spectrum per core is partitioned into 320 frequency slots of 12.5 GHz.

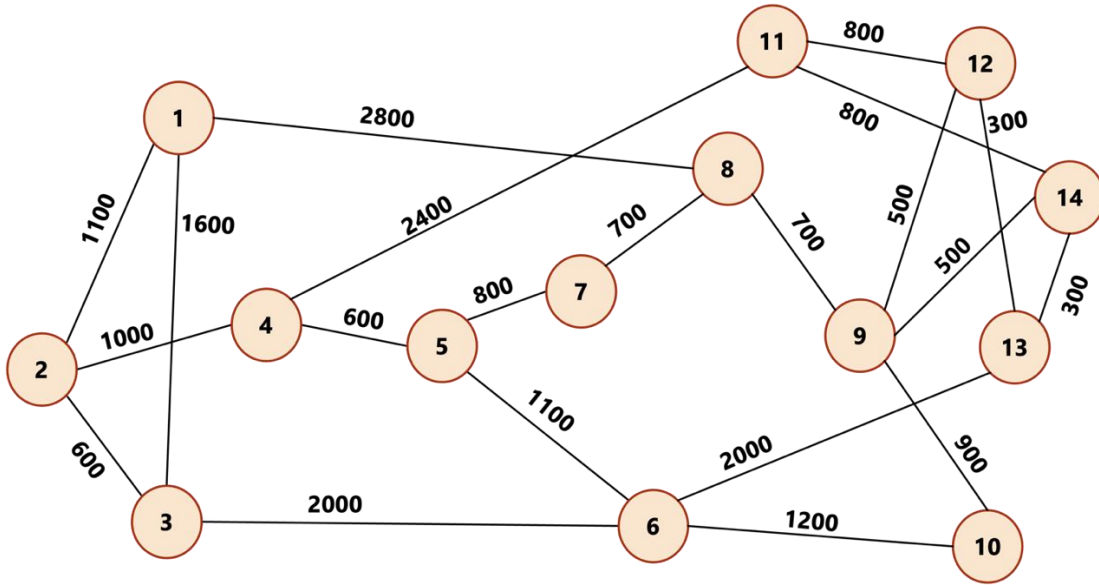


Figure 4. The NSFNET topology [77] (distances are given in km).

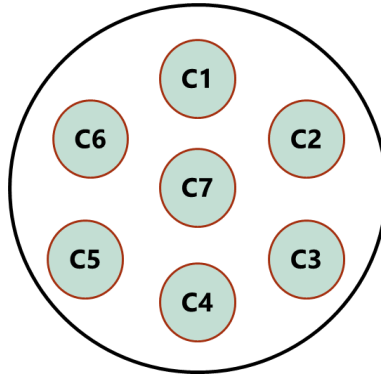


Figure 5. The even-wide hexagonal structure for a seven-core fiber.

Connection requests arrive at the network according to a Poisson process with average arrival rate  $\lambda$ , and the duration of each established connection ( $\tau$ ) is based on an exponential distribution with average  $T$ . The source and the destination nodes of each connection request are randomly selected considering a uniform distribution. A range of 12.5 Gb/s to 300 Gb/s in

steps of 12.5 Gb/s is considered as the potential data rate demanded by each connection request. The data rate associated to every connection request is randomly selected based on a uniform distribution from that range. Each slot has a capacity of 12.5 Gb/s if BPSK is used. Therefore, the number of required FSs for each connection,  $\gamma$ , follows a uniform distribution between  $\gamma_{min} = 1$  and  $\gamma_{max} = 24$  FSs, with an average of  $\gamma_{avg} = (\gamma_{max} - \gamma_{min}) / 2$ .

Since different connections may demand a different number of FSs, rather than using the classical traffic load in erlangs ( $\lambda T$ ), we use the normalized version given by Equation (4), which takes into account three additional parameters, namely, the average data rate of the connections ( $C_{avg}$ ), the maximum data rate of the connections ( $C_{max}$ ), and total number of nodes in the network ( $N$ ) [78].

$$Load = \frac{\lambda T}{N(N-1)} \frac{\gamma_{avg}}{\gamma_{max}}, \quad (4)$$

Transceivers in the network are assumed to be able to use BPSK, QPSK, 8QAM, and 16QAM modulation formats, subject to the transmission constraints and the spectral efficiency described in Table 1. Therefore, for establishing connections,  $\gamma_{modified}$  spectral slots should be reserved instead of  $\gamma$ . However, an additional slot should also be reserved for the connections to provide a spectral guard-band.

In each simulation,  $10^5$  requests are generated for warming up the network, but no metrics are collected during that phase. Then  $10^6$  additional requests are generated, for which performance metrics are retrieved.

### 3.3.1 Analysis for Different Numbers of $K$ -shortest Paths

First of all, we have analyzed the performance of EEMPR and the baseline algorithm, MPIRA [52], separately, for different numbers of  $K$ -shortest paths, setting  $K$  to 1, 3, 5 and 7. As we have mentioned, in EEMPR, all sublightpaths are routed through the same path; however, up to  $K$  different paths can be explored for resource availability. Four different metrics have been studied. First of all, Fig. 6 and Fig. 7 show the request blocking ratio (RBR) for EEMPR and MPIRA, respectively. The RBR is defined as the fraction of requests that are blocked. Results are represented together with 95% confidence intervals. Then, Fig. 8 and Fig. 9 represent the bandwidth blocking ratio (BBR) for both algorithms. The BBR takes into account that different requests need different bandwidths. Thus, BBR is computed as the quotient between the sum of the requested bandwidths ( $\gamma_{modified}$ ) associated with blocked requests and the sum of the requested bandwidths of all requests. Next, Fig. 10 and Fig. 11 show the energy required by network transponders for the transmission of a single bit. The energy consumption associated to the transmission through each core has been estimated by using the model by López *et al.* [79], considering the spectral resources employed in that core. Finally, Fig. 12 and Fig. 13 show the average delay of the longest distance sublightpath compared to that of the shortest distance path for both algorithms.

These metrics will be analyzed in more detail in the following subsection. At this point, our objective is to see the trade-off on blocking ratio vs other parameters when using different values of  $K$ . Increasing  $K$  leads to lower values of blocking ratio, but the energy consumption

per bit and the differential delay increase, when using either the EEMPR or the MPIRA algorithms. Our main goal is to minimize the blocking probability, and when going from  $K=5$  to  $K=7$ , there is no improvement on blocking probability (again, for both EEMPR and MPIRA). Therefore, in the following subsections we compare and analyze in detail the results for  $K=5$ .

Nevertheless, it should be noted that in some cases higher values of  $K$  may lead to increasing blocking rate for high traffic loads (as shown in Fig. 7 and 9). Higher values of  $K$  allow the use of additional, although typically longer, routes to establish connections. However, these longer routes require more network resources. Under low traffic loads, the availability of these additional routes can help prevent connection blocking by providing alternative paths that may not have been considered with lower  $K$ . This is feasible because sufficient resources remain available on other links, minimizing the impact on future incoming connections. However, under high traffic loads, where network resources are scarce, using longer routes may become counterproductive. The increased resource consumption of these paths can lead to a significant reduction in the network's ability to accommodate new connection requests, increasing the overall blocking probability in some cases.

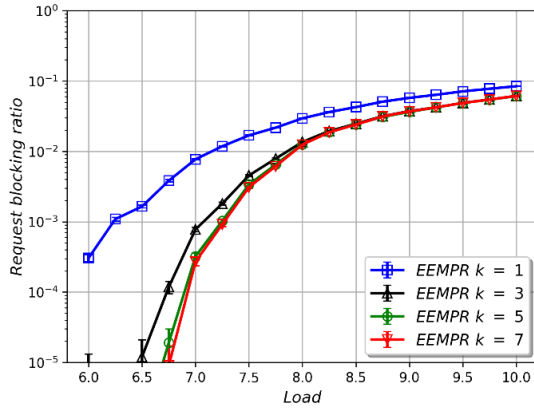


**Figure 6.** Request blocking rate of EEMPR in NSFNet at  $K=1, 3, 5, 7$

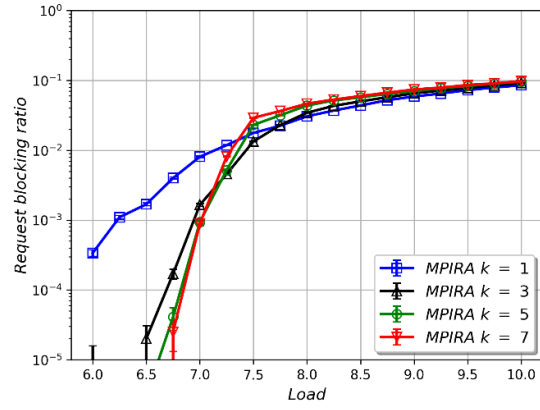


**Figure 7.** Request blocking rate of MPIRA in NSFNet at  $K=1, 3, 5, 7$

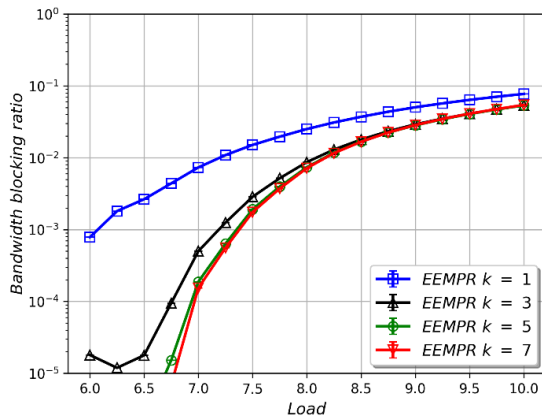


**Figure 8.** Bandwidth blocking rate of EEMPR in NSFNet at  $K=1, 3, 5, 7$

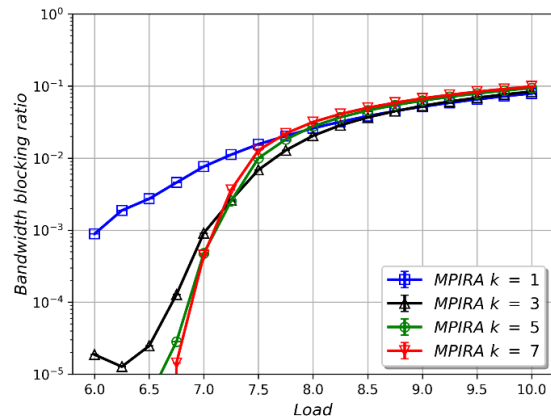


**Figure 9.** Bandwidth blocking rate of MPIRA in NSFNet at  $K=1, 3, 5, 7$

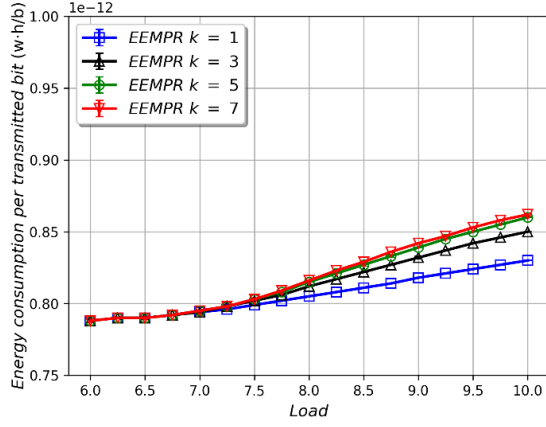


**Figure 10.** Energy consumption per transmitted bit of EEMPR in NSFNet at K=1, 3, 5, 7

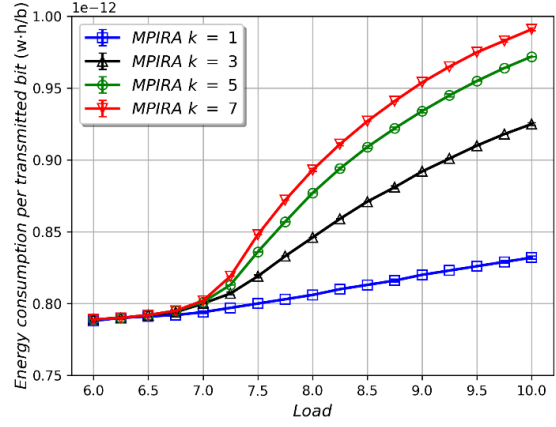


**Figure 11.** Energy consumption per transmitted bit of MPIRA in NSFNet at K=1, 3, 5, 7

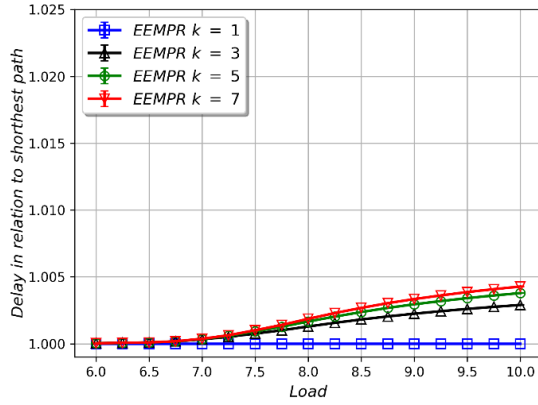


**Figure 12.** Delay relative to shortest path of EEMPR in NSFNet at K=1, 3, 5, 7

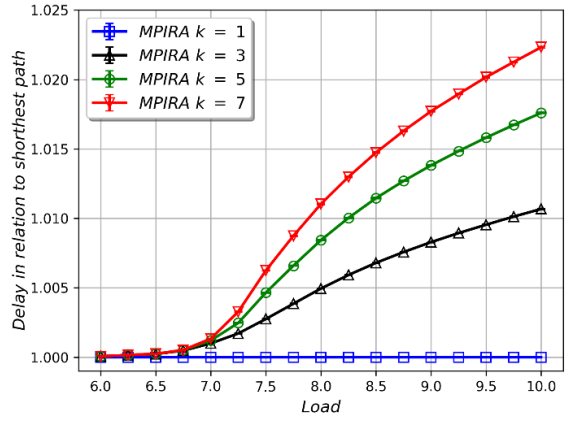


**Figure 13.** Delay relative to shortest path of MPIRA in NSFNet at K=1, 3, 5, 7

### 3.3.2 Comparison of EEMPR and MPIRA for K=5 Shortest Paths

We now focus on the K=5 case and plot the results for EEMPR and MPIRA in the same figures to facilitate comparison. First of all, Fig. 14 and Fig. 15 show the RBR and BBR, respectively, for different traffic loads. As it can be observed, EEMPR always obtains a lower blocking ratio than MPIRA, achieving approximately up to 50% reduction in RBR and BBR for a traffic load of 7.5.



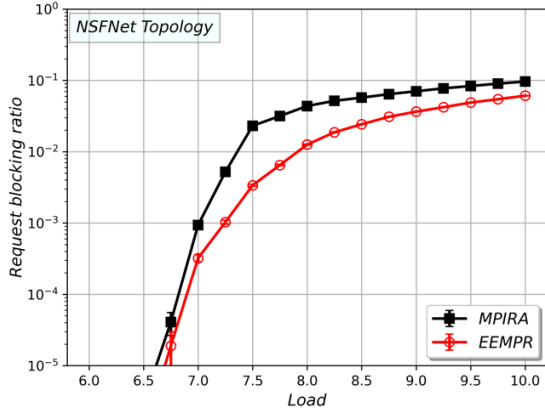


**Figure 14.** Request blocking ratio comparison in NSFNet topology at K=5.

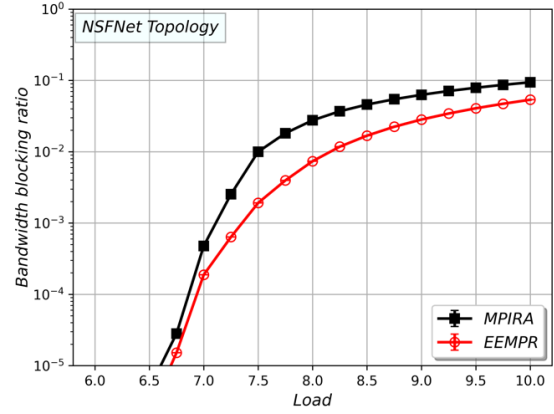


**Figure 15.** Bandwidth blocking ratio comparison in NSFNet topology at K=5.

Then, Fig. 16 shows the energy required by network transponders for the transmission of a single bit. As shown in Fig. 16, EEMPR leads to lower consumed energy per bit than MPIRA. This is mainly due to the fact that MPIRA typically requires a higher number of paths to satisfy a demand thereby leading to higher utilization of network transponders (especially at high loads). The savings in energy consumption per transmitted bit of EEMPR when compared with MPIRA are shown in Fig. 17. Employing only one single path to accommodate a connection request and only limiting the division of a demand just across the cores, like EEMPR does, leads to a decrease on the consumed energy per bit.

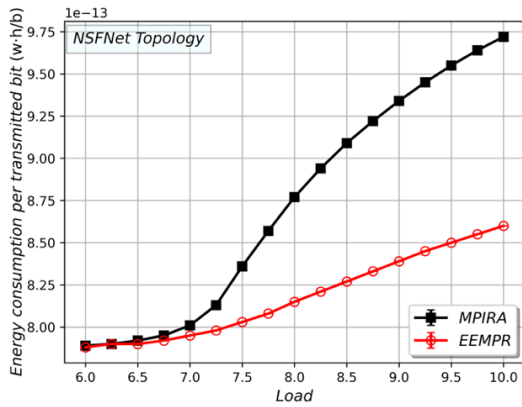


**Figure 16.** Energy consumption per transmitted bit comparison in NSFNet topology at K=5.

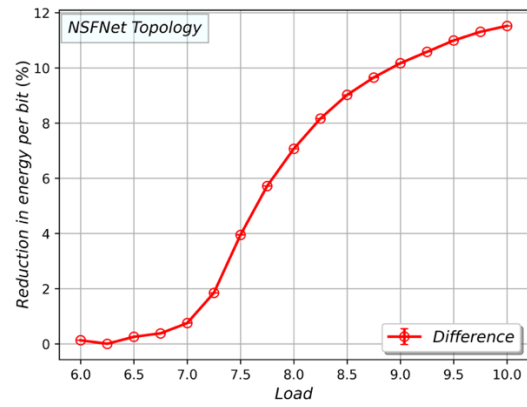


**Figure 17.** Reduction in energy per bit in NSFNet topology at K=5.

In multipath routing, a demand can be served by using several paths (sublightpaths). However, with EEMPR, the average number of sublightpaths required is much lower than with MPIRA, a reduction of more than 15% for a load of 7.5, as shown in Fig. 18. The reduction in number of sublightpaths, which is yielded by EEMPR leads to a more efficient use of transponders and spectrum as a lower number of guard-band slots are required.

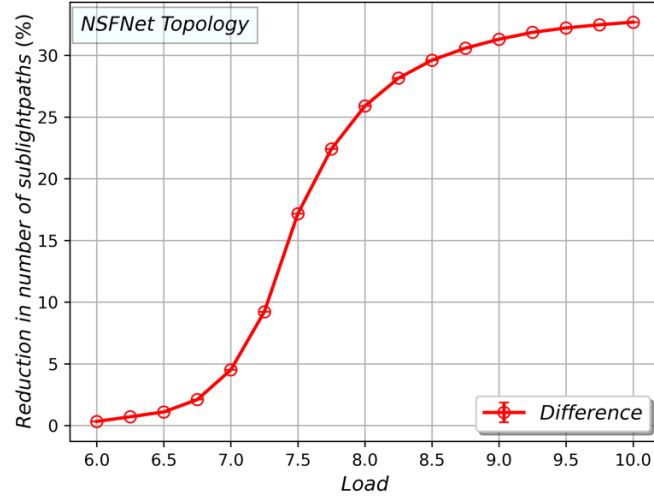


**Figure 18.** Reduction in number of sublightpaths in NSFNet topology at K=5.

A key advantage of EEMPR is that it removes the differential delay associated to transmission through different paths, since they all use the same route (just a different core). This fact is very important as a significant difference can cause the unneeded retransmission of packets and malfunctions (or inefficiencies) in the protocols of upper layers. Moreover, EEMPR also reduces the average delay in relation to the shortest distance path. The average delay of the longest distance sublightpath compared to that of the shortest distance path is shown in Fig. 19 for EEMPR and MPIRA, obtaining again better results with EEMPR.

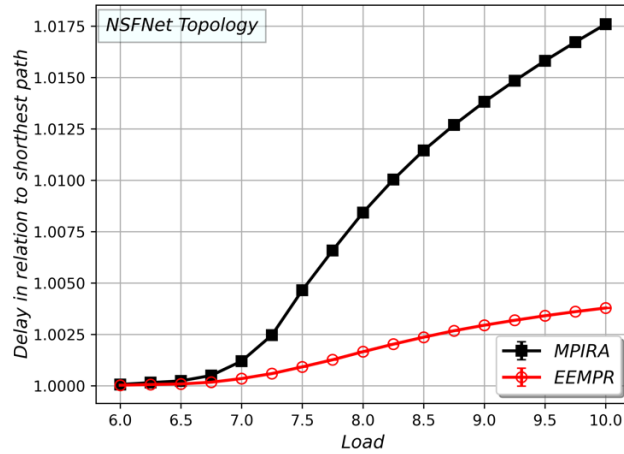
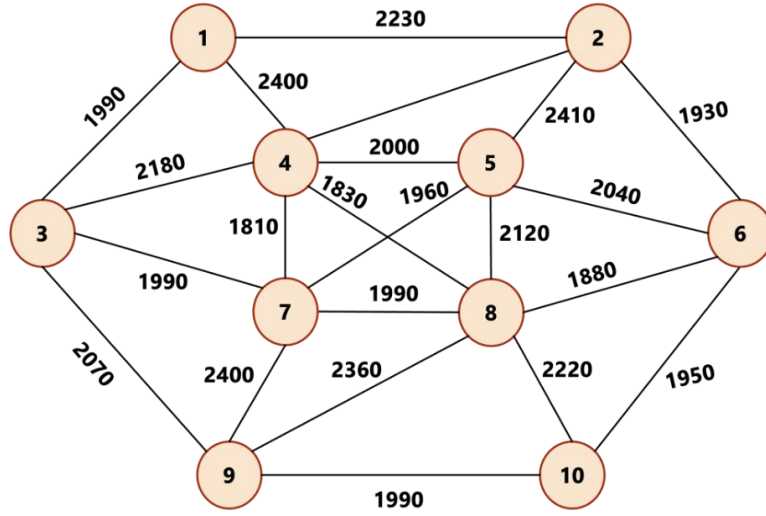


**Figure 19.** Delay in relation to shortest path comparison in NSFNet topology at K=5

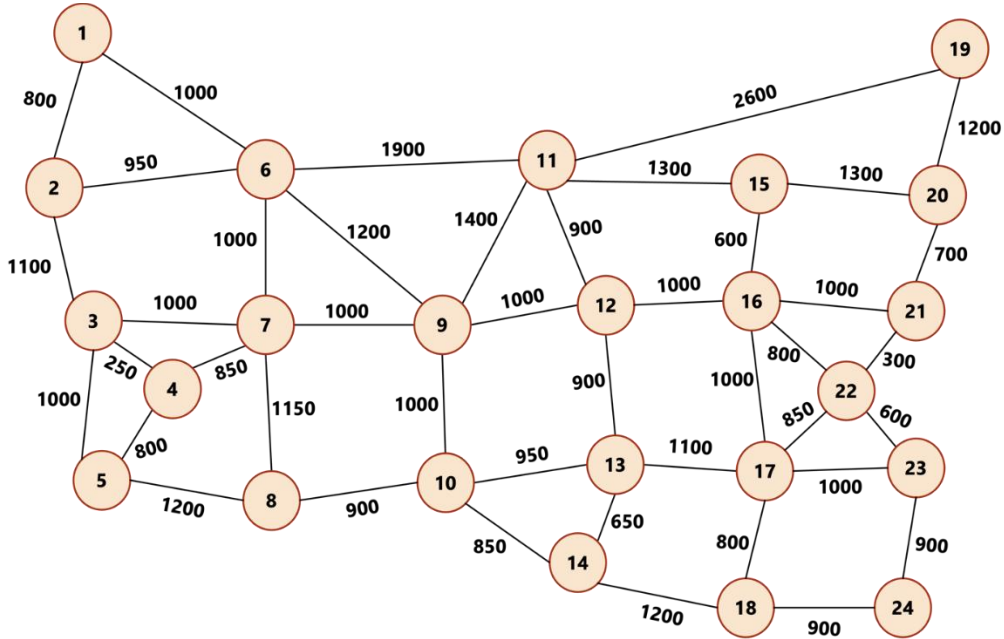
### 3.3.3 Analysis for Other Topologies

We have also analyzed the performance of EEMPR (compared with MPIRA) in four additional topologies: SmallNet [80], USNet [80], JPN12 [38] and Deutsche Telekom (DT) [81]. The

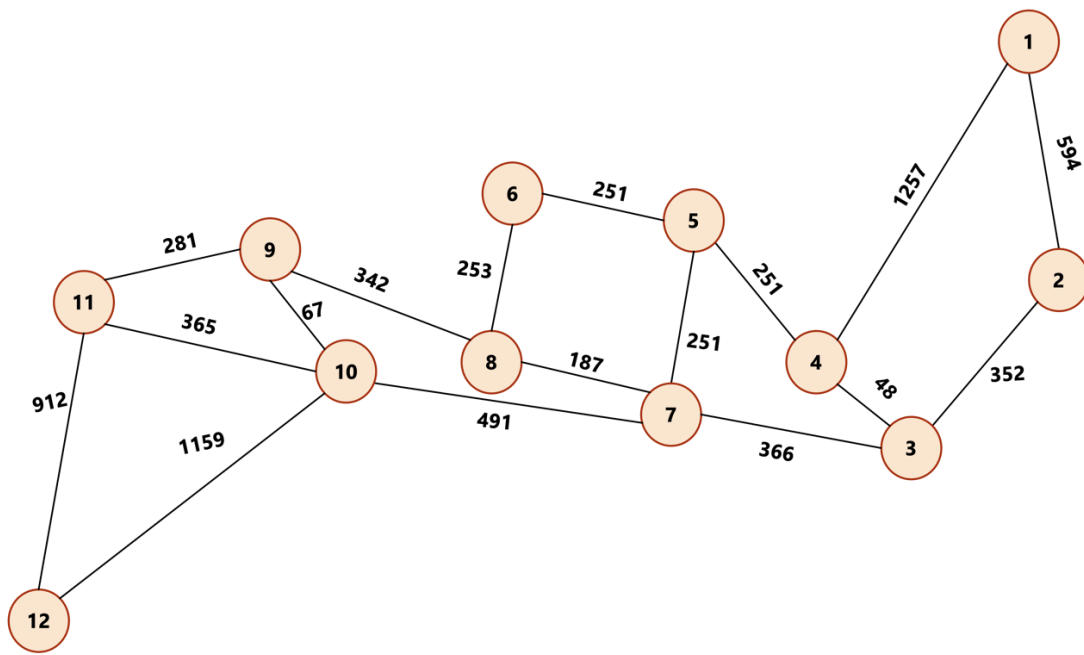
topologies are shown in Fig. 20, and their characteristics, together with those of the NSFNet, are shown in Table 3. The USNet topology has a higher number of nodes and links than the other topologies. Nevertheless, considering the length of the links, we can observe two distinct groups of topologies. The SmallNet, NSFNet and USNet topologies are characterized for having long links (around or higher than 1000 km), and thus the average length of the 5-shortest paths exceeds 4000 km for each of those networks. In contrast, the JPN12 and DT topologies have lower link distances (below 500 km), and the average length of the 5-shortest paths is less than 2000 km. Note that for paths with length lower than 2000 km, spectrally efficient modulation formats like 8QAM or 16QAM are employed (Table 1), while for paths exceeding 4000 km, BPSK must be used, which is more robust but less spectrally efficient. As we will show next, this feature has an impact on the results obtained.



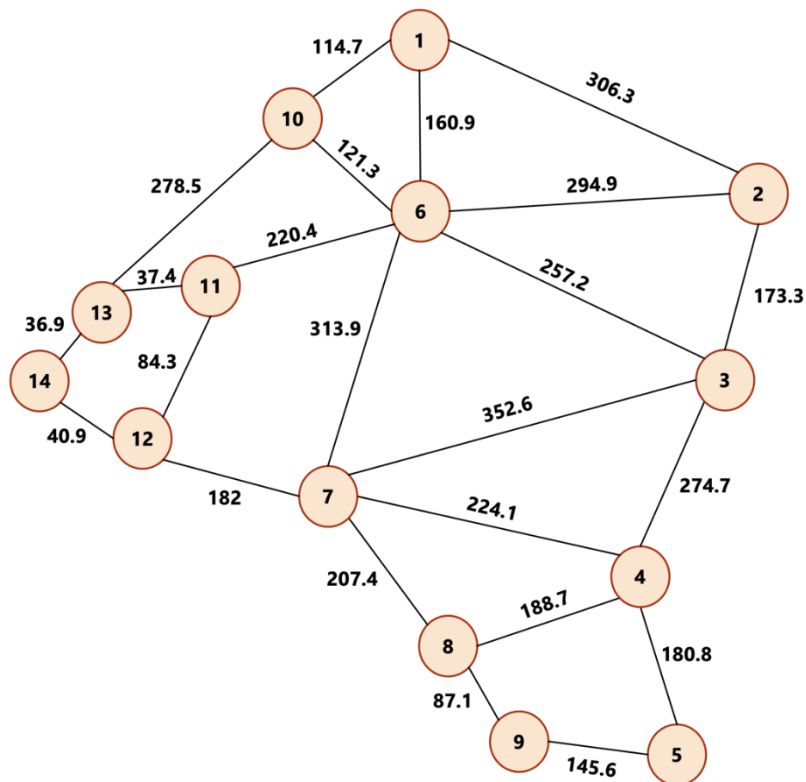
(a)



(b)



(c)



(d)

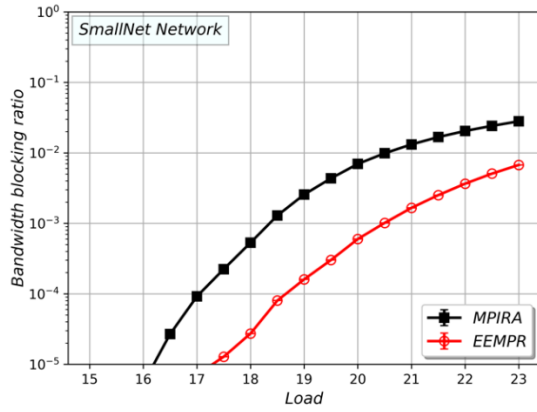
**Figure 20.** Network topologies (a) SmallNet [80], (b) USNet [80], (c) JPN12 [38], (d) DT [81] (distances in km).

**Table 3.** Characteristics of the five network topologies.

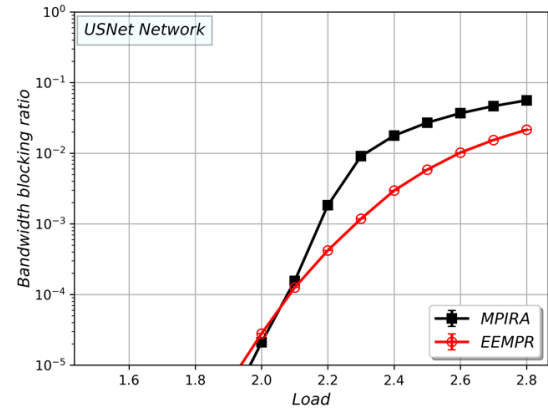
Topology	Number of nodes	Number of links	Avg. link length (km)	Min. length of the 5-shortest paths (km)	Avg. length of the 5-shortest paths (km)	Max. length of the 5-shortest paths (km)
SmallNet	10	22	2080.0	1810	5152.91	8820
NSFNet	14	21	1080.95	300	4341.09	9200
USNet	24	43	997.67	250	4012.13	8750
JPN12	12	17	436.88	48	1554.14	4003
DT	14	23	186.25	36.9	685.61	1379.6

First, the results for the topologies with long links, SmallNet and USNet, are shown in Fig. 21. The conclusions are similar to those obtained for the NSFNet (also a topology with long links). For most loads, EEMPR gets lower BBR than the baseline algorithm, MPIRA, and the reduction is particularly significant for the SmallNet topology. Moreover, EEMPR also reduces energy consumption, around 11% for SmallNet and 5% for USNet (considering the traffic loads leading to a BBR  $\sim 10^{-3}$ ) when compared with MPIRA, as well as the delay in relation to the shortest path.

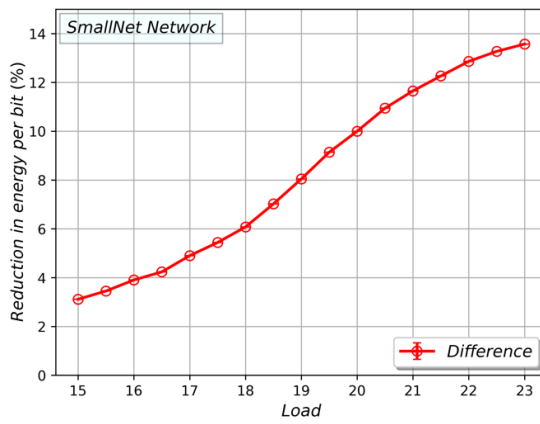
Then, the results for the topologies with shorter links, JPN12 and DT, are shown in Fig. 22. In this case, in contrast to the previous networks, the results are very similar for EEMPR and MPIRA, both in terms of BBR and energy consumption.



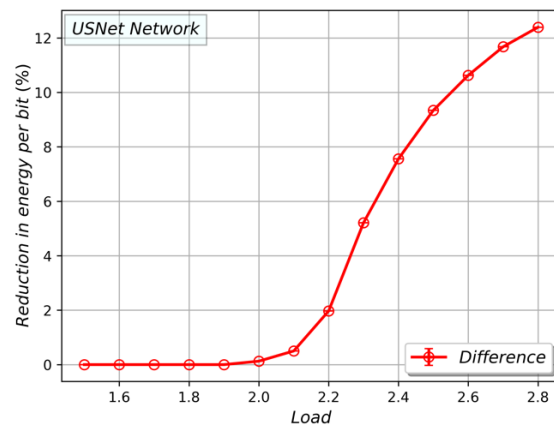
(a)



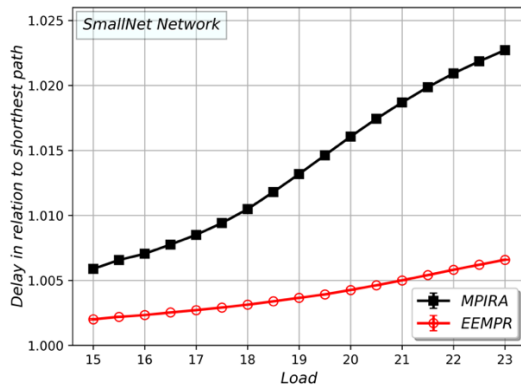
(b)



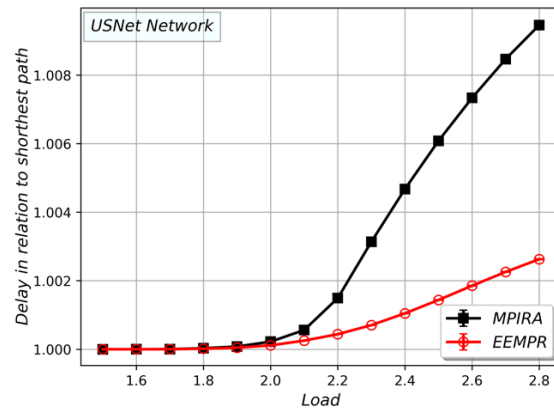
(c)



(d)



(e)



(f)

**Figure 21.** Analysis in the SmallNet (left column) and USNet (right column) topologies in terms of BBR (a and b), energy consumption (c and d) and delay in relation to shortest path (e and f).

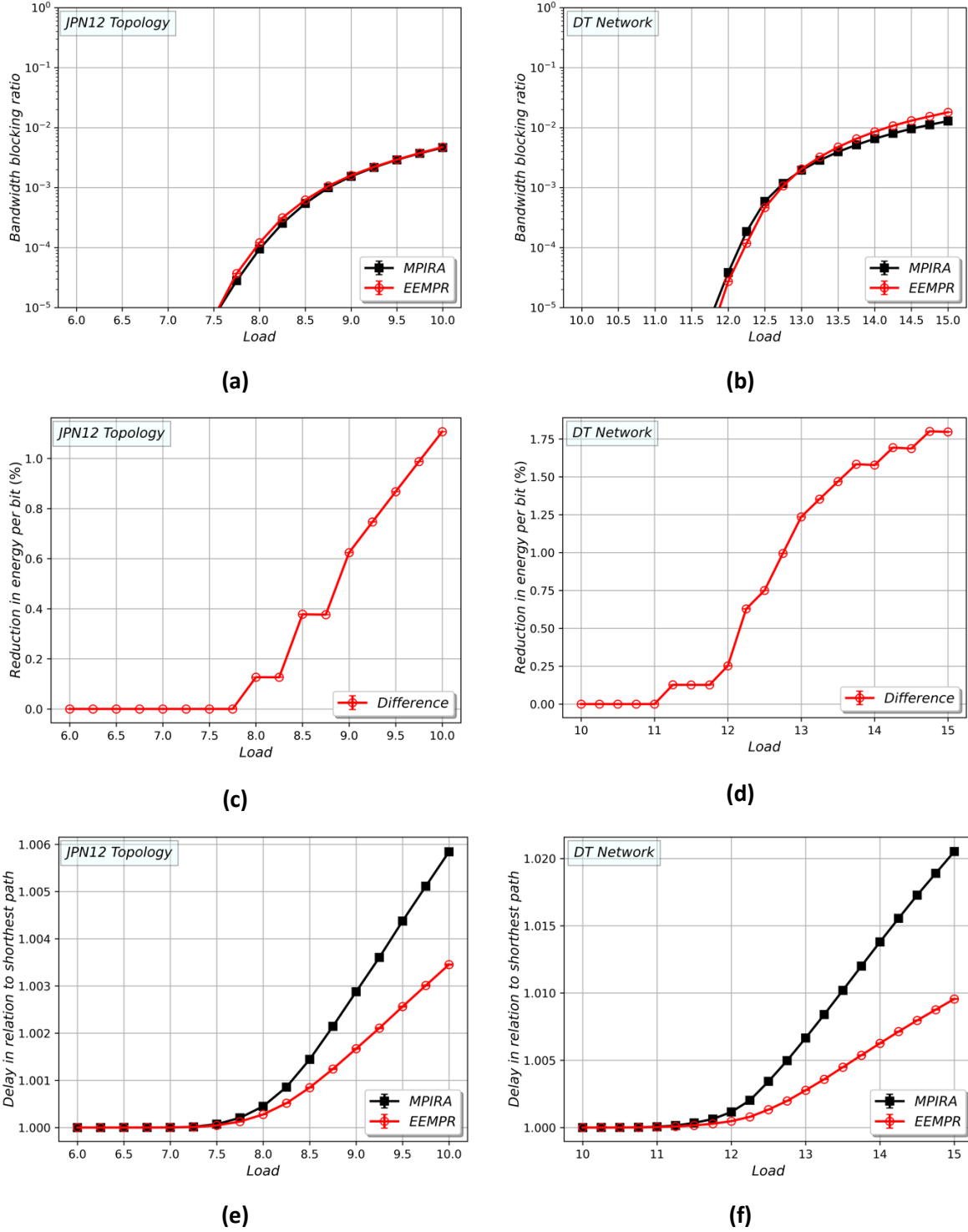


**Figure 22.** Analysis in the JPN12 (left column) and DT (right column) topologies in terms of BBR (a and b), energy consumption (c and d) and delay in relation to shortest path (e and f).

As shown in Table 3, SmallNet, NSFNet and USNet, have long links, and thus the length of the  $K$ -shortest paths is higher. In contrast, JPN12 and DT are smaller networks and thus have shorter  $K$ -shortest paths. Fig. 23 and Fig. 24 show the histogram of the length of the paths for

these five networks for  $K=5$ . The histograms also represent the modulation format associated with those paths, based on the limitations shown in Table 1.

In networks with long links, BPSK must be used for a considerable number of paths, resulting in increased bandwidth requirements (a higher number of spectral slots) to achieve a specific data rate. In contrast, for networks with short links, most connections can be established with 16QAM and 8QAM, so they require less bandwidth (and thus a lower number of spectral slots) to achieve a specific data rate. EEMPR is more efficient when dealing with requests demanding a high number of spectral slots than MPIRA and for that reason, EEMPR outperforms MPIRA in networks with long links. This is due to the fact that MPIRA has more constraints when searching for ‘rectangles’ in cores and frequency slots for resource allocation [52], while EEMPR operates with more freedom. This translates in EEMPR requiring a lower number of sublightpaths to serve the requests, which brings advantages in terms of energy consumption, and also in terms of requiring a lower number of guard-bands (and so additional spectral savings). The reduction in the number of sublightpaths is shown in Fig. 25. For instance, focusing on the traffic load for which the BBR is around  $10^{-3}$ , EEMPR, compared with MPIRA, reduces the number of sublightpaths in around 22% for USNet, 12% for NSFNet and 35% for SmallNet (i.e., in the networks with long links), and around 2% for JPN and 6% for DT (i.e., in the networks with short links).

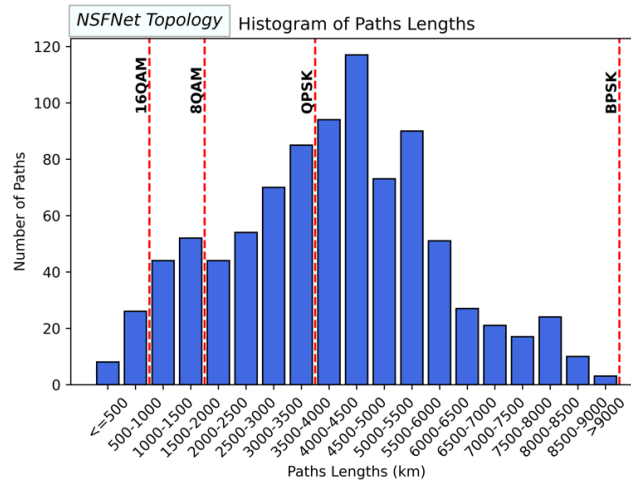


**Figure 23.** Histograms of the 5-shortest paths lengths for the NSFNet.



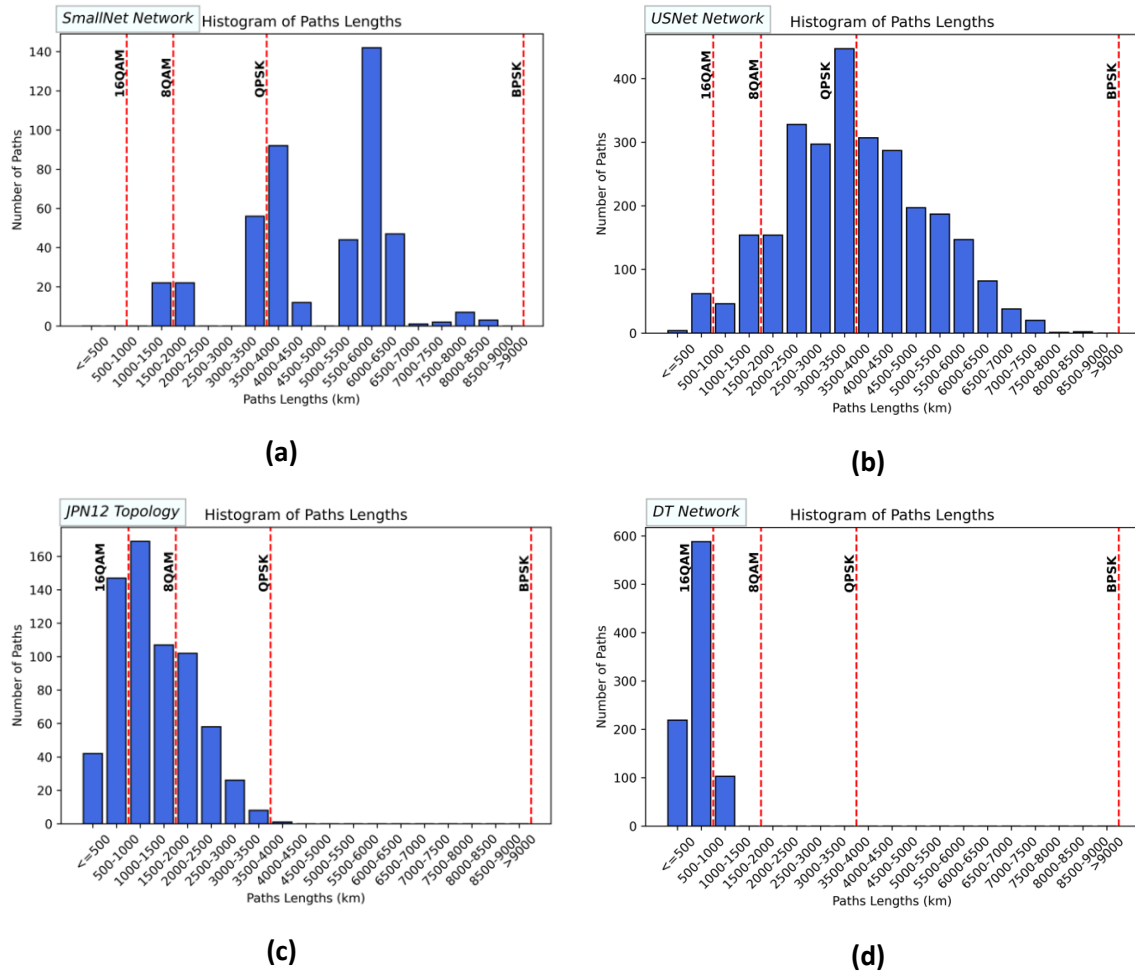


**Figure 24.** Histograms of the 5-shortest paths lengths for (a) SmallNet, (b) USNet, (c) JPN12 and (d) DT.

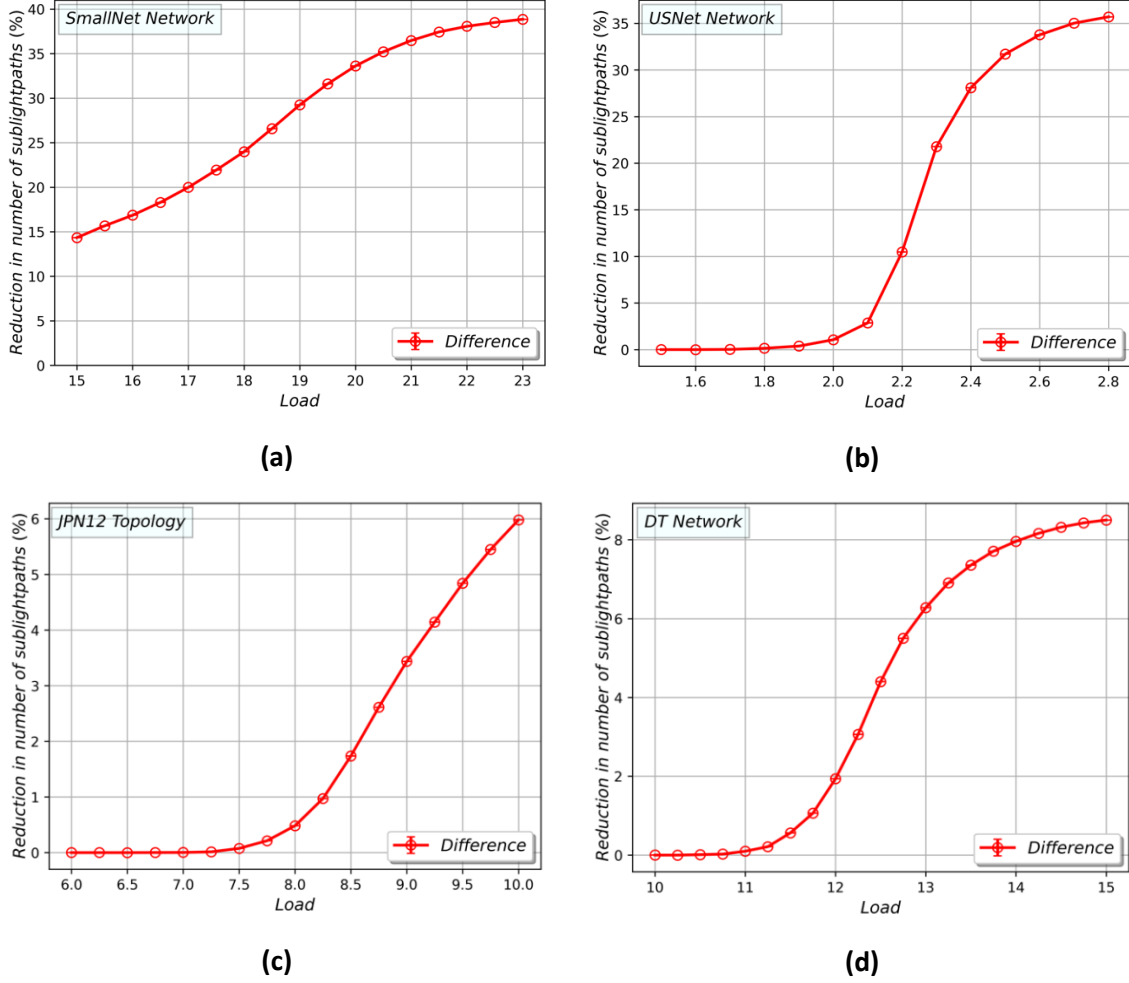


**Figure 25.** Reduction in the number of sublightpaths for (a) SmallNet, (b) USNet, (c) JPN12 and (d) DT.

As a conclusion, EEMPR is as efficient as MPIRA in networks with short links (typically national networks), while it clearly outperforms in networks with long links (large countries, continental and inter-continental networks).

### 3.4 Conclusions

In this chapter, we have proposed a new dynamic multipath routing, space, and spectrum assignment algorithm for SDM-EONs. It has been designed with the aim of decreasing blocking ratio and energy consumption, as well as setting the differential delay parameter arising in multipath strategies to zero. Since the appearance of inter-core crosstalk (XT) in SDM systems decreases the signal quality, the proposed method also checks that the accumulated XT does not exceed certain thresholds to validate the connection establishment. In case there are not enough resources to satisfy the demand with a single lightpath, the demand will be split, using the minimum number of cores as possible. Keeping the number of generated sublightpaths low is essential to prevent the use of many BVTs, and thus improving energy efficiency. The simulation study has been conducted considering different network topologies with different link distances. We have demonstrated that in network topologies with long links (like large

countries, continental or inter-continental networks), our proposal outperforms another proposal from the literature in both blocking ratio and energy consumption. Moreover, our proposal keeps the delay closer to that of the shortest path, and hence, it clearly improves network performance.



## Chapter 4.

### Efficient Migration from the C-band to C+L bands

As previously mentioned, one of the main problems with the SDM implementation via MFT is related to the availability of fibers. Even for incumbent operators, the number of unused fibers is scarce. Increasing the number of fibers could require civil work, which is slow and CAPEX demanding, or leasing dark fibers from an infrastructure operator. Therefore, the exploitation of the full potential capacity of the already deployed fibers is the main motivation for proposing MB-EONs as the future technological choice.

Despite the advantages offered by MB-EON, the high cost of the components required to upgrade a network to C+L-band optical line systems leads network operators to postpone the deployment of a complete upgrade and to adopt a partial migration strategy instead. In this way, it is necessary to identify which fibers (and associated equipment) should be migrated first. Therefore, in this chapter, we focus on the partial migration of EONs. A set of methods is proposed to identify a limited subset of fibers that should be upgraded within the network. The goal of this upgrade is to optimize dynamic performance, particularly by reducing the blocking probability during the process of dynamically establishing and releasing optical connections.

The rest of the chapter is organized as follows. First, in Section 4.1, we propose a basic heuristic algorithm to perform a partial upgrade of conventional EONs to C+L multi-band optical networks. Then, in Section 4.2, an integer linear programming (ILP) formulation is presented to identify which fibers should be upgraded to exploit C+L bands, subject to a constraint on the maximum number of fibers that can be upgraded. In Section 4.3, three heuristic algorithms, each pursuing a different objective, and two of them based on an ILP formulation, are proposed to determine which fibers to upgrade while adhering to a limit on the maximum number of EDFAs that can be upgraded. Finally, in Section 4.4, we analyze which type of transceivers should be acquired during the network migration from the C-band to C+L bands.

The proposals and simulation results presented in this chapter have been published in [82], [83], [84], [85].

#### 4.1 A Heuristic for the Partial Migration of EONs to C+L Bands

In this section, we propose a basic planning strategy to decide the set of the fibers to be upgraded with C+L amplifiers, and complement it with an algorithm (with two versions) to solve the dynamic RMLBSA problem and thus serve on-demand incoming connection requests.

The procedure of the proposed planning heuristic for the partial migration of a network is described as a pseudocode in Algorithm 2.

**Algorithm 2: Partial Migration**

**Given:** Physical network topology  $\mathcal{G} = (\mathcal{N}, \mathcal{E})$   
 Set of  $K$ -shortest hop paths for each  $s$ - $d$  pair

**Output:** Set of fibers to upgrade to L-band,  $F_{\text{upgrade}}$

```

0 fiber_usage_count = 0 # initialize fiber_usage_count
1 for each  $s$ - $d$  pair:
2   path = primary shortest_paths[ $s$ ][ $d$ ]
3   for each fiber in path:
4     increment_fiber_usage_count(fiber_usage_count, fiber)
5   end for
6 end for
7 prioritized_fibers = sort the optical fibers based on their usage.
8  $F_{\text{upgrade}}$  = prioritized_fibers

```

In the phase of network planning, firstly, we compute the shortest paths between each source-destination pair. Based on these pre-calculated shortest paths in terms of the number of the hops, the optical fibers are prioritized for band upgrade depending on the number of times that they might be utilized to establish a lightpath between each source-destination pair. Accordingly, whenever the network operator desires to improve the capacity of the network through the exploitation of other spectral bands, optical fibers are slowly migrated to C+L band based on their priority. In other words, the network operator provides the multi-band devices for those fibers which are more exposed to congestion.

The time complexity of Algorithm 2 is  $O(N^2H + F \log F)$ . Based on the given network topology, there are  $N$  nodes in the network. If it is assumed that the maximum number of hops corresponding to the paths between the  $s$ - $d$  pairs is  $H$ , the ‘for’ loops of the algorithm (lines 1-6) runs  $N^2H$  times. With the assumption of having  $F$  fibers within a network, sorting the fibers has a complexity of  $O(F \log F)$ . Therefore, the complexity of the algorithm would be  $O(N^2H) + O(F \log F)$ , which is equal to  $O(N^2H + F \log F)$ .

Later, we will analyze the impact of upgrading different numbers of fibers following the policy we have just explained.

Once the network has been upgraded, when a connection establishment request is received, the RBMLSA algorithm is executed. For addressing the routing problem, the  $K$ -shortest paths algorithm is used, and we consider two approaches: length-based and hop-based routing.

In the length-based approach, when a connection request arrives at the network, the algorithm searches through its potential paths, and the path with the minimum length ( $l$ ) in km is selected. Any other potential paths whose length is equal to  $l$  will be stored in a data structure. If all of the links of the selected path are equipped with multi-band devices (i.e., the L-band is lit up), in the phase of band selection, the priority will be given to the L-band. On the other hand, if at least one of the links only supports the C-band, for ensuring the continuity constraint of resource allocation (i.e., the same block of frequency slots should be assigned in all the links that a lightpath goes through), the C-band should be used. However, instead of doing this directly, it

is first checked whether any of the other stored paths (all of  $l$  length) could use the L-band. This process will be repeated while investigating any of the paths returned by the  $K$ -shortest paths algorithm to take the full advantage of the L-band of the upgraded fibers. Although getting several potential paths with equal distance when running the  $K$ -shortest paths algorithm does not occur frequently, this procedure leads to improve the blocking ratio.

On the other hand, many times the  $K$ -shortest path, when executed in terms of hops, retrieves several paths with the same number of hops. Therefore, applying the hop-based algorithm brings about better results in terms of blocking probability. In the hop-based resource allocation method, among different paths with the same number of hops, the path with the ability of utilizing the L-band would be prioritized.

#### 4.1.1 Simulation Setup

We employ the separate amplifiers architecture (Fig. 2) for the implementation of C+L band networks. In the simulation, we assume that the 400 GHz required guard-band while using this architecture is deducted from the beginning of the L-band spectrum. We also consider that the spectrum is divided into 12.5 GHz FSs. Thus, the C-band consists of 320 slots, while the L-band, after the guard band allocation, consists of 516 FSs. We evaluate the network performance assuming that the network operates in an online environment. In this way, the arrival of connection requests is modeled as a Poisson process with arrival rate ( $\lambda$ ). The holding time of each connection is modeled by an exponential distribution with an average of  $T$ . In case that a connection request is successfully established, it will be released after an exponentially distributed time. The source and the destination for the incoming connection requests are randomly chosen from a uniform distribution. It should be noted that no metrics are retrieved for the first  $10^4$  connection requests, as they are used for warming up the network simulator. Then, data gathering is done for the following  $10^5$  connection requests. The main metrics that we consider are the request blocking ratio (RBR) and the bandwidth-blocking ratio (BBR). The division of the blocked connections to the total incoming connections indicates the RBR. The BBR is computed by dividing the total number of blocked FSs by the number of total requested slots throughout the simulation.

The efficient utilization of spectrum allocation is met by considering three different levels of modulation, namely BPSK, QPSK, and 16QAM. Table 4 [86] shows the maximum optical reach for 16QAM and QPSK modulation formats, depending on the selected spectral band. For instance, if the length of a lightpath over the L-band is lower than 330 km, the 16QAM modulation format would be used (enabling the transmission of 4 bits per symbol). Alternatively, if the length of the lightpath is higher than 330 km and lower than 1600 km, the QPSK modulation format (2 bits per symbol) would be selected. Otherwise, the BPSK modulation format should be employed (1 bit per symbol). Assuming the BPSK modulation format, the demanded FSs for each connection range from 1 to 24 slots, which is translated to a spectrum request range from 12.5 GHz to 300 GHz. When the BPSK modulation format is used, every slot holds the capacity of 12.5 Gb/s. This value transforms to 25 Gb/s and 50 Gb/s for the QPSK and 16QAM modulation formats, respectively. Since 16QAM encodes more bits per symbol than the QPSK modulation format, it achieves higher spectral efficiency, offering higher data rates per unit of spectrum. This makes 16QAM preferred over QPSK. However,

this advantage comes at a cost, as it requires a shorter transmission distance to maintain the quality of the lightpath.

**Table 4.** Maximum Optical Reach for Each Spectral Band in C+L Line Systems [86].

Modulation Level	Multiband Optical Reach (km)	
	<i>C-band</i>	<i>L-band</i>
QPSK	1800	1600
16QAM	370	330

As the data rates demanded by different incoming connection requests are different, we employ a normalized version of the classic definition of the traffic load (or offered load) in erlangs ( $\lambda T$ ). The normalized traffic load is previously discussed (see Section 3.3) and is calculated using Equation (4) [78].

When a connection request enters the implemented C+L multiband optical network, the RBMLSA algorithm is employed. The routing problem between a pair of source and destination is solved following the execution of the  $K$ -shortest paths algorithm. This execution is performed based on the length-based approach in which a potential path with the shortest distance is prioritized. Then, the first path of the list is selected, and it is checked if it has available resources over the L-band fulfilling the spectrum continuity and spectrum contiguity constraints. If that is the case, the lightpath is established using that route and those L-band spectral resources. Otherwise, the availability of resources in the C-band of that path is assessed. If there are no resources, then the following paths of the list are considered, evaluating for each one of them the availability of resources in the L-band first and then in the C-band. If no resources are available for any of the paths in the list, the connection is blocked. In summary, if all the fibers of the selected path for the connection have been upgraded, the L-band is prioritized over the C-band. Otherwise, due to the spectrum continuity constraint, the connection is restricted to use the C-band.

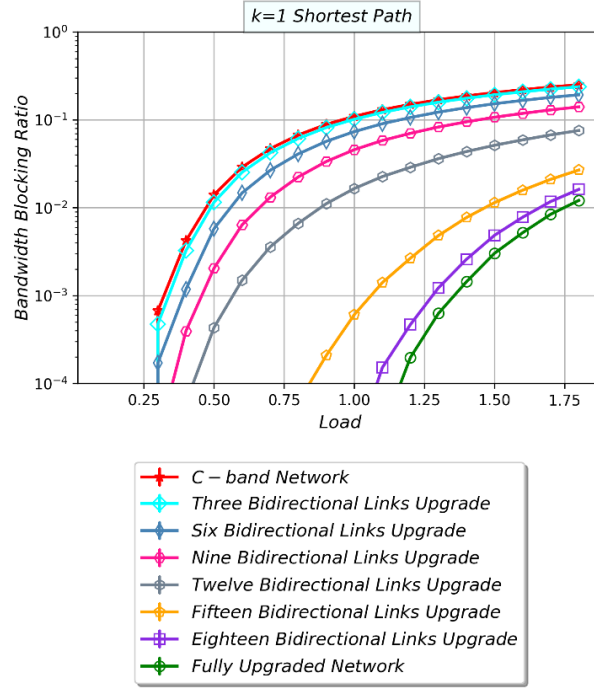
During the spectrum allocation phase, the Best-Fit policy [23], [24] is used for spectrum allocation. When using this policy, the entire spectral band under consideration (L- or C-band) is checked, and the set of contiguous unoccupied frequency slots whose size best matches the bandwidth required by the connection is assigned.

#### 4.1.2 Simulation Results

The analysis of the proposed heuristic has been conducted in the NSFNet topology, with 14 nodes and 21 bidirectional links. Fig. 26 shows the BBR versus traffic load with different number of links upgraded: from the current C-band elastic network to the fully upgraded one. The selection of the links to be upgraded follows the planning heuristic described in Section 4.1. Then, the RBMLSA problem is solved using the heuristic of Section 4.1 using  $K = 1$  shortest path in terms of distance. When using only one path, it is important to select the shortest



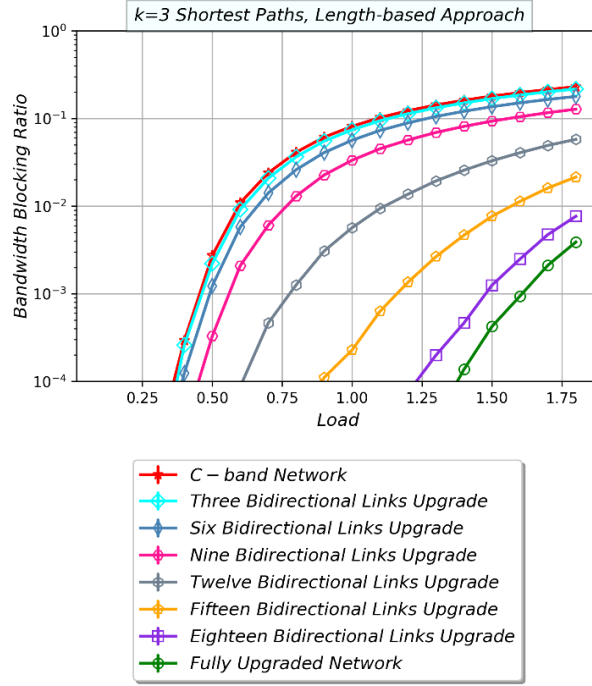
one in length to use the best modulation level as possible and reduce the number of slots required to establish the connections.



**Figure 26.** Bandwidth blocking ratio depending on the network load.  
Shortest path ( $K=1$ ) is used as routing strategy.

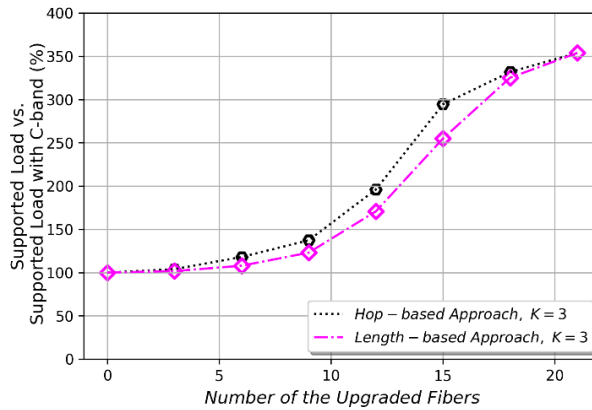
Fig. 26 shows that the BBR is reduced as the number of upgraded links increases. In fact, supposing  $10^{-3}$  as an acceptable value of BBR, the fully migrated network can transport more than 400% of the traffic of the initial C-band network. Note that the ratio in the available bandwidth of the C+L network compared with the C-band option is 262%. It is also possible to see that when up to 9 bidirectional links are upgraded (43% of the total), the network achieves a good reduction of the BBR and huge reduction is achieved from this point. Upgrading 12 fibers, the BBR is reduced more than one order of magnitude and the maximum load supported by the network (with  $BBR < 10^{-3}$ ) is double of the C-band network.

Fig. 27 exhibits the simulation results of the length-based RBMLSA strategy in terms of BBR using  $K = 3$ . As it can be observed in Fig. 27, the improvement in the BBR compared with C-band network is even higher. Therefore, by upgrading 12 bidirectional links it is possible to reduce the BBR in almost two orders of magnitude.



**Figure 27.** Bandwidth blocking ratio of length-based RBMLSA depending on the network load.  $K$  in  $K$  shortest paths algorithm is set to 3.

Fig. 28 summarizes the previous results and compares the two approaches for solving the RBMLSA problem: hop-based and length-based when  $K$  is set to 3. It represents the load increment with an acceptable value of BBR ( $BBR < 10^{-3}$ ) with different number of upgraded fibers. As can be seen in Fig. 28, the improvement is more noticeable from the upgrading of 9 fibers. However, a good increment of the load supported by the network can be obtained without upgrading all the fibers of the network. Moreover, the heuristic based on hops exploits better the L-band and it achieves better results than the one based on length when only a subset of fibers are upgraded. This is an important conclusion as most of proposals to solve RBMLSA problem when considering C-band or fully migrated networks use distances as it allows to use the best modulation format as possible. However, as shown in Fig. 28, it is better to use the hop-based approach.



**Figure 28.** Supported load with different number of upgraded fibers respect to employing only C-band.

### 4.1.3 Conclusions

In Section 4.1, we have evaluated the migration of the current EONs using C-band to multiband optical networks using C+L bands. One planning strategy was proposed to determine which fibers should be upgraded (upgrade in the amplifiers). Then, it is combined with two heuristics to solve the RBMLSA problem during network operation. The simulation study performed shows that networks will support more traffic thanks to the use of C+L multiband networks. However, it is not necessary to upgrade all the fibers to achieve a good increment in the supported traffic load. Therefore, finding a trade-off between the number of upgraded fibers and a satisfactory blocking ratio is important. Finally, the proposed heuristic to solve the RBMLSA problem based on hops leads to better results than using the shortest length paths when the network is not fully migrated.

## 4.2 An ILP Formulation for the Partial Migration of EON to C+L Bands

In Section 4.1, in order to determine which links should be upgraded from the C to the C+L-bands, we proposed a heuristic. However, since the main objective in Section 4.1, was to analyze the potential advantages of a partial upgrade of the network, the quality of the proposed heuristic was not analyzed in detail nor compared with other options.

Therefore, in this section, we extend that proposal by proposing an ILP formulation which determines the set of fibers that should be upgraded to the C+L-band line system. In this proposal, the spectrum continuity constraint is imposed and, therefore, each optical connection (or lightpath) should use the same slice of the spectrum in all the fibers of the path from the source to the destination node. Hence, an optical connection can be established using L-band spectral resources only if all the fibers traversed by that connection have been upgraded. Therefore, the aim of the ILP formulation is to determine which fibers should be upgraded so that the number of precomputed paths (used by the connections) that can benefit from the upgrade is maximized. However, maximizing the number of paths that can benefit from the upgrade (which is the metric that optimizes the formulation) does not necessarily translate into a minimization of the blocking ratio when the network operates dynamically. Therefore, the ILP formulation should be considered as an alternative (although more informed and better) heuristic for network migration, and not as an optimal method in terms of blocking probability reduction. Note that we are trying to get good dynamic operation by means of a good network planning. Thus, the performance in terms of blocking probability of the migration proposal obtained when solving the ILP formulation, and when using the heuristic proposed in Section 4.1, will be compared using three different geographically located network topologies, the North-American NSFNet [77], the Japanese JPN12 [38], and the European DT network [81].

### 4.2.1 Objective of the ILP Formulation

The objective of the formulation is to determine which links should be upgraded with the aim of maximizing the number of those precomputed  $s$ - $d$  paths that can benefit from the upgrade. Note that this approach is equivalent to minimizing the number of precomputed  $s$ - $d$  paths that cannot benefit from the upgrade.

### 4.2.2 Inputs for the ILP Formulation

The formulation takes as inputs the network topology, the maximum number of fibers that the network operator desires to upgrade, and a set of precomputed paths for each source-destination ( $s$ - $d$ ) pair of nodes in the network (which will be used for establishing dynamic optical connections when operating the network).

The first input for the ILP formulation is the network topology to be partially upgraded, which is represented by a connected graph  $G = (V, E)$ , where  $V$  denotes the set of nodes and  $E$  the set of bidirectional links. Then, the  $K$  shortest paths are precomputed between each source-destination ( $s$ - $d$ ) pair of nodes in the network. These  $K$  shortest paths will be eventually used for establishing end-to-end optical connections, so we focus our attention on them. In order to represent these precomputed paths, the binary variables  $r_{ij}^{sdk}$  are introduced. If the precomputed path  $k$  from node  $s$  to  $d$  traverses fiber  $(i, j)$ , then  $r_{ij}^{sdk}$  is set to 1, being 0 otherwise. On the other hand, let  $w_{ij}$  denote the number of times that fiber  $(i, j)$  is used in the first pre-calculated shortest paths (i.e.,  $k = 1$ ) of all  $s$ - $d$  pairs, that is,

$$w_{ij} = \sum_{sd} r_{ij}^{sd1}, \quad \forall i \in V, \forall j \in V \quad (5)$$

Moreover, let  $F$  denote the maximum number of unidirectional fibers that the network operator wants to upgrade by equipping them with multi-band devices. Finally, we also introduce a big constant in the formulation,  $U$ , which represents an upper bound on the length of the network paths, i.e., a number at least equal to the number of unidirectional fibers in the topology (or higher), and  $M$ , a very small constant. Additionally, a set of constants ( $\alpha_k$ ) are introduced as positive weighting factors in the objective function, but their meaning will be explained later, when the objective function is described.

### 4.2.3 Decision Variables

The output of the ILP formulation, i.e., the decision variables are as follows:

- $f_{ij}$  are the main variables to be found, as they indicate whether a fiber should be upgraded or not by equipping it with multi-band devices. Thus,  $f_{ij}$  is a binary variable which will be 1 if the fiber  $(i, j)$  is equipped with multiband devices; otherwise, it will be 0.
- $\Delta^{sdk}$  is an auxiliary variable which represents the number of fibers in the precomputed path  $k$  between nodes  $s$  and  $d$  which have not been upgraded. Thus, it is an integer number (0 or positive). The value 0 means that all fibers in the precomputed path  $k$  between nodes  $(s, d)$  have been upgraded, and therefore the end-to-end path (and thus connections using that path) can benefit from L-band resources. In contrast, a higher number means that end-to-end connections using that path cannot benefit from the L-band (since at least one of the fibers has not been upgraded) and thus must employ the C-band (to comply with the spectrum continuity constraint).

- $\delta^{sdk}$  is another auxiliary variable. It is a clipped version of  $\Delta^{sdk}$  becoming a binary variable. The value 0 means (as before) that all fibers in precomputed path  $k$  between  $(s, d)$  have been upgraded with multi-band devices, and 1 otherwise. If it is 0, the precomputed path can benefit from the upgrade. Otherwise, it cannot.

#### 4.2.4 ILP Formulation

The ILP formulation to determine the set of fibers that should be upgraded is as follows:

*minimize*

$$\sum_{sdk} \alpha_k \delta^{sdk} - M \cdot \sum_{ij} w_{ij} f_{ij} \quad (6)$$

*subject to:*

$$\sum_{ij} f_{ij} \leq F \quad (7)$$

$$f_{ij} = f_{ji}, \quad \forall i \in V, \forall j \in V \quad (8)$$

$$\Delta^{sdk} = \sum_{ij} r_{ij}^{sdk} - \sum_{ij} r_{ij}^{sdk} f_{ij}, \quad \forall s, d \in V, \forall k \in K \quad (9)$$

$$\Delta^{sdk} \leq U \delta^{sdk}, \quad \forall s \in V, \forall d \in V, \forall k \in K \quad (10)$$

$$f_{ij} \in \{0, 1\} \quad (11)$$

$$\delta^{sdk} \in \{0, 1\} \quad (12)$$

We will start by explaining the constraints, and finally the objective function. Equation (7) guarantees that the number of fibers to be upgraded does not exceed the maximum number of fibers that the network operator wants to equip with multi-band devices. Equation (8) forces the simultaneous upgrade of the fibers composing a link. That is, whenever the fiber  $(i, j)$  is upgraded to C+L bands, the fiber  $(j, i)$  must also be upgraded. Then, Equation (9) defines the auxiliary variable  $\Delta^{sdk}$ , which computes the number of fibers that are not equipped with multiband devices over the precomputed path  $k$  between nodes  $s$  and  $d$ . Note that the first term in the right-hand side of that equation is the length in hops of the path  $k$  between  $(s, d)$ . The second term is the number of fibers of that path that have been upgraded, so the difference (i.e.,

the value of  $\Delta^{sdk}$ ) is the number of fibers of the path which have not been upgraded. Equation (10) determines the value of  $\delta^{sdk}$  (a clipped, binary version of  $\Delta^{sdk}$ ). Since  $U$  is a big positive constant, note that if  $\Delta^{sdk}$  is higher than 0, constraint (10) forces the binary variable  $\delta^{sdk}$  to be set to 1. If  $\Delta^{sdk}$  is 0,  $\delta^{sdk}$  could be either 0 or 1. However, when considering how the objective function is set in Equation (6), the value 0 will be preferred, as it leads to minimizing the objective function. In sum,  $\delta^{sdk}$  works as a clipped (binary) version of  $\Delta^{sdk}$ . Finally, constraints (11) and (12) set the binary nature of  $f_{ij}$  and  $\delta^{sdk}$  variables.

The objective function is defined by Equation (6). The aim is to minimize the number of precomputed paths that cannot benefit from the upgrade in the links. As we have just described,  $\delta^{sdk}$  is 1 when path  $k$  between nodes  $s$  and  $d$  cannot benefit from the upgrade (and 0 otherwise), so adding these variables constitute the objective function. The  $\alpha_k$  in the equation are weighting factors (constants) set to values between 0 and 1, to model the relevance of the primary paths ( $k = 1$ ), secondary paths ( $k = 2$ ) and so on, when determining the set of fibers to be upgraded. When the network is operated dynamically, a usual strategy consists in using the first precomputed path ( $k = 1$ ) between nodes  $s$  and  $d$  for establishing a connection between those nodes if possible, and only resort to higher order paths if there are no resources on the first path. Therefore, it seems reasonable to set a higher weight  $\alpha_k$  for  $k = 1$  than for higher order paths. The second term of the objective function is introduced in order to break ties following the spirit of the heuristic in Section 4.1, i.e., in case of ties, updating fibers with higher values of  $w_{ij}$  is preferred. As the aim is to break ties,  $M$  is a very small constant (e.g., set to  $10^{-5}$  in the following tests).

As previously mentioned, it is very important to note that this ILP formulation finds the optimal set of links to be upgraded with the aim of maximizing the number of precomputed paths that fully benefit from the upgrade. Nevertheless, that does not necessarily mean that the blocking probability will be minimized when operating the network dynamically and using those paths for establishing the optical connections. The performance of the upgraded network in a dynamic scenario will be studied in the following subsection.

#### 4.2.5 Simulation Setup and Results

We have analyzed the performance of the proposed ILP formulation using the same simulation settings described in Subsection 4.1.1. In this regard, in order to evaluate the performance of the ILP formulation to determine the set of links to upgrade, and to compare with the heuristic proposed in Section 4.1, we have considered three different network topologies of similar size, the 14-node NSFNet [77], the 12-node JPN12 [38], and the 14-node DT topology [81].

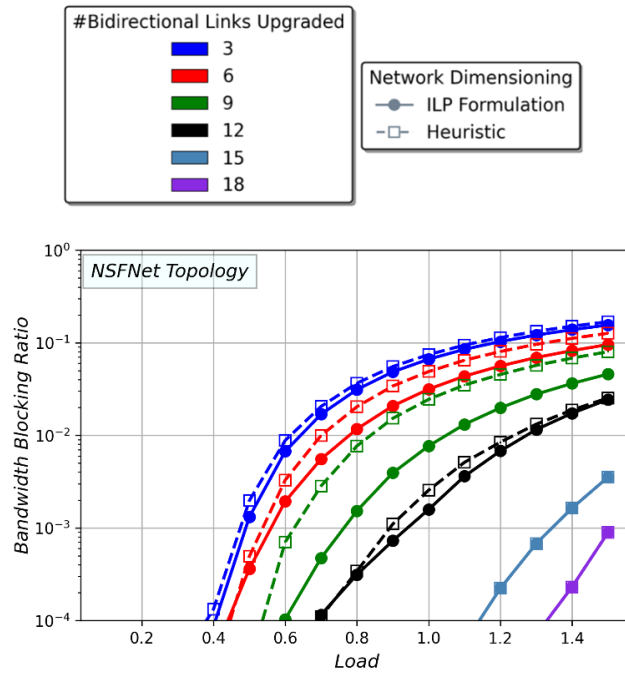
We have solved the ILP formulation using IBM ILOG CPLEX [87], in order to determine the fibers to upgrade in different scenarios, from 3 bidirectional links ( $F = 6$ ) to 18 bidirectional links ( $F = 36$ ), for each of the topologies (except for JPN12, where a maximum of 15 links have been upgraded). When solving the ILP formulation, only the shortest path between each source-destination pair has been considered, i.e.,  $K = 1$  (or equivalently,  $\alpha_1 = 1$  and  $\alpha_k = 0$  for  $k > 1$ ). This approach is consistent with the heuristic proposed in Section 4.1, which only considers the shortest path when determining the set of fibers to upgrade (i.e.,  $K = 1$ ). Despite being an ILP formulation, it can be solved very quickly in these scenarios. Each instance of the formulation

has been solved in less than 20 seconds in a laptop with an Intel(R) Core(TM) i7-4720HQ CPU processor, 2.60 GHz, and 16 GB RAM.

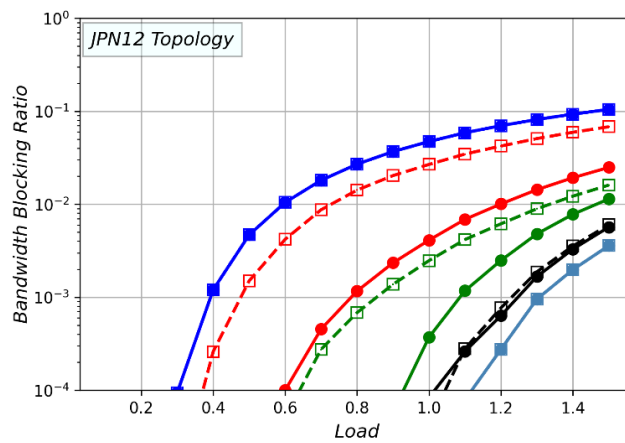
Bandwidth blocking ratio versus traffic load is depicted in Fig. 29 for the three topologies, NSFNet (Fig. 29.a), JPN12 (Fig. 29.b), and DT network (Fig. 29.c). In these figures, different colors represent different numbers of upgraded links. For each color, the continuous lines with filled circles represent the results obtained with the upgrade provided by the ILP formulation, and the dashed lines and hollow squares represent the results with the upgrade provided by the heuristic in Section 4.1.

As shown in these figures, the dynamic performance when upgrading the network according to the solution provided by the ILP formulation generally outperforms (or gets equal results) than the solution provided when using the heuristic in Section 4.1, i.e., lower or similar blocking probabilities are usually obtained.

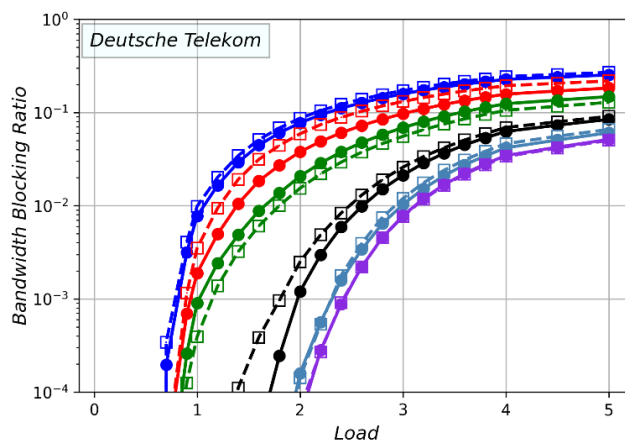
When just a few bidirectional links (3) or many links (18 for NSFNet and DT, or 15 in the case of JPN12) are upgraded, the dynamic performance of both approaches is very similar. It is for an intermediate number of upgraded links when the difference between the two methods is more significant.



(a)



(b)



(c)

**Figure 29.** Bandwidth blocking ratio depending on the network traffic load in (a) NSFNet, (b) JPN12, and (c) DT-network topologies.



The type of topology also has an impact on the results. For the NSFNet topology (Fig. 29.a), the ILP formulation provides better or at least equal results than the heuristic in Section 4.1 for all the upgrade scenarios. The JPN12 topology is the one that shows the major difference between the two methods, with a remarkable decrease on blocking ratio (around one order of magnitude for a traffic load of 0.8) when 6 or 9 bidirectional links are upgraded following the ILP solution compared with the heuristic in Section 4.1. Finally, for the DT-network topology, the results obtained with both techniques are similar.

In summary, a total of 17 upgrade scenarios have been analyzed (6 for NSFNet, 5 for JPN12, and 6 for the DT network). The configuration provided by the ILP formulation leads to better dynamic performance in 8 of those cases and provides similar performance in other 8, while the configuration provided by the heuristic in Section 4.1 is better in only 1 of the cases. The ILP formulation generally provides better results as it maximizes the number of precomputed end-to-end paths that can benefit from the upgrade, i.e., it takes into account that due to the spectrum continuity constraint all links in a path should be upgraded so that a connection following that path can use the L-band. In contrast, the heuristic in Section 4.1 does not take this issue into account and simply prioritizes the upgrades in those individual fibers used by a higher number of precomputed paths. Nevertheless, the simple heuristic proposed in Section 4.1 shows comparable performance in many cases, so being also a valuable technique. The heuristic is obviously quicker than the ILP formulation, although the ILP formulation can also be solved in a short time, in less than 20 seconds in the analyzed scenarios, which is insignificant for a planning (offline) method.

#### 4.2.6 Conclusions

In Section 4.1, we demonstrated that a partial upgrade of the network towards the use of C+L bands can bring significant improvements in blocking probability (and thus in increasing the supported traffic load) without the need of fully upgrading the whole network, and allowing the operator to perform gradual upgrades. However, in Section 4.2, we have presented a novel integer linear programming (ILP) formulation which determines the set of fibers that should be upgraded to support both C and L spectral bands, so that the number of precomputed paths that fully benefit from the upgrade (and which will be used when establishing optical connections) is maximized. However, it should be noted that that strategy does not necessarily imply that the blocking ratio will be minimized when operating the network dynamically.

This ILP approach has been compared with the heuristic proposed in Section 4.1 to determine which fibers to upgrade. We have demonstrated that the ILP formulation generally leads to better (or at least similar) results in terms of blocking ratio when the upgraded network is operated dynamically, and in some cases the improvement is very significant. For instance, for a 6-link upgrade of the JPN12, the network can support up to 60% more traffic when using the upgrade provided by the ILP formulation instead of using the solution provided by the heuristic in Section 4.1, while ensuring a blocking probability lower than  $10^{-3}$ . Although solving the ILP formulation is slower than using the heuristic proposed in Section 4.1, the solution can be obtained in less than 20 seconds in a regular laptop in all the scenarios analyzed (which include topologies with 12-14 nodes, and 17-23 links, where between 3 and 18 of those links are upgraded).

### 4.3 Partial Migration Subject to a Partial Upgrade of the Number of EDFAs

In Sections 4.1 and 4.2, the cost of upgrading different existing fibers to the L-band is assumed to be the same. However, if the EDFAs in the network were originally deployed to support only the C-band, that is not the case. Upgrading a link implies upgrading its EDFAs, and the number of amplifiers can vary from link to link. This implies different upgrading costs. Therefore, in this section, we focus on determining which fibers should be upgraded, subject to a constraint on the maximum number of C-band amplifiers that can be upgraded to support C+L bands, and the final objective is to minimize the blocking probability in a scenario where optical connections are dynamically established and released. For that aim, we propose three heuristics focused on three different auxiliary objectives, a) upgrading the most used fibers (as it was done in Section 4.1), b) upgrading the fibers which maximize the number of precomputed source-destination paths that benefit from the partial upgrade, and c) upgrading the maximum number of fibers as possible subject to the constraint on the number of EDFAs.

In particular, this section extends our previous works in Section 4.1 and Section 4.2, not only because of the consideration of the maximum number of EDFAs to be upgraded (in contrast to those works), but also because (1) we introduce and analyze two metrics to help understand which heuristic may lead to better performance in different scenarios, (2) we propose an additional (simple) heuristic to compare with, and (3) because we analyze the performance assuming not only uniform traffic but also non-uniform traffic, with the help of weighting factors included in the methods and tuned to operate providing better performance in those scenarios.

#### 4.3.1 Description of the Problem and Proposed Solution Strategies

Let us consider an optical network that is going to be partially upgraded from C to C+L bands, that is, just a subset of the network links will be migrated to support both bands. The topology of the network can be represented by a connected graph  $\mathcal{G} = (\mathcal{N}, \mathcal{E})$  where  $\mathcal{N}$  denotes the set of nodes and  $\mathcal{E}$  the set of bidirectional links. We assume that a link connecting two nodes  $i$  and  $j$ , is composed by two fibers,  $(i, j)$  and  $(j, i)$ , one in each direction. Moreover, each fiber  $(i, j)$  is equipped with a certain number of amplifiers,  $a_{ij}$ . Upgrading a link to support C+L transmission involves upgrading all the EDFAs located in the fibers in both directions of that link.

The objective is to determine which fibers should be migrated subject to a constraint on the maximum number of EDFAs that can be upgraded in the whole network ( $A_{max}$ ). The selection of the set of fibers to upgrade is done with the final objective of minimizing the connection blocking probability when the network faces dynamic traffic (i.e. when optical connection establishment and release requests are received during network operation).

Nevertheless, rather than directly minimizing the blocking probability, we adopt a simpler but pragmatic approach and propose three heuristics to determine the set of fibers to upgrade during the off-line planning phase of the network.

For that aim, the  $K$ -shortest paths are precomputed between each source-destination ( $s$ - $d$ ) pair of nodes in the network. These  $K$ -shortest paths will be eventually used for establishing end-to-

end optical connections, and for that reason we focus on these paths. To represent these precomputed paths, the binary constants  $r_{ij}^{sdk}$  are introduced. If the fiber  $(i, j)$  is traversed by the  $k^{th}$  shortest path between nodes  $s$  and  $d$ , then  $r_{ij}^{sdk}$  is set to 1, while it is set to 0 otherwise. Additionally, a set of weighting factors ( $\alpha^{sdk}$ ) can be employed to model the relevance of the different  $sd$  paths when determining the set of fibers to be upgraded. For instance, as we will describe and analyze later, these factors can be used to give more relevance to the end-to-end paths associated to those pairs of nodes  $(s-d)$  interchanging more traffic.

Therefore, in summary, the selection of the fibers to upgrade is done based on the following inputs:

- $\mathcal{G} = (\mathcal{N}, \mathcal{E})$ , the network topology.
- $a_{ij}$ , the number of amplifiers in each fiber of the network.
- $r_{ij}^{sdk}$ , the set of  $K$  precomputed shortest paths for each source-destination  $(s-d)$  pair of nodes in the network.
- $\alpha^{sdk}$ , the set of weighting factors for each  $sd$  path.
- $A_{\max}$ , the maximum number of amplifiers that the network operator desires to upgrade to operate in C+L bands.

The first of the three proposed heuristics, named MostUsed, upgrades the fibers that are most used by the precomputed shortest paths (similar to Section 4.1). The second heuristic, MaxPaths, upgrades the fibers which maximize the number of precomputed  $K$ -shortest paths that benefit from the partial upgrade towards the L-band. Finally, the third heuristic, MaxFibers upgrades as many fibers as possible. The last two methods are based on ILP formulations. However, since they optimize a target function which is different from the minimization of the blocking probability, they should be also considered as heuristic approaches to solve the problem.

The MostUsed and MaxPaths methods are extensions of our previous proposals in Section 4.1 and Section 4.2, respectively, where we did not consider that different links may have different number of amplifiers (and thus a different impact on the cost of the upgrade).

#### 4.3.2 The MostUsed Method

The MostUsed method prioritizes the optical fibers to be upgraded based on the number of times that they are utilized in the shortest path of all source-destination pairs. The number of times that a certain fiber  $(i, j)$  appears in the first precomputed shortest path (i.e.,  $k = 1$ ) of all  $s-d$  pairs ( $w_{ij}$ ) is:

$$w_{ij} = \sum_{sd} r_{ij}^{sd1}, \quad \forall i \in \mathcal{N}, \forall j \in \mathcal{N} \quad (13)$$

In contrast to Section 4.1, that definition can be enhanced by including the set of weighting factors,  $\alpha^{sd1}$ , to take into consideration the traffic associated with each source-destination pair and improve performance when facing non-uniform (but more realistic) traffic:

$$w_{ij} = \sum_{sd} \alpha^{sd1} r_{ij}^{sd1}, \quad \forall i \in \mathcal{N}, \forall j \in \mathcal{N} \quad (14)$$

In this way,  $w_{ij}$  represents the traffic that would traverse fiber  $(i, j)$  if all the traffic between each source-destination pair were successfully routed through its first precomputed shortest path. Thus, from now on, we will consider Equation 13 as the general definition of  $w_{ij}$ , since Equation 13 is a particular case of Equation 14 where  $\alpha^{sd1} = 1$ .

Algorithm 3 shows the operation of the MostUsed method. First of all, the fibers of the network are sorted in a list from the most used to the least used one, i.e., in decreasing order of  $w_{ij}$  (lines 1-2). Then, the algorithm works in an iterative fashion using that list, checking if each link can be upgraded without exceeding the maximum number of EDFAs that can be upgraded due to cost considerations,  $A_{\max}$  (lines 5-12). It should be noted that for a link to be upgraded both fibers composing the link must be migrated. For that reason, the number of amplifiers required in each direction of the link is considered (line 6). The abovementioned process is repeated until all the fibers have been analyzed.

#### Algorithm 3: MostUsed - Upgrade the Most-used Fibers

**Input:**  $(\mathcal{G}, a_{ij}, r_{ij}^{sd1}, \alpha^{sd1}, A_{\max})$

**Output:** Set of fibers to upgrade to L-band,  $F_{\text{upgrade}}$

```

0  Compute  $w_{ij}$  using Equation (14)
1   $F_{\text{not\_upgraded}}$  = list of fibers in the network in decreasing order of  $w_{ij}$ 
2   $F_{\text{upgrade}} = \emptyset$  # set of fibers selected for migration to L-band
3   $\text{upgraded\_EDFAs} = 0$ 
4  for each fiber  $(i, j)$  in  $F_{\text{not\_upgraded}}$ :
5      if  $\text{upgraded\_EDFAs} + a_{ij} + a_{ji} \leq A_{\max}$ :
6          # The fibers composing the link can be migrated
7          Add fibers  $(i, j)$  and  $(j, i)$  to  $F_{\text{upgrade}}$ 
8          Delete fibers  $(i, j)$  and  $(j, i)$  from  $F_{\text{not\_upgraded}}$ 
9           $\text{upgraded\_EDFAs} = \text{upgraded\_EDFAs} + a_{ij} + a_{ji}$ 
10     end if
11 end for
```

#### 4.3.3 The MaxPaths Method

The aim of the MaxPaths method is to maximize the number of precomputed paths that can use the L-band to establish optical connections (or lightpaths). As in most of previous works, we consider the spectrum continuity constraint. Taking this issue into account, the aim of the MaxPaths method is to determine which fibers should be upgraded with the objective of

maximizing the number of precomputed paths (which will be used by the connections) that can benefit from the upgrade. Note that this approach is equivalent to minimizing the number of precomputed  $s$ - $d$  paths that cannot benefit from the upgrade. In order to achieve this objective, a new ILP formulation is presented. It takes at inputs  $(\mathcal{G}, a_{ij}, r_{ij}^{sd1}, \alpha^{sdk}, A_{\max})$ .

In the formulation, we also introduce a big constant,  $U$ , which represents an upper bound on the length (in hops) of the precomputed paths. The longest path between a source and destination node could traverse all the unidirectional links in the topology. Therefore, the value of  $U$  must be set to a value equal or higher than the number of unidirectional fibers in the network. We also introduce  $M$ , a very small constant, which is used to break ties if there is more than one solution which minimizes the number of precomputed  $s$ - $d$  paths that cannot benefit from the upgrade.

The outputs of the ILP formulation, i.e., the decision variables, are defined as follows:

- $f_{ij}$  are the main output of the formulation, as these decision variables identify the fibers selected for migration. They are binary variables, where a value of 1 means that the fiber  $(i, j)$  should be upgraded, i.e., equipped with C+L-band EDFAs. On the other hand, a value of 0 means that no upgrade is performed. Thus, transmission through that fiber can only use the C-band.
- $\Delta^{sdk}$  is an auxiliary integer variable ( $\geq 0$ ) which represents the number of fibers in the  $k$  precomputed path between nodes  $s$  and  $d$  that have not been upgraded. When the ILP formulation is solved, if  $\Delta^{sdk}$  is 0, it means that all fibers along that path  $sdk$  have been equipped with multi-band devices, and therefore, the path benefit from the upgrade as connections using that path can work over C+L bands. On the contrary, if  $\Delta^{sdk}$  is higher than 0, it means that at least one of the fibers of the path has not been upgraded. Therefore, the path cannot benefit from the L-band, since connections using that path must necessarily use the C-band to comply with the spectrum continuity constraint.
- $\delta^{sdk}$  is an auxiliary variable that converts  $\Delta^{sdk}$  into a binary value by clipping its value. Thus, if  $\Delta^{sdk} = 0$ , then  $\delta^{sdk}$  is also 0, which means the path  $sdk$  benefits from the upgrade. If  $\Delta^{sdk} \geq 1$ , then  $\delta^{sdk} = 1$ , which means that the path cannot benefit from the upgrade.

The ILP formulation for the MaxPaths method is as follows:

*minimize*

$$\sum_{sdk} \alpha^{sdk} \delta^{sdk} - M \cdot \sum_{ij} w_{ij} f_{ij} \quad (15)$$

subject to:

$$\sum_{ij} a_{ij} f_{ij} \leq A_{\max} \quad (16)$$

$$f_{ij} = f_{ji}, \quad \forall i \in \mathcal{N}, \forall j \in \mathcal{N} \quad (17)$$

$$\Delta^{sdk} = \sum_{ij} r_{ij}^{sdk} - \sum_{ij} r_{ij}^{sdk} f_{ij}, \quad \forall s, d \in \mathcal{N}, \forall k \in K \quad (18)$$

$$\Delta^{sdk} \leq U \delta^{sdk}, \quad \forall s \in \mathcal{N}, \forall d \in \mathcal{N}, \forall k \in K \quad (19)$$

$$f_{ij} \in \{0, 1\}, \quad \forall i \in \mathcal{N}, \forall j \in \mathcal{N} \quad (20)$$

$$\delta^{sdk} \in \{0, 1\}, \quad \forall s \in \mathcal{N}, \forall d \in \mathcal{N}, \forall k \in K \quad (21)$$

Equation 15 shows the objective function of the formulation. The main objective (modeled by the first term of the equation) is to minimize the number of precomputed paths that cannot benefit from the partial migration of the network. As previously mentioned, if  $\delta^{sdk} = 1$ , it means that the path  $sdk$  cannot benefit from the upgrade, so adding these variables constitute the core of the objective function. The objective function also includes the set of weighting factors,  $\alpha^{sdk}$ . On the one hand, it can be used to give a higher weight to the end-to-end paths associated to those pairs of nodes  $(s, d)$  interchanging more traffic. On the other hand, when the network is operated dynamically, a usual strategy consists in using the first precomputed path ( $k = 1$ ) if possible, and only resort to higher order paths if there are no resources on the first path. Therefore, it seems reasonable to set a higher weight for  $k = 1$  than for higher order paths. Equation 15 has a second term, which is used to break ties if there is more than one solution that minimizes the number of precomputed paths that cannot benefit from the upgrade. In that case, the tie is broken by selecting the solution that upgrades the most used set of fibers, i.e., the set of fibers that appear in the highest number of precomputed shortest paths ( $k = 1$ ). As the aim is to break ties,  $M$  is set to a very small constant.

Regarding the constraints, Equation 16 guarantees that the number of EDFAs to be upgraded to operate in C+L bands does not exceed the bound imposed by the network operator,  $A_{\max}$ . As a bidirectional link is composed by two fibers in different directions, Equation 17 ensures that either both fibers of the link are upgraded or none of them. Equation 18 defines the auxiliary variable  $\Delta^{sdk}$ . The first term in the right-hand side of that equation computes the length in hops of the path  $sdk$ . The second term counts the number of fibers of that path that have been selected to be upgraded. Therefore, the difference is the number of fibers of that path that will not be upgraded, i.e.,  $\Delta^{sdk}$ . Then, Equation 19 is used to determine  $\delta^{sdk}$ , the clipped binary version of  $\Delta^{sdk}$ . Since  $U$  is a large positive constant, if  $\Delta^{sdk}$  is higher than 0, the binary variable  $\delta^{sdk}$

is forced to take the value of 1 to comply with Equation 19. On the other hand, if  $\Delta^{sdk}$  is 0, the  $\delta^{sdk}$  variable could be either 0 or 1 and still satisfy Equation 19. However, it will take the value of 0, as it leads to minimizing the objective function (sum of  $\delta^{sdk}$  variables) in Equation 15. In this way,  $\delta^{sdk}$  works as a clipped binary version of  $\Delta^{sdk}$ . Finally, Equation 20 and Equation 21 set  $f_{ij}$  and  $\delta^{sdk}$  as binary variables.

#### 4.3.4 The MaxFibers Method

The third method, MaxFibers, aims at maximizing the number of optical fibers that are migrated (subject to the constraint imposed on the number of upgraded EDFAs). An algorithmic implementation of this method can be done by selecting the links to upgrade in increasing order of the number of amplifiers that they have. Equivalently, the MaxFibers method can be defined by means of an ILP formulation (which is, in fact, a simplified version of the MaxPaths formulation, with fewer constraints and a different objective function):

*maximize*

$$\sum_{ij} f_{ij} - M \cdot \sum_{ij} a_{ij} f_{ij} \quad (22)$$

*subject to:*

$$\sum_{ij} a_{ij} f_{ij} \leq A_{\max} \quad (23)$$

$$f_{ij} = f_{ji}, \quad \forall i \in \mathcal{N}, \forall j \in \mathcal{N} \quad (24)$$

$$f_{ij} \in \{0, 1\}, \quad \forall i \in \mathcal{N}, \forall j \in \mathcal{N} \quad (25)$$

#### 4.3.5 Simulation Results

We have analyzed the performance of the proposed techniques using the same simulation settings described in Subsection 4.1.1. Three different strategies for network upgrading that we have just discussed determine the set of links to be migrated from the C-band to the C+L-band, subject to a constraint on the maximum number of EDFAs that can be upgraded. The three proposed methods employ different approaches: upgrading the most used fibers, upgrading the fibers that maximize the number of precomputed paths that benefit from the upgrade, and upgrading the maximum number of fibers. However, the final objective is to analyze and compare the performance of the network when it is upgraded according to each of these three strategies, and then operates dynamically. Therefore, once the network is partially migrated, we assume lightpath establishment and release requests are dynamically received. Connection

establishment requests will be handled by an RBMLSA algorithm and its performance in terms of BBR will be assessed. Three different network topologies, with similar size in terms of number of nodes and links, the American NSFNet [77], the Japanese JPN12 [38], and the European DT network [81], have been considered. However, the distances involved in these topologies are very different, being the lowest for the DT and the highest for the NSFNet, which translates into different numbers of required amplifiers. The exact location and distance between amplifiers (and thus the number of amplifiers per link) depends not only on the length of the link but also on other factors of each particular link, like the class of fiber employed, or the type and configuration of the amplifiers. However, our aim is not to accurately model amplifier placement, but to create a set of simulation scenarios where different links may have different numbers of amplifiers. Therefore, for the sake of simplicity, we have assumed that an amplifier is required every 80 km in all network links. Thus, the total number of C-band amplifiers in these networks ( $A_{\text{network}}$ ) ranges from 86 amplifiers for the DT and 554 for the NSFNet. Table 5 summarizes the characteristics of these three topologies.

**Table 5.** Characteristics of the evaluated network topologies.

Topology	Number of Nodes ( $N$ )	Number of Bidirectional Links	Number of Amplifiers ( $A_{\text{network}}$ )
NSFNet	14	21	554
JPN12	12	17	172
DT	14	23	86

We have analyzed different scenarios in terms of the maximum percentage of network amplifiers that can be upgraded, from no upgrade (0%) to full upgrade (100%), including partial upgrades in steps of 20% (that is, we have set  $A_{\text{max}} = p \cdot A_{\text{network}}$ , with  $p = 0, 0.2, \dots, 1$ ). In order to determine which fibers to migrate to C+L bands, the three heuristics described in Section 4.3 have been used.

Regarding traffic, we have assumed two different models:

- Uniform traffic, i.e. all source-destination pairs have the same average traffic load.
- Non-uniform traffic, i.e., different source-destination pairs have different traffic loads. In particular, we have assumed a population-based traffic matrix, where the average traffic load between nodes  $s$  and  $d$  is proportional to the product of the population ( $P$ ) of the cities where nodes  $s$  and  $d$  are located, i.e.  $vP_sP_d$ , where  $v$  is a proportionality constant. For simplicity, but without loss of generality, we assume  $v = 1$ . The 2023 population data for the cities (or states) where the nodes are located has been obtained from [88]. Additionally, the traffic matrixes that we have generated and used in this research have been made accessible on GitHub [89].

Moreover, we have only considered the primary shortest path between each source-destination pair (i.e.,  $K=1$ ) to propose the potential fibers for the migration. This approach is consistent



with the MostUsed heuristic, which also only considers the shortest path to determine which fibers to upgrade. Therefore, the constants  $\alpha^{sdk}$  have been set as  $\alpha^{sd1} = 1, \forall s, d$ , and  $\alpha^{sdk} = 0, \forall s, d$  and  $k > 1$  for the uniform traffic case. The value of the very small constant to break ties,  $M$ , has been set to  $10^{-5}$ . For the non-uniform traffic case, the constants  $\alpha^{sdk}$  have been set as  $\alpha^{sd1} = P_s P_d, \forall s, d$ , and  $\alpha^{sdk} = 0, \forall s, d$  and  $k > 1$ . In this case,  $M$  has been set to  $1/[F \sum_{s,d} (P_s P_d)]$ , where  $F$  is the number of unidirectional fibers in the network. However, in order to compare the results, we have also analyzed the performance when the network faces non-uniform traffic, but the network has been upgraded using the output of the heuristics using the weighting factors of the uniform scenario ( $\alpha^{sd1} = 1$ ).

Then, the IBM ILOG CPLEX solver has been used to solve the ILP formulations. An interesting point regarding all the proposed methods, including the ILP formulations, is that they provide the solution very quickly. The list of fibers to be upgraded in each scenario when using any of the three methods is obtained in less than 5 seconds in a laptop with an Intel(R) Core(TM) i7-4720HQ CPU processor, 2.60 GHz, and 16 GB RAM.

As previously mentioned, once the network is upgraded, we evaluate its performance under dynamic traffic. The arrival of connection requests is modeled as a Poisson process with arrival rate ( $\lambda$ ). The holding time of each connection is modeled by an exponential distribution with an average of  $T$ . For the uniform traffic case, a uniform random distribution is used to select the source and destination node for each connection. For the non-uniform case, the probability of selecting a source-destination pair is proportional to the traffic between those nodes, in particular,  $P_s P_d / \sum_{s,d} (P_s P_d)$ .

#### 4.3.5.1 Uniform Traffic

When assuming uniform traffic, the BBR versus traffic load is depicted for the three employed topologies, NSFNet (Fig. 30.a), JPN12 (Fig. 30.b), and DT (Fig. 30.c). Different colors in these figures correspond to different scenarios in terms of the maximum percentage of network amplifiers that can be upgraded, from no upgrade (0%) to full upgrade (100%) in steps of 20%. The type of line (dashed, solid or dotted) represent the results associated to the heuristics employed for fiber selection, MostUsed, MaxPaths or MaxFibers, respectively.

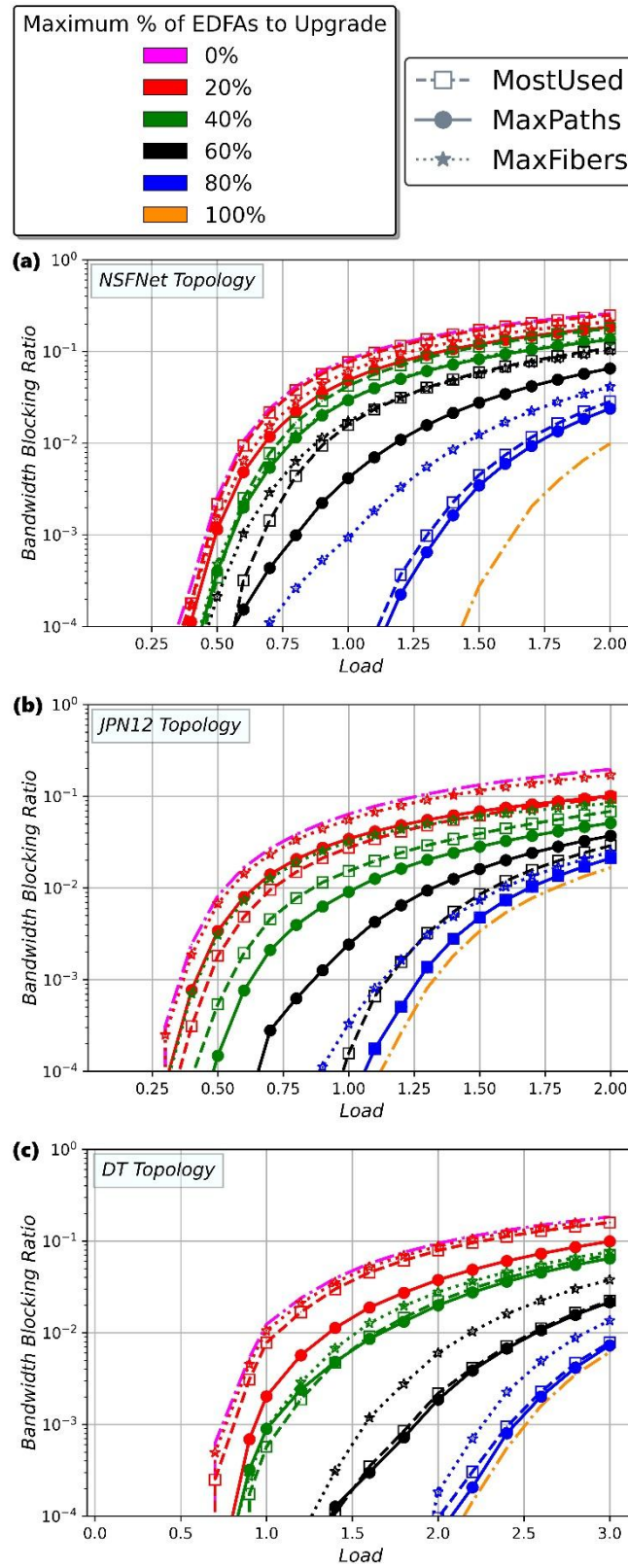


**Figure 30.** Bandwidth blocking ratio depending on the network traffic load considering uniform traffic in (a) NSFNet, (b) JPN12, and (c) DT-network topologies.

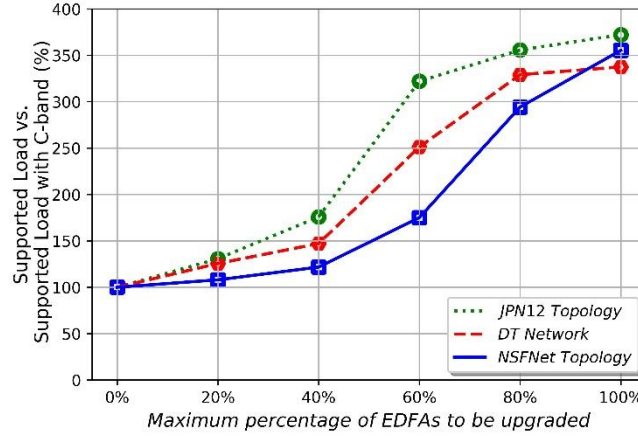


**Figure 31.** Maximum supported traffic load in a partially upgraded network with blocking probability  $\leq 10^{-3}$ , considering uniform traffic.

Obviously, as the percentage of upgraded amplifiers increases, the BBR reduces, since a higher number of network links have additional spectral resources in the L-band. Anyway, before commenting Fig. 30 in detail, Fig. 31 summarizes and quantifies this improvement. It represents the increase of the traffic load supported by the upgraded network, compared to a C-band only network, if we assume that the maximum acceptable BBR is  $10^{-3}$ , and considering different percentages of upgraded amplifiers. When the network is fully upgraded to the L-band (100% upgrade), the traffic load increase supported by the network, for the three topologies, is around 350% when compared to the C-band only counterpart. However, the figure demonstrates that even with a partial upgrade of the network, significant increases in the supported traffic loads can be achieved. The most significant rise in improvement is obtained when 60% to 80% of the EDFAs in the network are upgraded. Nevertheless, the amount of improvement on supported traffic load depends on the percentage of upgrade, but also on the topology, ranging from 175% for the NSFNet to 322% for the JPN12 (both for a 60% upgrade). In order to obtain Fig. 31, for each percentage of upgrade we considered the solution provided by the heuristic leading to the lowest BBR (which is an issue that we analyze next, coming back to Fig. 30).

Fig. 30 shows the BBR results when the three heuristics to select which fibers to upgrade (MostUsed, MaxPaths and MaxFibers) are used, considering different scenarios in terms of the maximum percentage of network amplifiers that can be upgraded. As shown in Figs. 30.a to 30.c, the MaxFibers heuristic never obtains the best results in terms of BBR when compared with the other two algorithms. Therefore, we will focus on the comparison between the MostUsed and the MaxPaths methods.

For the NSFNet topology (Fig. 30.a), the solution provided by the MaxPaths method leads to lower values of BBR in all the partial upgrade scenarios (from 20% to 80%). In contrast, for the JPN12 topology (Fig. 30.b), the MostUsed method obtains better or similar BBR than MaxPaths except for the 40% upgrade, where MaxPaths leads to lower BBR. Finally, for the DT network (Fig. 30.c), the MaxPaths method provides lower or at least similar BBR than MostUsed. Therefore, the MaxPaths method, which maximizes the number of precomputed paths that benefit from the upgrade, usually leads to better results. However, in some cases, as

we have seen in the JPN12 topology (mainly for the 60% upgrade), the MostUsed method, which prioritizes the upgrade of the fibers that are most used by the precomputed paths, can lead to a lower BBR.

In the following, we explain why in some cases one of the heuristics leads to better results than the other. For that aim, we compute two metrics for each of the solutions (i.e., for the sets of fibers to upgrade which are provided by each heuristic).

- Number of precomputed shortest paths that benefit from the upgrade, i.e.,  $N(N-1) - \sum_{sd} \delta^{sd1}$
- Congestion in not upgraded fibers, defined as the number of times that the most used but not upgraded fiber appears in the list of precomputed shortest paths, i.e.,  $\max_{(i,j)} w_{ij}$ , such that  $f_{ij} = 0$ .

It should be noted that the MaxPaths method always obtains the optimal (maximum) value for the first metric, as it is the objective of the associated ILP formulation, while the MostUsed method obtains the optimal (minimum) value for the second metric. Tables 6 to 8 report the values of these metrics for the different heuristics and the NSFNet, JPN12 and DT topologies, respectively. Although the focus is on the comparison between the MaxPaths and MostUsed heuristics, we also provide the results for MaxFibers for completeness. The values in bold in Tables 6 to 8 correspond to the solution which provides the best results in terms of BBR. If two different solutions provide very similar results, both of them are marked in bold.

The congestion metric for the solutions of the MostUsed and MaxPaths methods is the same or nearly the same for the NSFNet topology (Table 6) for the 20% and the 40% upgrades. However, the number of paths that benefit from the upgrade is much higher for the MaxPaths method in those two cases (around 20 percentage points more than MostUsed in the first case and 26 in the second). This translates into a lower BBR for the solution provided by the MaxPaths methods.

In contrast, in the 20% upgrade for the JPN12 network (Table 7), the number of paths that benefit from the upgrade when using the solutions provided by the MaxPaths and the MostUsed method are very similar, as they only differ in 2.3 percentage points. However, the congestion in not upgraded fibers is much higher for MaxPaths (22) than for MostUsed (11). Therefore, a highly congested link in the MaxPaths solution is becoming a bottleneck, compared to the solution provided by MostUsed, and translates in a higher BBR for the MaxPaths solution.

Therefore, these two metrics that we have introduced are indicators of the performance that can be expected when operating the network dynamically, and provide a hint of which planning method may provide a lower BBR in dynamic operation without the need of performing a simulation. If the congestion metric is similar, but there is a significant difference in the number of paths that benefit from the upgrade, the MaxPaths method will generally lead to lower BBR. If the number of paths that benefit is similar, but there is a significant difference in terms of congestion, the MostUsed method will usually lead to better results. Nevertheless, as shown in the table, there are many situations where the two metrics are different for the MostUsed and MaxPaths methods, and thus, there is a trade-off between the impact of congestion and the

number of precomputed paths that benefit from the upgrade on BBR. MaxPaths generally leads to lower (or at least similar) BBR results than MostUsed. However, a network operator desiring to upgrade the network should run a simulation to assess the performance of the upgrades provided by MostUsed and MaxPaths in order to take the final decision.

**Table 6.** Metrics of the upgrade solutions for the NSFNet (uniform traffic).

Metric	Method	Maximum % of EDFAs to upgrade			
		20%	40%	60%	80%
# paths that benefit from the upgrade	MostUsed	8 4.4%	26 14.3%	52 28.6%	117 64.3%
	MaxPaths	<b>44</b> 24.2%	<b>74</b> 40.7%	<b>111</b> 61%	<b>144</b> 79.2%
	MaxFibers	30 16.5%	65 35.8%	91 50%	130 71.5%
Congestion in not upgraded fibers	MostUsed	14	13	10	8
	MaxPaths	<b>14</b>	<b>14</b>	<b>14</b>	<b>13</b>
	MaxFibers	14	14	14	14

**Table 7.** Metrics of the upgrade solutions for the JPN12 (uniform traffic).

Metric	Method	Maximum % of EDFAs to upgrade			
		20%	40%	60%	80%
# paths that benefit from the upgrade	MostUsed	<b>29</b> 22%	60 45.5%	<b>90</b> 68.2%	<b>118</b> 89.4%
	MaxPaths	32 24.3%	<b>70</b> 53.1%	98 74.3%	<b>118</b> 89.4%
	MaxFibers	27 20.5%	60 45.5%	98 74.3%	100 75.8%
Congestion in not upgraded fibers	MostUsed	<b>11</b>	10	<b>7</b>	<b>6</b>
	MaxPaths	22	<b>11</b>	10	<b>6</b>
	MaxFibers	24	22	10	10

**Table 8.** Metrics of the upgrade solutions for the DT (uniform traffic).

Metric	Method	Maximum % of EDFAs to upgrade			
		20%	40%	60%	80%
# paths that benefit from the upgrade	MostUsed	18 9.9%	<b>62</b> 34.1%	<b>108</b> 59.4%	<b>153</b> 84.1%
	MaxPaths	<b>36</b> 19.8%	<b>84</b> 46.2%	<b>114</b> 62.7%	<b>159</b> 87.4%
	MaxFibers	24 13.2%	48 26.4%	89 45.1%	129 70.9%
Congestion in not upgraded fibers	MostUsed	16	<b>12</b>	<b>7</b>	<b>5</b>
	MaxPaths	<b>20</b>	<b>18</b>	<b>10</b>	<b>5</b>
	MaxFibers	20	20	20	20

#### 4.3.5.2 Non-uniform Traffic

We now analyze the performance of the methods when considering a non-uniform traffic matrix. We will focus on MaxPaths and MostUsed methods since they obtained better results than MaxFibers (and they can be tuned by means of the  $\alpha^{sdk}$  parameters to consider non-uniform traffic). As previously mentioned, we assume a population-based traffic matrix, where the average traffic load between nodes  $s$  and  $d$  is proportional to the product of the population of the cities where nodes  $s$  and  $d$  are located, i.e.  $P_s P_d$ . Our aim is to answer two research questions here. First of all, to determine whether setting the weights  $\alpha^{sdk}$  according to the associated load of each source-destination pair really improves the selection of fibers to upgrade, that is, it leads to a reduction of the BBR when the network operates dynamically. Secondly, to analyze whether the MaxPaths heuristic also usually leads to better results than MostUsed in this scenario.

In order to answer the first question, we have focused on the MaxPaths method and have compared the dynamic performance when the network is upgraded like in the previous subsection, that is, setting  $\alpha^{sd1} = 1, \forall s, d$  (and 0 for other values of  $k$ ), and when setting the weights so that  $\alpha^{sd1} = P_s P_d, \forall s, d$  (and  $\alpha^{sdk} = 0, \forall s, d$  and  $k > 1$ ). It should be noted that in the latter case, due to using those weights, the objective function of the MaxPaths method is not really the maximization of the number of paths that benefit from the partial upgrade of the network, but the maximization of the amount of end-to-end traffic that benefits from the upgrade (or equivalently, the minimization of the amount of end-to-end traffic that cannot benefit from the partial upgrade of the network).

Fig. 32 shows the results for the NSFNet, JPN12 and DT-network topologies. In nearly all cases, the results are always better when  $\alpha^{sd1}$  is set proportional to the load of each source-destination pair than when it is set to 1 for all pairs of nodes. The only exceptions have been

obtained for the NSFNet (Fig. 32.a) when 80% of EDFAs are upgraded and for the JPN12 network (Fig. 32.b) for the 20% upgrade. Nevertheless, in those cases the results are quite close with both methods. However, it can be seen that setting  $\alpha^{sd1}$  proportional to the load leads to significant improvements in many cases. For instance, for the NSFNet (Fig. 32.a), the dynamic performance when upgrading 40% of the amplifiers according to the solution obtained when setting  $\alpha^{sd1} = P_s P_d$  is even better than when upgrading 60% of the amplifiers according to a solution obtained with  $\alpha^{sd1} = 1$ . A similar behavior can be observed in the DT network (Fig. 32.c): the performance for the 40% amplifiers upgrade using  $\alpha^{sd1} = P_s P_d$  is again better than for the 60% upgrade using  $\alpha^{sd1} = 1$ .

In summary, the impact of the value of  $\alpha^{sd1}$  on the performance of the MaxPaths method considering non-uniform traffic has been analyzed in 12 different configurations. In only two of the cases,  $\alpha^{sd1} = 1$  provides slightly better results. However, in the rest of cases, setting the value of  $\alpha^{sd1} = P_s P_d$  leads to better results, and the improvement is very significant in several cases.

We have also compared the performance of the MostUsed method, considering non-uniform traffic, when setting  $\alpha^{sd1} = 1$  and  $\alpha^{sd1} = P_s P_d$ . The results are consistent with those obtained for MaxPaths. In all cases except two, the use of  $\alpha^{sd1}$  proportional to the traffic load between each pair of nodes leads to better results in terms of BBR (the exceptions are for the 20% upgrade of the JPN12 and the 80% upgrade of the DT network).

In conclusion, setting  $\alpha^{sd1}$  proportional to the load carried by each source-destination pair generally results in a selection of fibers to upgrade that leads to better dynamic performance. In this regard, if the real traffic deviates from the traffic that has been considered when determining which fibers to upgrade (e.g., assuming uniform traffic but having non-uniform traffic, as in the simulation just presented), a decrease in the dynamic performance is to be expected.

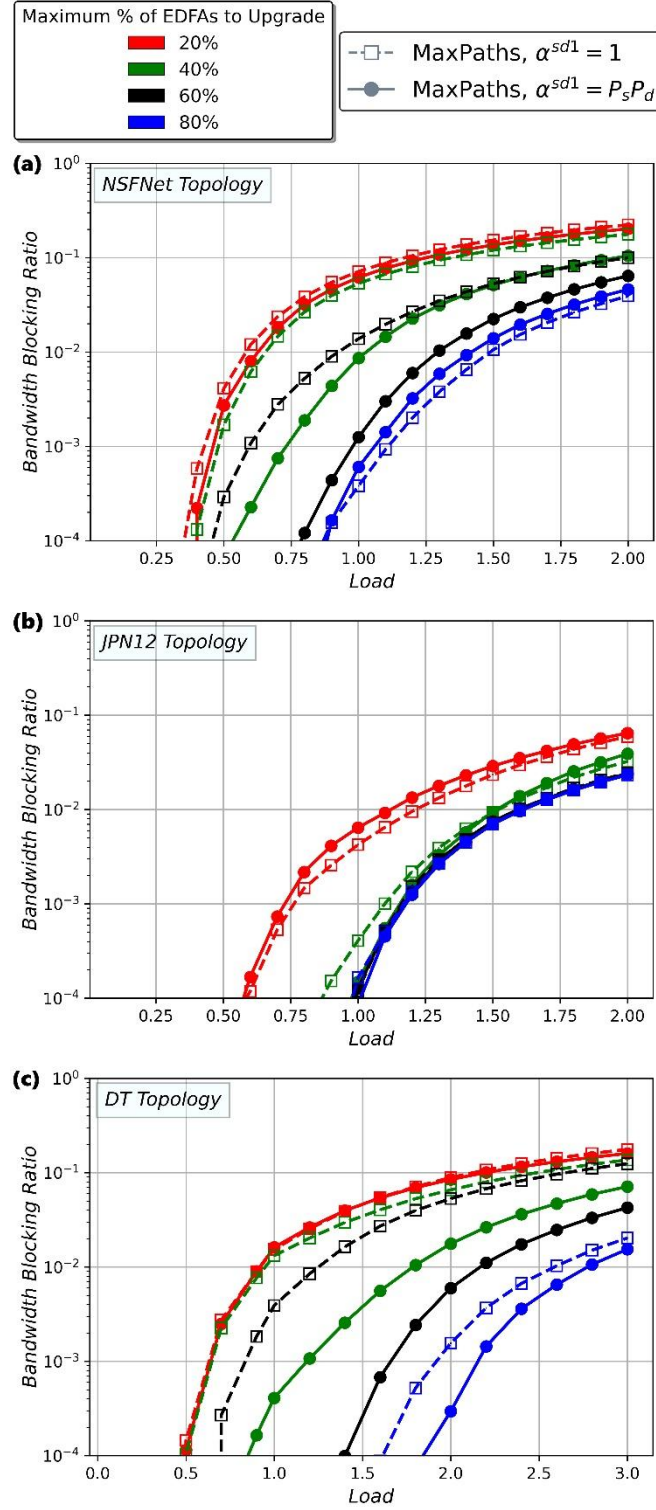


**Figure 32.** Bandwidth blocking ratio depending on the network traffic load considering non-uniform traffic in (a) NSFNet, (b) JPN12, and (c) DT-network topologies, for MaxPaths when different policies to set the  $\alpha^{sd1}$  weights are used.

We now address the second question and compare the MaxPaths and MostUsed methods when considering the non-uniform population-based traffic and setting in both algorithms  $\alpha^{sd1} = P_s P_d, \forall s, d$  (and  $\alpha^{sdk} = 0, \forall s, d$  and  $k > 1$ ). When using these weights, the MostUsed method



prioritizes those fibers that carry more traffic to be upgraded, while the MaxPaths method minimizes the amount of end-to-end traffic that cannot benefit from partial upgrade.

The results in terms of BBR are shown in Fig. 33. For the NSFNet topology (Fig. 33.a), MaxPaths leads to lower BBR than MostUsed in all the analyzed scenarios except for the 80% upgrade. For the JPN12 topology (Fig. 33.b), MaxPaths and MostUsed obtain very similar BBR in all cases, while in the DT network (Fig. 33.c), MaxPaths works better (or similar) than MostUsed in all scenarios, except for the 20% upgrade (where it is just slightly worst).

In summary, when dealing with non-uniform traffic, again MaxPaths usually provides better, or at least equal, results compared to MostUsed (when both methods use weights set according to the traffic load).

As we did in the uniform traffic case, in order to analyze in more detail this comparison, we compute the same metrics, but normalizing them by the total traffic in the traffic matrix, i.e.  $\sum_{s,d}(P_s P_d)$  in order to avoid having very big numbers, and taking into account that  $\alpha^{sd1}$  is not 1 but  $P_s P_d$ . Thus, we will analyze:

- The fraction of end-to-end traffic that benefits from the upgrade, defined as  $1 - \sum_{s,d}(\alpha^{sd1} \delta^{sd1}) / \sum_{s,d}(P_s P_d)$
- The traffic congestion in not upgraded fibers, defined as,  $\max_{(i,j)} w_{ij} / \sum_{s,d}(P_s P_d)$ , such that  $f_{ij} = 0$ . (Note that  $w_{ij}$  is computed using Equation 14, and thus considers  $\alpha^{sd1} = P_s P_d$ ).

These metrics are reported in Tables 9 to 11. Again, the values in bold correspond to the solutions which provide the best results in terms of BBR. If two different solutions provide very similar results, both of them are marked in bold.

Similar conclusions can be drawn from these metrics as in the uniform case. If the congestion metric is very similar for the two heuristics, and also does the other metric, then the dynamic performance is, in general, very similar for the two heuristics. This is what happens, for instance, for all the upgrade scenarios for the JPN12 topology, where the metrics are identical or very similar in all cases, (Table 10) and thus the performance results for MostUsed and MaxPaths are also very similar (Fig. 33.b). If the congestion metric is similar for both heuristics, but there is a significant difference in the fraction of traffic that benefits from the upgrade, the MaxPaths method will generally lead to lower BBR. That happens in the 40% and 60% upgrade of the NSFNet (Table 9). However, to be honest, in the DT network (Table 11) according to the obtained metrics one would expect a more similar performance for both heuristics for 60% and 80% upgrades, but MaxPaths provides better results. That is, as previously mentioned, these two metrics are indicators of the performance, but obviously a simulation is more trustworthy.

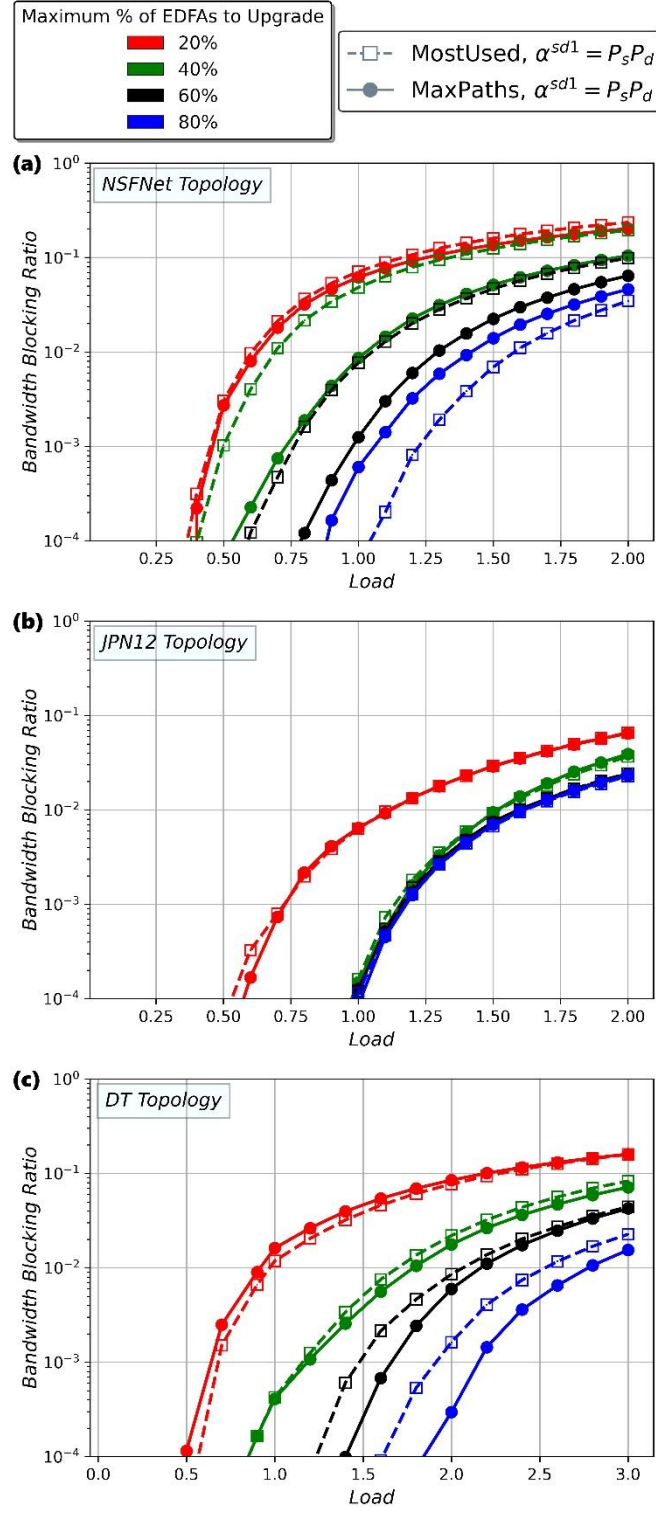


**Figure 33.** Bandwidth blocking ratio depending on the network traffic load considering non-uniform traffic in (a) NSFNet, (b) JPN12, and (c) DT-network topologies, for MostUsed and MaxPaths.

**Table 9.** Metrics of the upgrade solutions  
for the NSFNet (non-uniform traffic,  $\alpha^{sd1} = P_s P_d$ ).

Metric	Method	Maximum % of EDFAs to upgrade			
		20%	40%	60%	80%
Fraction of traffic that benefits from the upgrade	MostUsed	0.06	0.17	0.41	<b>0.72</b>
	MaxPaths	<b>0.22</b>	<b>0.48</b>	<b>0.63</b>	0.81
Traffic congestion in not upgraded fibers	MostUsed	0.07	0.06	0.05	<b>0.03</b>
	MaxPaths	<b>0.12</b>	<b>0.07</b>	<b>0.07</b>	0.07

**Table 10.** Metrics of the upgrade solutions  
for the JPN12 (non-uniform traffic,  $\alpha^{sd1} = P_s P_d$ ).

Metric	Method	Maximum % of EDFAs to upgrade			
		20%	40%	60%	80%
Fraction of traffic that benefits from the upgrade	MostUsed	<b>0.56</b>	<b>0.85</b>	<b>0.94</b>	<b>0.98</b>
	MaxPaths	<b>0.56</b>	<b>0.86</b>	<b>0.94</b>	<b>0.98</b>
Traffic congestion in not upgraded fibers	MostUsed	<b>0.09</b>	<b>0.02</b>	<b>0.016</b>	<b>0.011</b>
	MaxPaths	<b>0.09</b>	<b>0.03</b>	<b>0.016</b>	<b>0.011</b>

**Table 11.** Metrics of the upgrade solutions  
for the DT (non-uniform traffic,  $\alpha^{sd1} = P_s P_d$ ).

Metric	Method	Maximum % of EDFAs to upgrade			
		20%	40%	60%	80%
Fraction of traffic that benefits from the upgrade	MostUsed	<b>0.19</b>	0.39	0.59	0.80
	MaxPaths	0.25	<b>0.50</b>	<b>0.64</b>	<b>0.84</b>
Traffic congestion in not upgraded fibers	MostUsed	<b>0.10</b>	0.06	0.04	0.03
	MaxPaths	0.14	<b>0.10</b>	<b>0.07</b>	<b>0.04</b>

#### 4.3.6 Conclusions

As fully upgrading a C-band EON towards the use of C+L bands in all links imposes a high cost to network operators, we have focused on strategies for a partial upgrade. We have analyzed which fibers should be upgraded in an EON with the aim of improving the performance when the network operates dynamically. In contrast with previous works, we have considered that the cost of upgrading different fibers is different, as the number of amplifiers in each link may be different.

In particular, we have proposed three different heuristics to select which fibers to upgrade subject to a constraint on the maximum number of EDFAs than can be upgraded. The heuristics are:

- MostUsed, which upgrades the most used links;
- MaxPaths, which upgrades the links that maximize the number of precomputed  $s$ - $d$  paths that benefit from the upgrade;
- MaxFibers, which upgrades as many fibers as possible.

All these methods, even those based on ILP formulations, can be solved in a few seconds in networks with around a dozen of nodes. Amongst them, MaxPaths is the method that generally leads to lowest BBR when the upgraded network operates dynamically, although in some scenarios the MostUsed method can obtain better results. We have defined two metrics, the number of paths that benefit from the upgrade and the congestion in not upgraded fibers, which provide an indicator of which of the proposed methods may lead to best performance. Moreover, we have demonstrated that a partial upgrade of the network can lead to significant increases in the supported traffic load by the network. The most significant rise in improvement is obtained when 60%-80% of the EDFAs are upgraded.

Besides analyzing the performance of the heuristics when dealing with uniform traffic, we have also analyzed the case of non-uniform traffic patterns. The MostUsed and MaxPaths heuristics incorporate weighting factors that effectively consider the traffic load associated with each source-destination pair and use this information to determine which set of fibers should be upgraded. We have demonstrated that when the weights of the heuristics are tuned considering the expected traffic load, better dynamic performance is generally obtained. Therefore, network operators should leverage on monitoring data from their networks and employ traffic prediction techniques to get a good estimate of the traffic matrix. Moreover, again, for the case of non-uniform traffic scenarios, MaxPaths usually yields better (or at least equal) results than MostUsed.

### 4.4 Cost-effective Transceivers in the Process of Partial Migration

In Section 4.3, we analyzed the effects of partial migration with a focus on link equipment, specifically amplifiers. In this section, our focus is on transceivers. We begin with the realistic premise that current operators are already operating their networks in the C-band and have an adequate number of transceivers for this purpose. To accommodate higher traffic loads using both the C and L bands, operators have two alternatives:

- Option A: acquire single band transceivers, i.e., C-band transceivers for new lightpaths established over that band, and L-band transceivers for those to be established in the L-band.
- Option B: acquire new multi-band transceivers capable of operating in both C+L bands.

This section provides insights into the matter of choosing one of these options, considering that the network operates dynamically. Through simulation analysis, we offer an estimate of the potential savings in the number of transceivers if the multi-band option is chosen, and we also present a techno-economic analysis. This information empowers network operators to make more informed decisions by taking equipment costs into account. Additionally, this research could be valuable for the optical industry in order to decide in which direction to lead the transceiver development efforts.

In the previous sections of Chapter 4 (Sections 4.1, 4.2, and 4.3), the transceivers that should be purchased in order to realize the C+L band systems were not considered, even though they have an important impact on the upgrade costs. In this section, the set of links to be upgraded will be determined based on the method proposed in Section 4.2. However, we now shift the focus to transceivers, and analyze the question of whether it is worthwhile for network operators to invest in multi-band transceivers to accommodate increased network traffic loads, as opposed to using separate C-band and L-band transceivers for that aim. Our study is based on the premise that network operators already have C-band transceivers deployed in the network. However, as traffic increases and the network should be upgraded, the acquisition of new transceivers becomes necessary. If the network operates dynamically, having multi-band transceivers offers more flexibility, as these transceivers can be employed for establishing connections in any band to adapt to traffic conditions. The question is whether that advantage is significant enough.

#### 4.4.1 Simulation Setup and Results

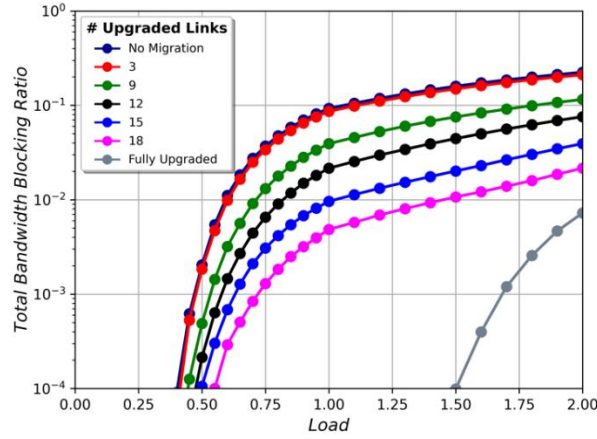
The simulation was created following the assumptions detailed in Subsection 4.1.1. It is considered that the transceivers should be allocated at both the source and destination nodes. As the aim is to identify new transceivers to be purchased, if there are no idle transceivers for a new connection, we assume instant acquisition of new transceivers along the simulation with no restrictions. Note that the simulation, and the assumption of instant acquisition, are used as planning mechanisms. In this way, we keep track of the total number of transceivers required, and thus determine how to dimension the network and the number of new transceivers that should be purchased.

In Option A, single-band transceivers are considered. If a lightpath is to be established in the C-band and there are available C-band transceivers at the source and destination, those resources are used, eliminating the need for new equipment. If no idle resources are available, new C-band transceivers must be acquired. The same process applies if the lightpath is to be established in the L-band (in that case acquiring L-band transceivers).

In Option B, only multi-band transceivers will be acquired. If a lightpath is to be established in the C-band and there are idle C-band or multi-band transceivers at the source and destination nodes, the control plane utilizes them for the request. Otherwise, new multi-band transceivers

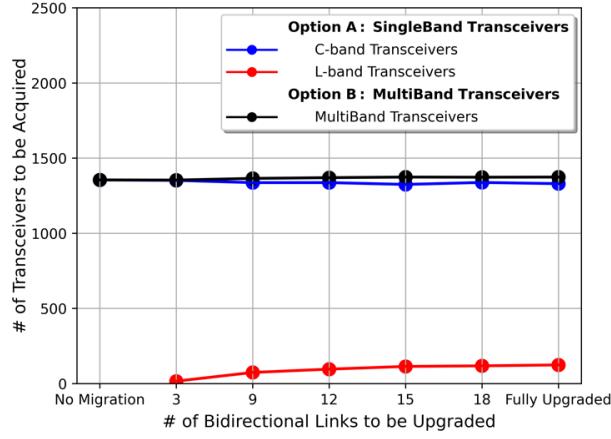
will be acquired. If the lightpath is to be set up in the L-band and no idle multi-band transceivers exist, new multi-band transceivers will be purchased.

Fig. 34 represents total BBR depending on the traffic load for different scenarios of partial migration. The traffic load is defined according to Equation 4, which is a normalized version of the classic definition of traffic load in Erlangs. As expected, upgrading more fibers results in better dynamic performance. According to Fig. 34, the improvement in the supported traffic load while maintaining  $BBR < 10^{-3}$  can be increased approximately 1.5 times through the migration of 18 bidirectional links to the C+L bands. Here, as it is mentioned, during the band selection of an upgraded link, the C-band is prioritized over the L-band. However, according to the results of previous Sections 4.1, 4.2, and 4.3, the blocking ratio could be further improved if priority were given to the L-band, even if it requires a higher number of new transceivers. Nevertheless, the aim of this section is to analyze the most cost-effective solution for minimizing the transceivers costs.



**Figure 34.** Bandwidth blocking ratio for different number of links upgraded.

Fig. 35 shows the number of C-band/L-band/multi-band transceivers to be acquired depending on the number of migrated links, and assuming that the traffic in the network increases to a normalized load of 0.6. Acquiring transceivers following Option A or Option B leads to the same BBR. Note that even in the 'no migration' scenario, new transceivers should be acquired, as the network was dimensioned assuming a (lower) normalized traffic load of 0.2. As shown in that figure, the number of multi-band transceivers to be acquired (Option B) is very similar to the number of additional C-band transceivers to buy if Option A is employed. Therefore, the red line, which corresponds to the L-band transceivers to buy for Option A, can be considered (roughly) as the number of transceivers that can be saved by the usage of multi-band transceivers. If 15 links are upgraded, 65 less transceivers are required if multi-band transceivers are used (1,374 vs 1,439).



**Figure 35.** Number of transceivers to be acquired (if traffic load increases to 0.6).

Table 12 provides a comparison between single-band and multi-band transceivers in terms of the number of required transceivers and the associated costs. The techno-economic model in [90] assumes that the cost of a C-band and an L-band transceiver is 36 cost units (c.u.) and 43.2 c.u., respectively (where 1 c.u. is equal to the cost of a C-band EDFA). No data is provided for C+L multi-band transceivers, but it is sensible to assume a higher cost due to higher complexity. Nevertheless, in Table 12 we assume a best-case cost scenario, assuming that the cost of a multi-band transceiver is equal to that of the L-band transceiver (43.2 c.u.). Even with that optimistic assumption, the use of single-band transceivers leads to lower total costs. It should be noted that the analysis is performed on a network that operates initially with a traffic load of 0.2. Thus, the corresponding values for that load (first row of Table 12) are all zero as no upgrades are required for that load. For a traffic load of 0.6, 15 bidirectional links need to be upgraded to the L-band to achieve  $\text{BBR} < 10^{-3}$ . In that scenario, 1,325 additional C-band transceivers and 114 L-band transceivers must be purchased if single-band transceivers are used. Therefore, the total number of new transceivers would be 1,439. However, this number is 1,374 if multi-band transceivers are used. Considering the costs previously mentioned for each type of transceiver, the use of single-band transceivers leads to around 11.3% savings in cost (even considering a best-case cost scenario for multi-band transceivers). In fact, the cut point for the multi-band transceivers is 38.3 c.u. (for 0.6 and 0.8 loads), which is lower than the cost of an L-band transceiver. If the cost of multi-band transceivers is higher than that cut point, the use of single-band transceivers is a more cost-effective option. Hence, although the use of multi-band transceivers leads to a reduction in the number of transceivers to be acquired, the use of single-band transceivers is the most cost-effective option when considering the techno-economic model in [90].

**Table 12.** Number of elements and cost to upgrade the network with the two alternatives considering  $BBR < 10^{-3}$ .

Load	Number of links to be upgraded. $BBR < 10^{-3}$	Option A			Option B	
		Number of C-band transceivers to be acquired	Number of L-band transceivers to be acquired	Cost (c.u)	Number of C+L transceivers to be acquired	Cost (c.u)
<b>0.2</b>	0	0	0	0.0	0	0.0
<b>0.4</b>	0	562	0	20,232.0	562	24,278.4
<b>0.6</b>	15	1325	114	52,624.8	1374	59,356.8
<b>0.8</b>	21	2316	269	94,996.8	2479	107,092.8

#### 4.4.2 Conclusions

We have evaluated the total transceiver costs when migrating a C-band towards a C+L multi-band network. We have demonstrated that the total number of additional transceivers required is lower if multi-band transceivers are purchased than if single-band transceivers are used (ensuring  $BBR < 10^{-3}$ ). However, the reduction in the number of transceivers does not translate into a reduction in the total cost compared to the purchase of single band transceivers (if the techno-economic model of [90] is considered). Therefore, the deployment of separate L-band transceivers when migrating from the C-band to C+L bands is a more cost-effective action than the use of multi-band transceivers.



## Chapter 5.

### Survivability Against Network Failures in MB-EON

While increasing the capacity of the optical networks, the importance of preserving the transmission of large amounts of data against network failures should be emphasized. The concept of survivability as a critical prerequisite for launching an optical transport network has been extensively studied in the literature in EONs [25], [26], [27] and SDM networks [91], [92], but has not yet been completely analyzed taking into account the characteristics of MB-EONs.

In the next sections, different survivability methods are analyzed in a fully and partially upgraded C+L multiband optical network. Specifically, in Section 5.1, we propose several protection methods to ensure resiliency against at least single amplifier failures in a fully upgraded network. Then, in Section 5.2, we consider a partially upgraded network, and analyze the most effective protection methods discussed in Section 5.1 when the separate amplifiers architecture (previously shown in Fig. 2) is used. Finally, in Section 5.3, the focus is set on the evaluation of network performance when considering different levels of partial migration and comparing the use of dynamic restoration versus dedicated protection.

The proposals and simulation results presented in this chapter have been published in [72], [93], [94].

#### 5.1 Survivability in a Fully Upgraded C+L band Network

In this subsection, we propose and compare different methods to achieve survivability, at least against single amplifier failures, in a fully upgraded C+L band systems, considering dedicated protection, and assessing two different amplifier architectures. We compare different strategies with different trade-offs in terms of protection capabilities and blocking ratio performance, and demonstrate that one of the proposed mechanisms (which leverages on one of the amplifier architectures) provides superior results if the aim is to protect at least against amplifier failures, or if service level agreements (SLA) with differentiated protection capabilities are enabled.

Amplifiers are active components prone to failures, whose repairment requires significant OPEX efforts since their implementation is outside the plant [95]. Moreover, according to [96] the failure rate of amplifiers is approximately 45 times higher than that of fiber failures (assuming amplifiers are located every 100 km); thus, providing resiliency against amplifier failure is of paramount importance. In classical EONs (using only the C-band), the establishment of disjoint end-to-end path connections protects against both amplifier and fiber failures. However, as will be shown later, in MB-EONs it is possible to increase the network performance at the expense of protecting all connections only against the most likely failure (i.e., amplifier failure). For this reason, we focus on protection against single amplifier failures, although we also consider the possibility of protecting some connections against link failures.

As previously mentioned, optical amplification in a MB-EON can be implemented through several architectures (Fig. 36). In separate amplifiers architecture (Fig. 36(a)), the signal amplification is performed using a single EDFA along with its associated demultiplexer/multiplexer structure. An alternative model (Fig. 36(b)) employs a wideband amplifier architecture, and thus does not suffer the bandwidth waste that affect the separate amplifiers architecture.

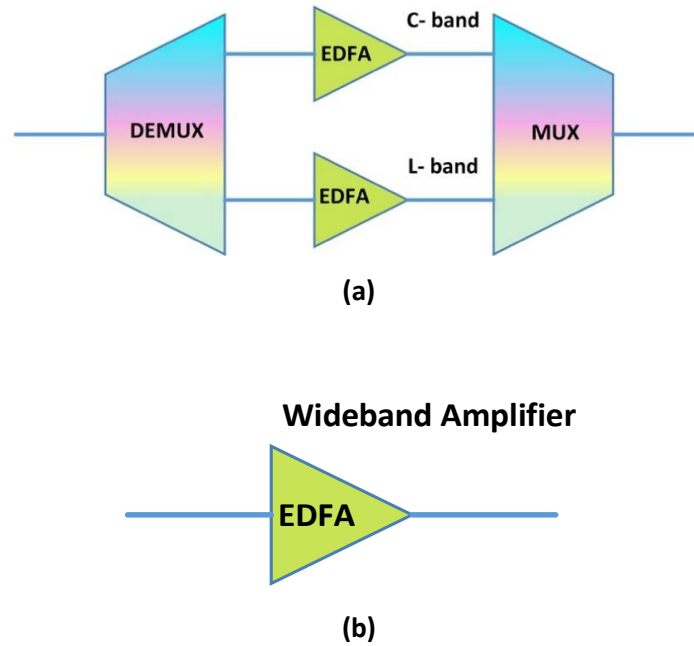


**Figure 36.** The implementation of C+L band networks through **(a)** separate amplifiers architecture and **(b)** wideband amplifier architecture [54].

In terms of survivability, when using the wideband amplifier architecture (Fig. 36(b)), the use of disjoint paths for primary and backup connections is a must to get protection against amplifier failures, and this also provides protection against fiber failures. When using the separate amplifiers architecture (Fig. 36(a)), and considering only protection against single EDFA failures, it is possible to route the primary and backup connections over the same fibers but using different spectral bands. Since primary and backup connections use different EDFAs (due to the separate amplifiers architecture), this approach offers resiliency against amplifier failures. Nevertheless, this strategy does not provide protection against fiber failures (in contrast with the use of a disjoint fiber path, which obviously, can also be used if this architecture is employed).

Therefore, in the case of using the wideband amplifier architecture, two link-disjoint paths for the primary and backup connection must be used when solving the survivable RBMLSA problem. In this scenario, the full spectrum (C+L bands) can be used to establish the primary and backup connections.

When the separate amplifier architecture is employed, different methods are proposed to solve the survivable RBMLSA problem, using dedicated protection. The first method (from now on,

“*basic approach*”) consists in using the same path for the primary and the backup connection but using different spectral bands for each one. There are two alternatives: using C-band for the primary and L-band for the backup, or vice versa. The second method (called, from now on, the *hybrid* method) exploits the advantage of using the separate amplifiers architecture, but allowing the primary and the backup connections to follow different end-to-end disjoint paths if needed. The hybrid strategy starts by following the same procedure as the first method: using the same path for both connections but using different spectral bands for each one. If no solution is found due to the unavailability of resources to establish the primary and backup connections, it explores the alternative of routing the primary and the backup connection following two link disjoint end-to-end paths. The primary connection is limited to use one single spectral band (always C or always L), while the backup path can utilize both the C and L spectral bands. It should be noted that connections protected in this way (with an alternate end-to-end path) are resilient not only to amplifier failures but also to fiber failures. Thus, the hybrid method provides amplifier failure resiliency for all connections, and additional fiber failure resiliency for a subset of them.

### 5.1.1 Simulation Setup and Results

The simulation was designed based on the settings described in Subsection 4.1.1. The NSFNet topology is used to evaluate the performance of the protection methods. The request blocking ratio versus traffic load is displayed in Fig. 37 for all studied scenarios, and the bandwidth blocking ratio is shown in Fig. 38. The request blocking ratio is defined as the fraction of requests that are blocked. The BBR as previously mentioned takes into account that different requests need different bandwidths. Thus, BBR is computed as the quotient between the sum of the requested bandwidths (once considering the selected modulation format) associated with blocked requests and the sum of the requested bandwidths of all requests. Besides the strategies mentioned in Section 5.1 (survivability in a fully upgraded C+L band Network), for comparison purposes, we have also evaluated the use of multiband (C+L) without protection when using the separate amplifiers architecture and the wideband amplifier architecture. Obviously, the lowest blocking ratio is obtained for the unprotected transmission, since no resources are used for protection. The results are slightly worse for the separate amplifiers architecture due to the guard-band between C and L bands. These results are only shown to provide a baseline of the blocking ratio that can be achieved without protection, but from now on we focus on resilient solutions.

The blocking ratio for the separate amplifiers architecture with the basic resiliency strategy is the same independently of which band (C or L) is used for primary connections (and the other for backup connections). Since the same number of resources must be reserved for both connections, the lower number of available slots in the C band (320 vs 512) is the limiting factor. Consequently, a significant part of the L band is not utilized.

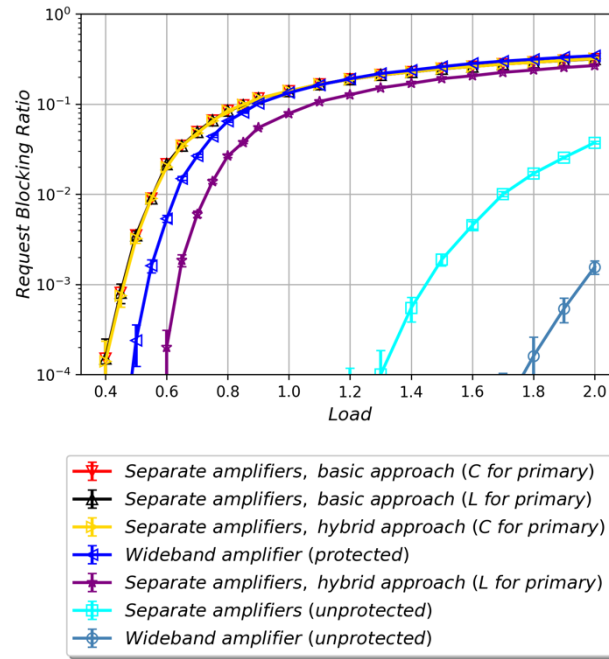


**Figure 37.** Request blocking ratio depending on the network load.

In contrast, the use of the wideband architecture with dedicated path protection uses all available spectrum in the C and L bands, and thus provides better results in terms of blocking ratio than the previous alternative, besides providing protection not only for EDFA failures but also for fiber failures.

However, for the separate amplifiers architecture we also proposed a variation to achieve resiliency, the hybrid technique. Fig. 37 shows that when the hybrid technique is used, and the L band is used for the primary connections, a significant decrease on the blocking ratio is obtained compared to all the previous cases with resiliency (using either the separate amplifiers or the wideband amplifiers architectures). It should be noted that when the hybrid technique is used, all connections are resilient to EDFA failures but only a portion of them are also resilient to fiber failures.

Therefore, in terms of resiliency, as expected, the end-to-end disjoint paths approach (which is used with the wideband amplifier architecture) is the most suitable one. However, the use of separate amplifiers and the hybrid protection technique leads to much lower blocking ratio (more than one order of magnitude for traffic loads lower than 0.6). Thus, that technique allows for a more efficient use of resources but requires SLA differentiation, where some connections are protected by means of an alternate disjoint path (thus being resilient to fiber and EDFA failures), while others are protected by using a different spectral band of the same route (being resilient to EDFA failures).

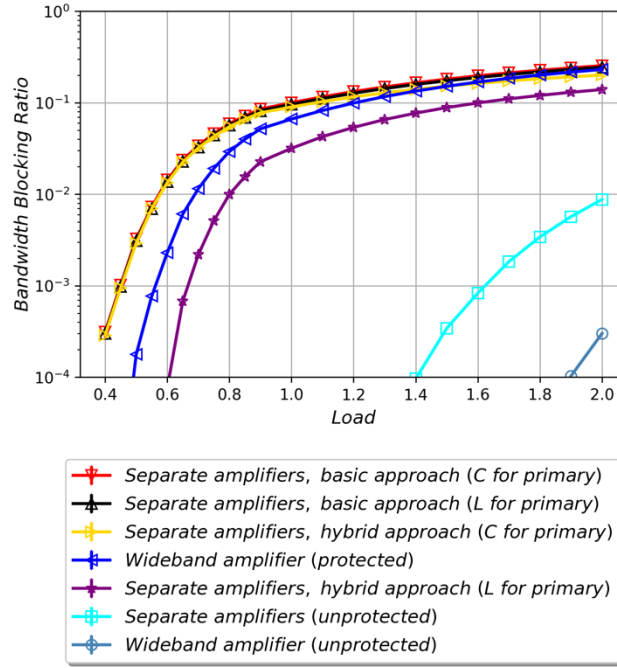


**Figure 38.** Bandwidth blocking ratio depending on the network load.

### 5.1.2 Conclusions

We have proposed and compared different strategies to provide survivability against, at least, amplifier failures in multi-band (C+L) EONs considering two different amplifier architectures: separate amplifiers vs wideband amplifier. We have demonstrated that the use of the separate amplifiers architecture together with the hybrid protection technique has significant performance advantages in terms of blocking ratio, thus enabling the network to support higher traffic loads.

## 5.2 Survivability in a Partially Upgraded C+L-band Network

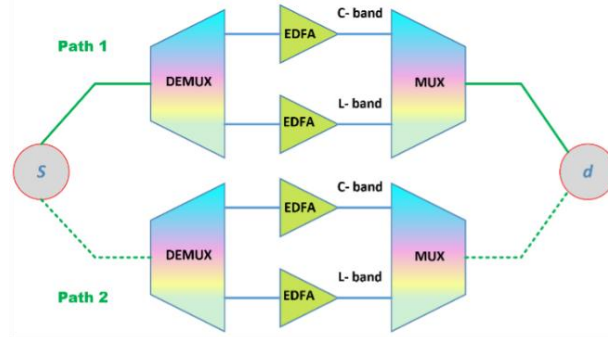
This section is an extension of Section 5.1, and our objective is to adapt the protection technique in Section 5.1 to be able to operate efficiently in a partially migrated network in which not all links have been migrated to support the L-band, and to evaluate its performance in terms of blocking probability.

Fig. 39 represents the method of classical protection in a C+L band system. Reserving the resources over two link-disjoint paths provides the established connections with data persistence against single EDFA failures as well as fiber failures simultaneously. In the classical path protection method, two link-disjoint paths are selected for the primary and backup connections. Then, in the phase of band selection of the RBMLSA algorithm, the algorithm checks whether all the links in the selected paths are migrated to the L-band or not. If the answer is true, the L-band is prioritized. Otherwise, or in case of not finding the required resources for serving the connection in that band, the C-band spectrum slots would be analyzed.

In Section 5.1, we proposed a protection technique for fully upgraded C+L networks, called “hybrid approach”. Several variants were analyzed, but we present here the one that gave the

best results. When using that technique, primary and backup connections are routed through the same path, but the L-band is dedicated to primary connections, and the C-band is employed for backup connections. Considering the use of the separate amplifiers architecture (also shown in Fig. 36(a)), this method ensures survivability against single EDFA failures (but not against fiber failures). If there are insufficient resources to establish the primary and backup connections in that way (which may occur since the available spectrum in the C-band is less than in the L-band), a second phase is run where it is checked whether it is possible to establish them using two link-disjoint paths (the primary using the L-band, but allowing the backup to use either the C or the L band). If the second phase is successful, the established connection is protected against both amplifier and fiber failures. It is worth noting that, in Section 5.1, a fully upgraded network was considered so all links had, potentially, spectral resources in the L-band. Moreover in Section 5.1, it was also demonstrated that the use of the hybrid approach instead of the classical method leads to a reduction of the BBR of the network.

Here, we focus on partially upgraded networks, where there are links not upgraded to C+L-band. In those scenarios, directly using the hybrid approach as defined in Section 5.1 leads to a very high blocking ratio. This is because the fibers that have not been upgraded to the L-band become the limiting factors. Therefore, in this section, we consider a variation of the hybrid approach where in the second phase of the hybrid approach, the primary connections are able to use the whole spectrum of both C+L bands rather than only the L-band. The backup connections can use C+L bands like in the proposed hybrid approach of Section 5.1.



**Figure 39.** Example of the use of disjoint paths in classical path protection and the use of separate amplifiers (i.e., a different EDFA to amplify each band).

### 5.2.1 Simulation Setup and Results

Fig. 40 shows the request blocking ratio for the classical path protection method and the hybrid approach (with the variation introduced in this section) when the network is partially upgraded through the migration of 3, 9, 15, and 18 bidirectional links in the NSFNet topology (Fig. 40.a) and in the DT network (Fig. 40.c). As the JPN12 topology has 17 bidirectional links, we have also considered a 12 bidirectional links upgrade scenario instead of the impossible 18 links upgrade (Fig. 40.b). The set of fibers to migrate in each case was selected using the method proposed in Section 4.2. As shown in Fig. 40, lightpath protection using the hybrid approach leads in most of cases to lower blocking ratio when compared to the classical method (an

exception for this behavior is obtained in the NSFNet for an 18 links upgrade). For the NSFNet and DT topologies, hybrid and classical methods have almost the same performance when a few links are upgraded (e.g., 3 bidirectional links upgraded). In fact, in the DT network, for the first two upgrade scenarios, both classical and hybrid protection methods yield very similar results. However, the hybrid approach outperforms the classical protection in other upgrade scenarios for the DT network. The JPN12 topology is the one that holds a greater advantage for the hybrid approach in different upgrade scenarios. We also obtained the BBR with similar results and conclusions for all the studied topologies.

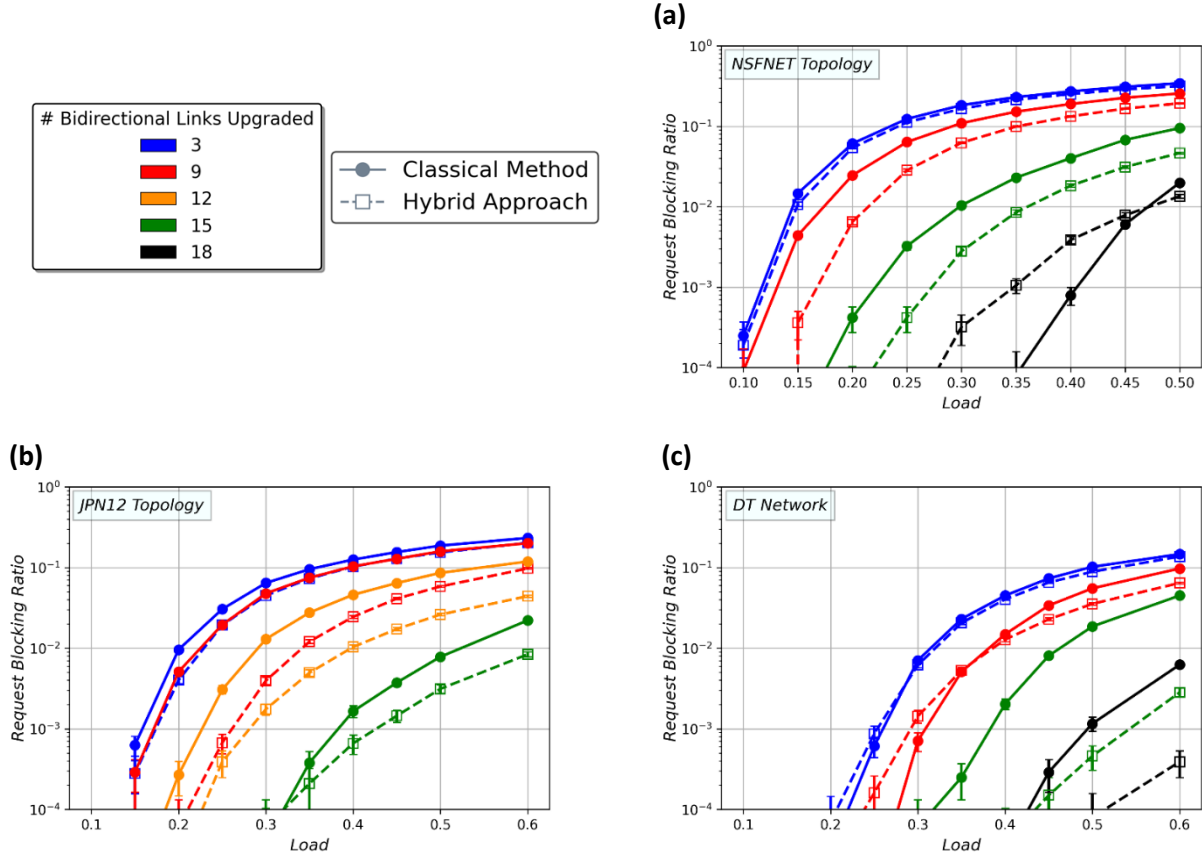
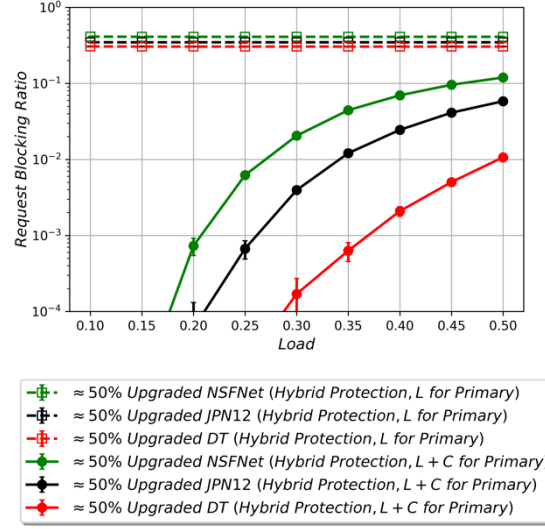


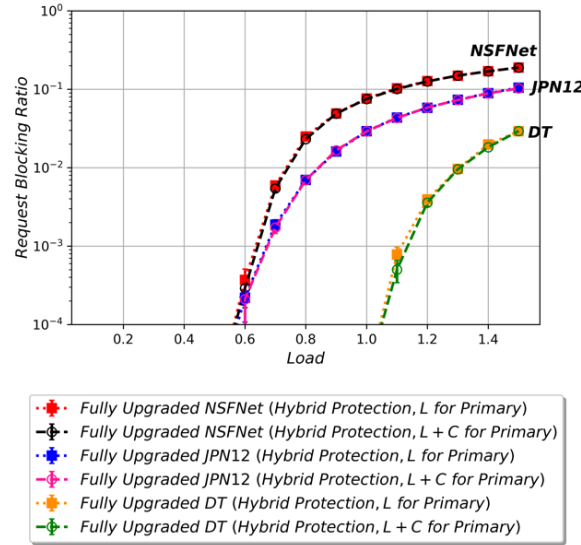
**Figure 40.** Request blocking ratio depending on the network traffic load in the (a) NSFNet topology, (b) JPN12 topology, and (c) DT network under different upgrade scenarios.

As previously mentioned, the proposed modification of the hybrid approach (L+C for Primary) provides good performance in a partially upgraded network in contrast with the original hybrid approach proposed in Section 5.1 (only L for Primary). Fig. 41 (a) compares the discussed hybrid approaches for a scenario where around 50% of the bidirectional links of the NSFNet (12 out of 21), JPN12 (9 out of 17), and DT (12 out of 23) topologies have been upgraded. It can be observed that the employment of the modified hybrid approach presented in this section significantly reduces the blocking ratio compared to the original approach (which in fact leads to very high blocking ratios in partially upgraded networks). We did the same analysis with different levels of migration and obtained similar results: the new proposal outperforms the one in Section 5.1. We have also analyzed if that good behavior in a partially upgraded network for the new variation comes at a cost, compared with the original proposal, when it is used in a

fully upgraded. Fig. 41 (b) compares the performance of the new and the original version of hybrid protection when they are used in a fully upgraded network. As shown in Fig. 41 (b), both options behave similar in a fully upgraded network but, when the network is partially migrated, the new approach clearly overperforms the original version (Fig. 41 (a)).



(a)



(b)

**Figure 41.** Comparison of the hybrid approaches (L-band for primary connections vs. L+C bands for primary connections) in (a) 50% upgraded and (b) fully upgraded NSFNet, JPN12, and DT topologies.

### 5.2.2 Conclusions

In this section, we have analyzed the performance of a protection method proposed in Section 5.1, the hybrid approach, when operating in a partially upgraded network. Simulation results have shown that the original hybrid approach in 5.1, in which primary connections can only use L-band resources, is not effective in a partially upgraded network, as it performs poorly in terms of blocking probability. However, modifying the algorithm leads to the same performance as



the original one when the network is fully upgraded and enables efficient operation in partially upgraded networks. This modification is performed by allowing the primary connections to be also established in the C-band. Classical path protection and the modified hybrid approach have been investigated in different upgrade scenarios. Simulation results indicate that the modified hybrid approach generally leads to better results in terms of blocking ratio compared to the classical path protection method. Although the hybrid approach generally works better in terms of blocking probability, the classical approach is more effective for network survivability, as it provides protection against both amplifiers and fiber failures.

### 5.3 Dynamic Restoration in a Partially Upgraded C+L-band Network

In this section, we evaluate the performance of dedicated protection and dynamic restoration for different levels of partial migration. The process of achieving different levels of partial migration of a network is performed using the algorithm proposed in Section 4.2. The objective of this section is to analyze the performance of a network in the presence of dynamic restoration during the process of migration from the C-band to the C+L bands.

#### 5.3.1 Failure Scenarios and Survivability Strategies

We consider that every 500 connection requests, a single link failure is introduced, with a link being randomly selected for failure. Also, we consider that the failure is repaired after a random repairment time (which is selected randomly to match the interval of receiving from 1 up to 100 connection requests). Nevertheless, we have also decreased the frequency of failures by considering 1000 connections as the successive points of failure occurrence.

It should be noted that a link consists of two fibers, one per direction. Therefore, a link failure implies the failure of both fibers, and thus disrupts all lightpaths traversing any of those fibers. We consider two different survivability strategies. A first option is to rely on dynamic restoration. When a failure takes place, attempts are made to reroute the affected connections. Therefore, for a certain affected connection, the RBMLSA algorithm will be re-executed. In case that among the precomputed link disjoint paths, the required bandwidth can be allocated successfully, the affected connection request will be re-established and thus recovered. Otherwise, it will be marked as an unrecovered connection. The second option is to employ path protection, so that for every connection request two disjoint lightpaths are established, so that the communication will be effectively protected against single link failures.

It is worth noting that we employed dynamic restoration and classical path protection methods as proposed in the literature. Since optical fibers are more commonly chosen for failure scenarios in the literature, we followed the same approach by selecting fibers rather than amplifiers. In this section, our main focus is on evaluating a partially upgraded network when protected using these protection methods.

#### 5.3.2 Simulation Setup and Results

We start the performance evaluation results by analyzing the dynamic restoration method in a partially upgraded network in terms of incoming BBR and total BBR. The incoming BBR metric indicates the proportion of total requests that cannot be established upon reception. This occurs when there are insufficient resources to establish a connection at the specific moment

the request is received, accounting for the current state of the network. The total BBR is the fraction of requests that either cannot be initially established or, if initially established, cannot be successfully recovered due to an eventual subsequent link failure during their lifetime.

Fig. 42 represents the incoming and the total BBR versus traffic load when the (a) NSFNet topology, (b) JPN12 topology, and (c) DT network rely on dynamic restoration for survivability. Different levels of partial migration are displayed in the figure with different color lines. In that figure, the total BBR and the incoming BBR are specified by the solid lines and the dashed lines, respectively. In Fig. 42, the expected outcome is realized for all the analyzed topologies and the total BBR is higher than the incoming BBR, since rerouting for the already established connections that may experience the link-cut due to the introduced failure is not always executed successfully due to lack of network resources. As the focus of this section revolves around analyzing the impact of partial migration on a network, which is equipped with a survivability method, let us analyze the total BBR considering different scenarios of network migration. Assuming that an acceptable value of the total BBR is  $10^{-3}$ , Fig. 42(a) demonstrates that upgrading 12 bidirectional links of the NSFNet topology, which is translated to providing L-band optical components for 57% of the network links improves the supported network traffic load by around 1.5 times compared to the C-band only network when the network is protected using the dynamic restoration method.

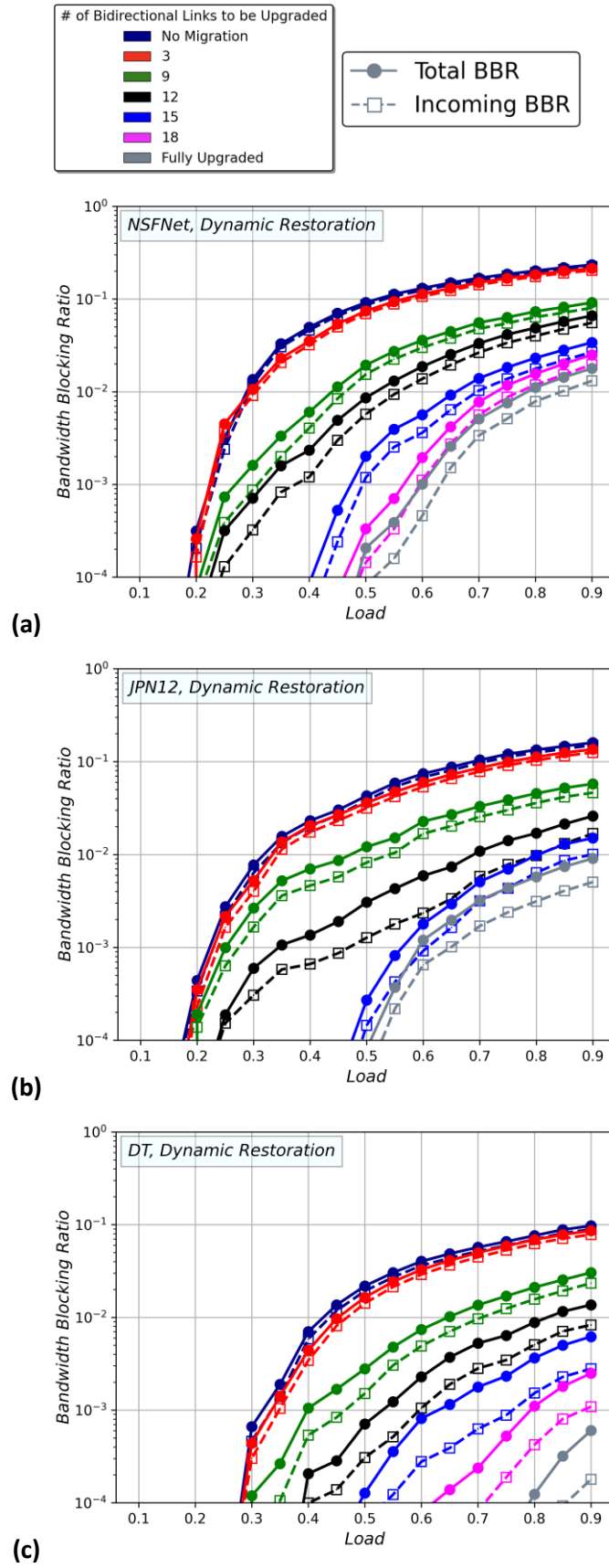


**Figure 42.** BBR depending on network load considering partial migration and dynamic restoration in the (a) NSFNet, (b) JPN12, and (c) DT topologies.

Besides the NSFNet topology, the results for the JPN12 topology and the DT network verify the suitability of the application of partial migration for different network topologies when the dynamic restoration is employed. For better understanding of the advantages of joint application of dynamic restoration and partial migration, in Fig. 43, we compare the traffic load increment when dynamic restoration is used instead of dedicated protection during the migration of network links. The points represented in that figure correspond to cases where the BBR is lower than  $10^{-3}$ . The solid line represented in Fig. 43 corresponds to the NSFNet topology, while the dashed line and the dotted line refer to the JPN12 topology and the DT network, respectively. It should be noted that in Fig. 42 and in Fig. 43, it is assumed that the network suffers from quite frequent failures in optical fibers. In other words, a new failure appears in every 500 incoming connections. As shown in Fig. 43, the percentage of bidirectional links to be upgraded to the L-band is specified on the x-axis and the percentage of additional traffic load that can be supported using the dynamic restoration versus dedicated protection is plotted on the y-axis. As can be seen in that figure, due to the better use of resources, the application of dynamic restoration leads the supported traffic load to be significantly improved compared to the use of dedicated protection.

Fig. 43 also shows that for the NSFNet and DT topologies, upgrading of 60% of the total number of bidirectional links contribute to a significant boost in the supported traffic load. For the JPN12 topology, it can be observed that in the middle stages of partial migration, while we increase the percentage of the upgraded links, the excellence of the dynamic restoration over the dedicated protection remains constant. More interesting, it can be concluded from Fig. 43 that the application of the partial migration up to 60% of the bidirectional links within the analyzed topologies brings about more advantages in terms of the supported traffic load than the fully upgraded network compared to the classical protection. Therefore, in case of having limited financial resources, the joint employment of the partial migration and the dynamic restoration method could be an interesting option for the network operators.

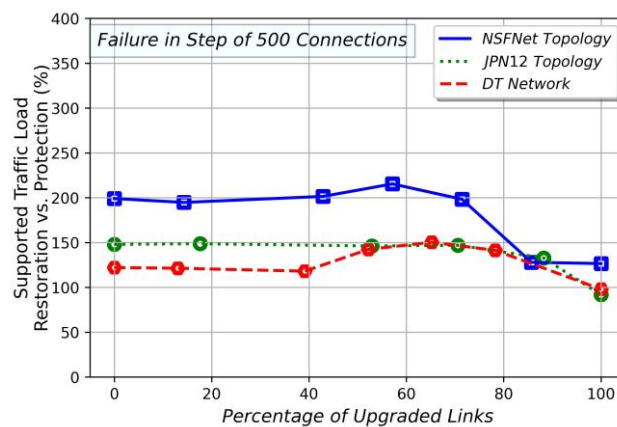


**Figure 43.** Supported traffic load with different levels of partial migration using the dynamic restoration with respect to the dedicated protection (failure rate = every 500 connections).

We proceed with the simulation results analysis by changing the time between failures. Firstly, we assess the performance of the employed survivability methods, namely classical path protection and dynamic restoration in a partially upgraded network taking into account that no

failure is introduced to the network. The additional load that can be supported when using dynamic restoration compared to the protection in no failure scenario is shown in Fig. 44. Once again, in Fig. 44, it can be observed that upgrading 60% of the bidirectional links to the L-band in the NSFNet and DT topologies significantly improves the excellence of the dynamic restoration over the dedicated protection. In fact, this improvement is around 650% and 500% for the NSFNet topology and the DT network, respectively. Based on Fig. 44, when optical fibers within the analyzed topologies do not experience any failure during the simulation, performing the partial migration of around 60% for the NSFNet and DT topologies would provide interesting results. According to Fig. 44, the interesting level of migration for the JPN12 topology changes to 70% of the bidirectional links.

Then, we investigate the network performance considering that the link failure is introduced to the network at each 1,000 connections milestone. A similar assumption as before is considered for the time interval that a link failure may remain in the network. Fig. 45 confirms that for the network operators, during the process of network migration, the employment of dynamic restoration is highly recommended as it leads to remarkable increase in the supported traffic load compared to the classical protection method.

The results achieved so far in this subsection are based on the assumption that during the resource allocation phase in the RBMLSA algorithm, the priority is given to the L-band. Therefore, firstly, the L-band is analyzed in terms of the availability of resources. Then, in case that the required block of FSs is not available in the L-band, attempts are made to meet the requested bandwidth through searching over the C-band spectrum. Another strategy for the resource allocation is also used in which the C-band is prioritized over the L-band while the dynamic restoration method is employed. The comparison between the potential strategies for performing the resource allocation algorithm shows that giving the prioritization to the L-band over the C-band significantly improves the total BBR. For instance, for the traffic load of 0.45 while 15 bidirectional links are upgraded in the NSFNet topology, providing the L-band with the higher priority results in around two orders of magnitude lower blocking ratio than if the C-band is prioritized.

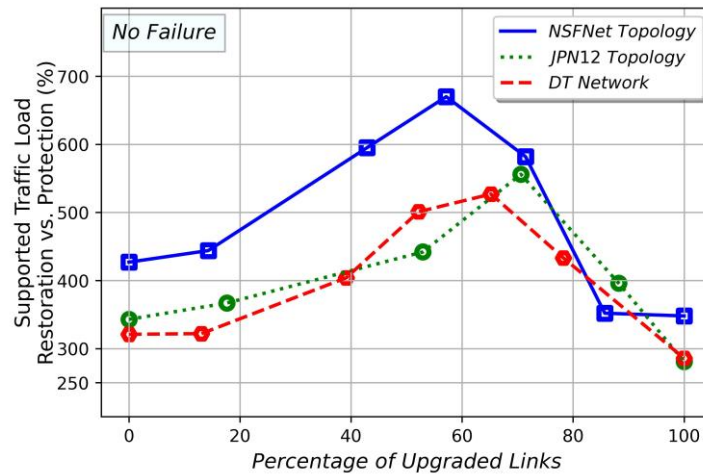


**Figure 44.** Supported traffic load with different levels of partial migration using the dynamic restoration with respect to the dedicated protection (fiber-cut failure is not introduced to the network).

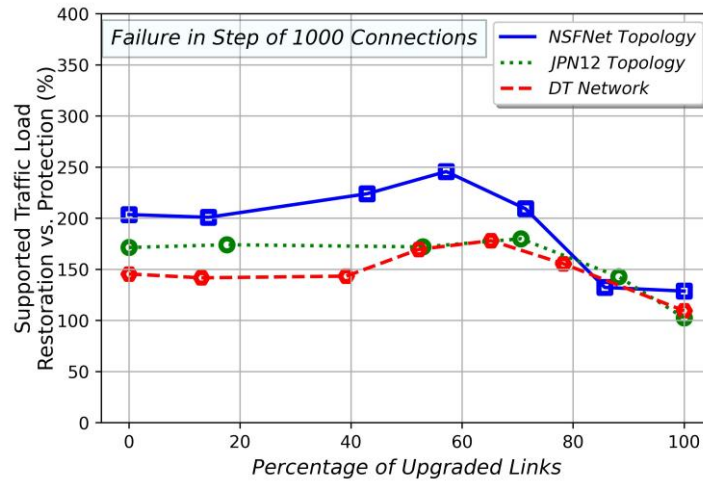


**Figure 45.** Supported traffic load with different levels of partial migration using the dynamic restoration with respect to the dedicated protection (failure rate = every 1000 connections).

### 5.3.3 Conclusions

In this section, we have analyzed the advantages of using restoration instead of protection during the migration from current C-band to C+L bands optical networks. For that aim, we have evaluated the performance of the NSFNet topology, the JPN12 topology, and the DT network set up with the classical path protection and the dynamic restoration in different levels of partial migration. The simulation results have demonstrated that in case of having financial challenges, upgrading of around 60% of the links within the NSFNet topology and the DT network in which the dynamic restoration is employed would lead the BBR to be improved more than one order of magnitude compared to the C-band network. For the JPN12 topology, this achievement is obtained by upgrading around 70% of the links (assuming no failures or very infrequent ones).

In this section, different scenarios for introducing a link failure to the network when the dynamic restoration is employed have been investigated. Firstly, it has been assumed that the network experiences a link-cut every 500 connection requests. Then, we have evaluated the network performance through an increase in the interval between failures. Furthermore, it has been considered that fixing a link failure may take time and the following 100 incoming connections may suffer from the lack of resources due to the introduced failure. It has been shown that equipping the network with the dynamic restoration method in the middle stages of partial migration could significantly increase the supported traffic load compared to the employment of classical path protection method.

Finally, a preliminary analysis suggests that the prioritization of the L-band over the C-band during the resource allocation phase improves the BBR in a partially upgraded network. Nevertheless, a more extensive analysis remains as a future research line.

## Chapter 6 .

### SLA-Differentiated Protection in MB-EONs

As it is previously noted, moving from the C-band to the C+L-band increases the capacity of optical networks by more than two times. Hence, the failure in any network component will lead to huge data loss, thus making the provisioning of the C+L band systems with survivability methods a critical issue. In Chapter 5, optical fibers and EDFAs have been considered as the network elements most prone to failures. In that chapter, we introduced a new method of protection, (EDFA protection (“*basic approach*”)) to provide C+L multiband optical networks with survivability against a single failure in EDFAs (assuming the separate amplifiers architecture shown in Fig. 36(a) is used). To achieve EDFA protection, the primary and backup lightpaths are established along the same end-to-end path, but utilizing the L-band for the primary and the C-band for the backup connection. Using different spectral bands to transmit primary and backup connections together with the utilization of the separate amplifiers architecture (Fig. 36(a)), ensures that both lightpaths employ different amplifiers, thus protecting the network against a single EDFA failure. This technique enables an improvement in network capacity utilization, at the expense of providing protection only against a single EDFA failure, but not against fiber cuts. In a network with the separate amplifiers architecture, the DPP method obviously outperforms the EDFA protection technique (“*basic approach*”) introduced in Chapter 5 (and previously described) in terms of the provided level of survivability. This is because it uses different disjoint paths for the provisioning of primary and backup connections, and in case of a single failure in EDFAs or optical fibers, the backup lightpath would be activated. The protection level offered by the SBPP is similar to the DPP method, but with improved efficiency, as the spectral resources over the common backup lightpaths can be shared. In Chapter 5, we also introduced a new and more efficient protection method in C+L band networks over the separate amplifiers architecture, called “*hybrid approach*”, which is the combination of EDFA protection (“*basic approach*”) and DPP method.

On the other hand, optical networks are designed to serve a large number of users and services, and the required quality of service (QoS) may differ for each of them. Therefore, offering a service level agreement (SLA) differentiation method by network providers is crucial to effectively manage network resources and to enhance network performance. Implementing SLAs enables operators to categorize clients based on service quality and usage, thereby fostering a more structured and efficient network. This stratification not only enhances customer satisfaction through tailored service offerings but also maximizes economic benefits by aligning resource allocation with revenue potential. The provisioning of QoS-aware classification for data traffic has been studied in the literature, considering EONs [97], [98],

[99]. Therefore, in this chapter, we propose a technique to offer an SLA-differentiated protection mechanism. Firstly, we consider network users subscribing to “gold” and “silver” categories, with the former having more stringent requirements on survivability: connections of “gold” clients are protected against EDFA and fiber failures using DPP method, while connections of “silver” clients are only protected against EDFA failures, using the EDFA protection method (“*basic approach*”). Then, we employ the “*hybrid approach*” for C+L multi-band optical networks, and introduce a new SLA level of protection, labeled “silver plus”.

This is, to the best of our knowledge, the first reported case where a differentiated level of protection is offered to different types of users in C+L multiband networks. In particular, the key contributions of this Chapter are as follows:

- 1) Improvement of the C+L optical network performance in the presence of the SLA-differentiated protection. In this way, three different SLA categories are introduced: “gold”, “silver”, and “silver plus”. The performance of the C+L band systems with “gold” and “silver plus” users is compared with “gold” and “silver” users. Additionally, rather than relying solely on DPP for “gold” users, we also analyze the use of shared backup path protection (SBPP) for these “gold” clients in the context of the proposed SLA-differentiated protection approach.
- 2) Analysis of an AC mechanism to increase the chances of success for the establishment of “gold” connections through managing the spectrum resources in the C+L band systems.
- 3) Analysis of the proposed SLA-differentiated method considering non-uniform traffic to provide more realistic results.
- 4) Proposal and analysis of a new policy for SLA-differentiated protection. In this regard, rather than splitting users or clients into “gold” and “silver plus” categories, a percentage of the traffic associated to each user is assigned to “gold” category and the remaining to “silver plus” category, thus providing a minimum guaranteed highly protected bandwidth to each client.

This chapter firstly presents the survivability methods employed in our proposal to achieve SLA-aware service provisioning in Section 6.1. Then, an AC mechanism, designed to improve the performance of high priority services is discussed in Section 6.2. A new strategy for scenarios where a fraction of traffic coming from a user or client is highly protected while the remaining fraction has a lower degree of protection is proposed in Section 6.3. Next, Section 6.4 provides numerical results associated to dynamic network performance evaluation. Finally, the chapter is concluded by reporting the main findings in Section 6.5.

The ideas and findings presented in this chapter have been proposed and published in [100] and [101].



## 6.1 SLA Differentiation Protection Techniques

In this section, we consider four different types of protection methods: (1) Dedicated Path Protection (DPP); (2) Shared Backup Path Protection (SBPP); (3) EDFA protection; and (4) hybrid protection. Table 13 summarizes the main characteristics of each of these techniques (and their relationship with different SLA categories, which will be later explained).

The DPP method provides protection against a single failure in fibers or EDFAs in C+L band systems by using link-disjoint paths. Both primary and backup connections can employ either the C or the L band.

The SBPP method also offers protection against single fiber or EDFA failures, but enables backup lightpaths to share spectral resources over the common links if the corresponding primary lightpaths are disjoint.

As previously mentioned, the EDFA protection method is aimed to ensure network survivability in case that a failure in EDFAs occurs. The primary and backup lightpaths are established along the same end-to-end path, utilizing the L-band for the primary and the C-band for the backup connection, and thus using different amplifiers as the separate amplifier architecture is used. An alternative protection strategy to the basic EDFA protection method, which we also introduced in Chapter 5, is called the hybrid approach. When a request is received, the basic EDFA protection method is initially used, that is, the primary and the backup lightpaths follow the same path but use different bands (L for the primary and C for the backup). Since there is less bandwidth in C-band than in L-band (Fig. 1), C-band becomes a limiting factor leading to blocking. When the hybrid approach is used, if there are no available resources to establish the primary and backup lightpaths through the same route, a second phase is executed to search for two disjoint paths, considering only the L band for the primary lightpath, and allowing the use of the C or L bands for the backup lightpath.

The hybrid protection method is illustrated in Fig. 46. It should be noted that in the hybrid approach, survivability against single EDFA failures is achieved for all the established connection requests. However, those connections that are served in the second phase are also protected against single fiber failures (as link-disjoint paths are used for the primary and backup lightpaths).

It should be noted that DPP, EDFA protection and hybrid protection techniques support both 1+1 and 1:1 strategies. In the 1+1 strategy, the same data is transmitted simultaneously through the primary and backup lightpaths. This consumes more energy but ensures zero recovery time when a failure occurs, as the data is already available on both paths. In contrast, the 1:1 strategy transmits data only through the primary lightpath, switching to the backup lightpath when a failure occurs, which slightly increases the recovery time. However, it is worthy to note that during normal operation with 1:1, the backup lightpath can be used to transmit low priority, pre-emptable traffic. This effectively increases the network transmission capacity compared to the 1+1 strategy, doubling the capacity under normal conditions. Obviously, in the event of a failure, this "extra capacity" cannot be used, as the backup resources are committed to protect the primary, failing lightpath.

When SBPP is used, backup resources on each link are shared to protect multiple connections (enabling a 1:N-like strategy). Since these resources are shared, and potentially among different primary connections in each link, the recovery time is higher than in the previous approaches. This is because, during the recovery process, the backup lightpaths must be configured based on the specific fiber that has failed, adding to the recovery time. In [102], Kumar *et al.* quantified the recovery time, finding it to be nearly twice as long for shared protection compared to dedicated protection across two network topologies. Furthermore, unlike the other approaches, SBPP does not allow the backup resources to be used for transmitting low priority, preemptable traffic, meaning it does not offer the “extra network capacity” available in the other methods.

From a computational perspective, the time required to determine the route and the spectral resources to allocate for the backup lightpath varies depending on the protection strategy employed (DPP, SBPP, EDFA protection, or hybrid protection). This will be analyzed in Subsection 6.4.1.

Regarding Service Level Agreements, we first consider “gold” SLA clients, whose demands are served using DPP, and “silver” SLA clients, whose demands are served with the basic EDFA protection method. Then, a different SLA category is proposed, “silver plus” SLA clients, which consists in employing the hybrid protection strategy rather than the basic EDFA protection approach. Furthermore, we also consider here the use of the SBPP method for the accommodation of high priority (“gold”) users.

A summary of the characteristics of the different SLAs considered in this chapter (“gold” with the DPP and SBPP options, “silver”, and “silver plus”) is presented in Table 13. It should be noted that “gold” SLA categories ensure survivability against a single fiber or EDFA failure, while “silver” or “silver plus” categories only guarantee protection against single EDFA failures.

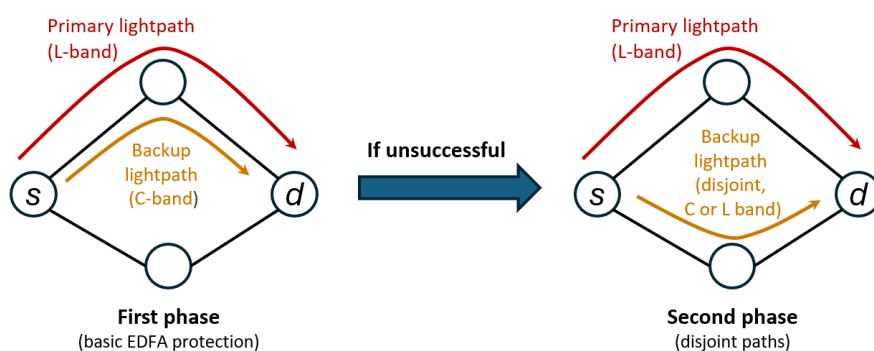


**Figure 46.** Hybrid protection method.

**Table 13.** Specifications of different SLA categories<sup>1</sup>.

SLA Type	Protection Method	Routing		Spectral Band		Protection Paradigm	Recovery Time	Computing Time	Extra Capacity <sup>*</sup>
				Primary	Backup				
Gold (DPP)	Dedicated Path Protection	Two disjoint paths		L+C	L+C	1:1 or 1+1	Zero (1+1) Low (1:1)	Low	Yes (for 1:1)
Gold (SBPP)	Shared Backup Path Protection	Two disjoint paths (backup resources shared, if possible)		L+C	L+C	1:N-like	Moderate	Moderate	No
Silver	EDFA Protection	One path		L	C	1:1 or 1+1	Zero (1+1) Low (1:1)	Low	Yes (for 1:1)
Silver Plus	Hybrid Protection	Phase #1	One path	L	C	1:1 or 1+1	Zero (1+1) Low (1:1)	Low	Yes (for 1:1)
		Phase #2	Two disjoint paths	L	L+C				

\* Extra capacity: Possibility of the backup lightpath being used to transmit low priority, pre-emptable traffic during normal operation.

<sup>1</sup> The SLA categories are based on the methods described earlier in Section 6.1.

Independently of the type of protection considered, in order to establish the required connections, the RBMLSA problem should be solved. The routing problem between a pair of source and destination is solved following the execution of the  $K$ -shortest paths algorithm. This execution is performed based on the length-based approach in which a potential path with the shortest distance is prioritized. The band allocation strategy that is considered is summarized in Table 13, although it should be mentioned that based on the simulation setup (see Subsection 4.1.1), for those cases where both bands can be used, the L-band is prioritized, which means that searching through the C-band spectrum is performed only if the requested bandwidth is not available over the L-band.

## 6.2 Admission Control (AC)

In order to improve the performance of “gold” services, the proposed SLA policy can be complemented with an AC scheme. Specifically, an incoming “silver plus” connection can be accommodated only if the vacant FSs in the L-band spectrum is higher than a certain operator-defined threshold of the total resources provided by the L-band. In other words, a fraction of the L-band spectrum is always exclusively available for “gold” services, and that percentage acts as a threshold in the AC mechanism for the “silver plus” connections. While this strategy reduces the blocking probability of “gold” connections, it increases the blocking probability of “silver plus” connections. Therefore, we will later analyze whether this trade-off is beneficial.

### 6.3 Enhanced SLA-Differentiated Protection

In the SLA categories described earlier, it was assumed that all traffic coming from a client requires the same level of protection. However, there may be cases where a client aims to transmit traffic with different priorities, and thus may require the highest level of protection (DPP/SBPP) only for a given fraction of its traffic and rely on EDFA or hybrid protection for the remaining part. Therefore, network operators should have flexible mechanisms to accommodate these diverse client needs, and categorize clients based on the percentage of highly protected traffic stated in their contracts.

In order to deal with these new SLA types, we propose the splitting of connection requests into two smaller sub-demands: one will be served with DPP or SBPP and the other with hybrid protection. (Since we will show that hybrid protection outperforms EDFA protection, our focus will be on hybrid protection for the low priority traffic.) Note that this process results in the establishment of four lightpaths in the network (a primary and a backup lightpath for each sub-demand) instead of only two lightpaths. However, each lightpath uses fewer spectral resources since the traffic demand, and thus the required bandwidth, is divided among the sub-demands. For instance, let us assume a certain connection request associated to a client in which 50% of the traffic requires DPP/SBPP (i.e. the “gold” type of protection), while the remaining 50% requires hybrid protection (i.e. the “silver plus” type). If the total data rate demanded by the request is  $R$  Gb/s, the connection request will be split into two sub-demands: one that requires  $R/2$  Gb/s with a high level of protection (DPP/SBPP, i.e. two link disjoint lightpaths), while the remaining traffic requires moderate protection (hybrid protection, i.e. two lightpaths not necessarily disjoint). If both sub-demands, with their corresponding level of protection, can be allocated in the network, the connection will be established. Otherwise, if the requirements of only one or none of the sub-demands are met, the connection will be blocked.

### 6.4 Simulation Setup and Results

In this section, the dynamic performance of a C+L band network that provides differentiated services based on the proposed methods is assessed in terms of blocking ratio. To this end, the same simulation setup as in Subsection 4.1.1 is considered. Then, the different SLA categories shown in Table 13 will be analyzed individually, demonstrating additional strengths and weaknesses together with those already outlined in the table. Based on that analysis, the potential of different combinations of SLA categories will be explored, mainly under uniform traffic, but also considering non-uniform traffic. Finally, the overall network performance will be evaluated under a scenario with enhanced SLA-differentiated protection, i.e. considering clients requiring high protection only for a portion of their traffic.

#### 6.4.1 Analysis of the SLA Categories

We first consider a network scenario with a single type of client, meaning all incoming connections correspond to a single SLA: “gold” with DPP, “gold” with SBPP, “silver” or “silver plus”. Fig. 47 shows the request blocking ratio versus the offered load for each of these SLA categories. This figure highlights the advantage of the two SLA categories (“gold (SBPP)” and “silver plus”) over the SLA-differentiated protection mechanism with “gold (DPP)” and

“silver” SLA. The use of “silver plus” reduces the blocking ratio by an order of magnitude (for loads lower than 0.6) when compared with “gold (SBPP)”, making it the most effective technique in terms of reducing the request blocking ratio. This allows the network to carry more traffic while maintain a low blocking ratio. However, it is important to note that the “silver” and “silver plus” SLA categories only protect against EDFA failures and not fiber cuts. For those clients or services that require a higher level of protection, it seems reasonable to differentiate SLAs based on protection needs and optimize the use of network capacity by supporting both categories. This approach will be explored in the following subsection.

Besides comparing the different SLA categories in terms of blocking ratio, computing time has also been considered. Fig. 48 shows the average computing time per request for each SLA category in the same scenarios as in Fig. 47. As expected, the computing time associated with SBPP is the highest, exceeding the other methods by more than two orders of magnitude. It should be noted that dynamic scenarios have been considered, where the speed of the algorithm is crucial. While the specific results depend on the implementation, it is clear that SBPP requires an exhaustive search to identify previously reserved resources that can be shared with an incoming request. In our implementation (a Python-based simulator, running on a server equipped with an AMD EPYC Rome 7552 2.2 GHz CPU and 128 GB RAM, with Ubuntu 20.04 LTS), for loads lower than 0.6, the use of SBPP takes more than a second to determine the paths and spectral resources for both the primary and backup lightpaths, whereas the other approaches complete resource assignment in less than 10 ms in the considered scenarios.

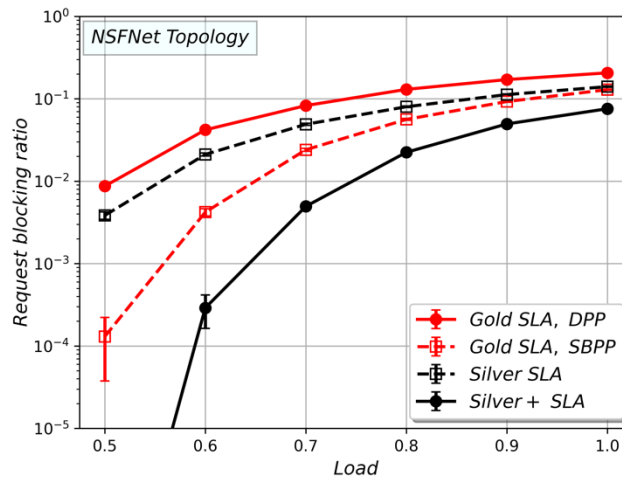


**Figure 47.** Request blocking ratio of different SLA categories depending on network traffic load.

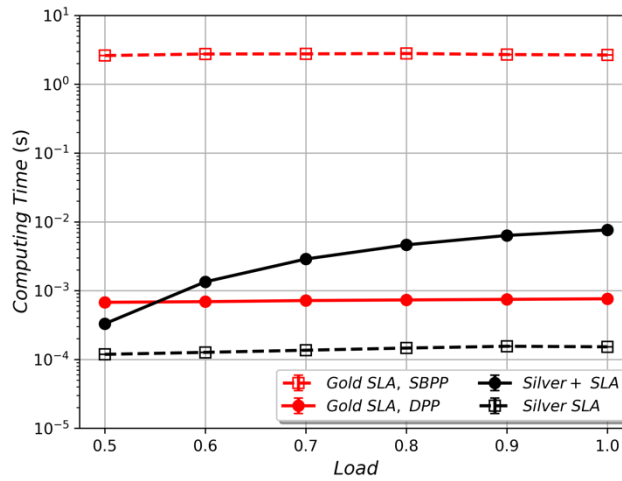


**Figure 48.** Average computing time per request of different SLA categories depending on network traffic load.

As shown in Table 13 and through Figs. 47 and 48, the SLA categories differ in terms of the level of protection provided (against fiber and/or EDFA failures), recovery time, computation time, efficient use of resources and potential extra capacity for the transmission of low priority traffic under normal operation. This reinforces the idea that enabling SLA-differentiated protection is a promising solution for efficiently using network capacity according to user needs. Therefore, in the following subsections, we explore different combinations to provide SLA-differentiated protection.

#### 6.4.2 Analysis of SLA-Differentiated Protection Techniques under Uniform Traffic: “Gold (DPP)” and “Silver” or “Silver Plus”

We now consider a network scenario where there are two different types of clients. We will initially consider “gold (DPP)” and “silver” clients. Later, in this subsection, we will analyze the use of the “silver plus” SLA category instead of “silver”. For simplicity, throughout this subsection, we will refer to the “gold” SLA, with the understanding that it specifically refers to “gold (DPP)”.

Fig. 49 represents the global request blocking ratio obtained in the network (i.e., without differentiating the category of the requests) as a function of the percentage of “gold” clients (and thus “gold” connections) in the network for different traffic loads. As previously discussed, “gold” connections employ the classic disjoint path protection or DPP (and are therefore protected against fiber and EDFA failures), while “silver” connections only rely on EDFA protection. Three main conclusions can be extracted from this figure. First, as expected, for higher traffic loads, the request blocking ratio increases. Secondly, for each traffic load, the global blocking ratio is always lower than if only the classic DPP protection method were used for all requests, i.e., without having SLA-differentiated protection (note that scenario corresponds to having 100% of requests of “gold” type). Moreover, there is a sweet spot. For instance, for a traffic load of 0.5 when 20% of connections are of “gold” type (and 80% of

“silver” type), the global blocking ratio is minimized, and is close to two orders of magnitude lower than the case of 100% “gold” connections.

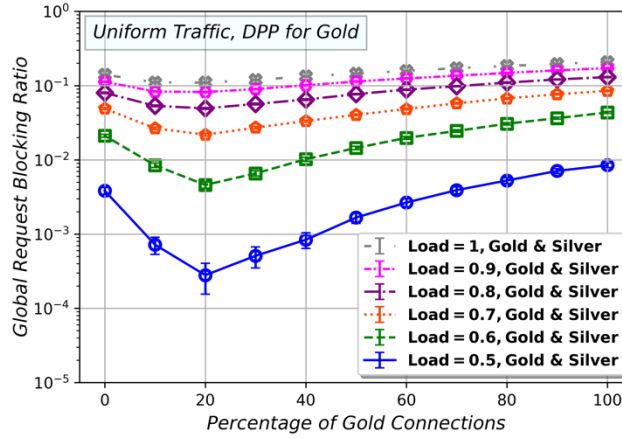


**Figure 49.** Global request blocking ratio with respect to the network load and the percentage of “gold” connections, when considering “gold (DPP)” and “silver” clients

Fig. 50 shows the blocking ratio of “gold” and “silver” requests separately for a network load of 0.5 (which corresponds to the blue line in Fig. 49). In Fig. 50, it can be observed that as the percentage of “gold” connections decreases, its blocking ratio also decreases. For the lowest percentages of “gold” connection requests, “silver” connections are obviously the predominant type in the network. It should be noted that for “silver” connections, as the primary and backup lightpaths are routed through the same path (but using the L-band for the primary and C for the backup) their lengths are equal, so they generally use the same modulation format (with some exceptions due to different optical reaches, as shown in Table 4) and thus use the same number of slots in each band. Since the C-band consists of 320 slots and the L-band of 516, the C-band becomes the limiting factor for “silver” connections. Therefore, even when “silver” connections are the predominant type, the L band has a set of slots that can only be exploited by “gold” connections, and thus helps reducing the blocking ratio of “gold” connections in those scenarios. Again, Fig. 50 shows that thanks to the use of SLA-differentiated protection, it is possible to reduce the blocking ratio of both “gold” and “silver” connections when compared with only using the classic protection method, DPP, for all requests (i.e. when 100% of the requests are of “gold” type).

Additionally, it should be noted that the differentiation between “gold” and “silver” clients is based on resiliency rather than on blocking ratio. “Gold” connection requests have more flexibility in the use of spectral resources yet may require more spectral resources than “silver” connections due to longer routes needed to establish two disjoint paths. As a result, “gold” clients may experience higher blocking probabilities than “silver” clients in some cases (as shown in Fig. 50, when the percentage of gold connections is between 20% and 50%), although they are all low values, around  $10^{-3}$  or lower.

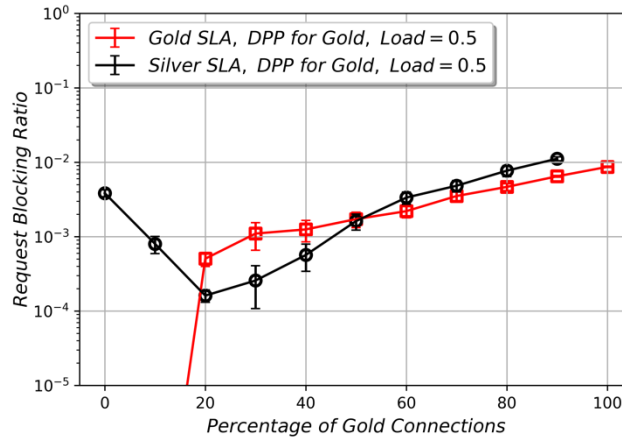


**Figure 50.** Request blocking ratio of each SLA category with respect to the network load and the percentage of “gold” connections, when considering “gold (DPP)” and “silver” clients.

We now propose to consider “gold” and “silver plus” SLA categories. This strategy will be analyzed assuming the same simulation scenario, and then compared with the previous strategy.

Fig. 51 shows the global request blocking ratio in this case. Again, having higher traffic loads increases the blocking ratio of the network, and when SLA-differentiated protection differentiation is employed (i.e. when the percentage of “gold” connections is lower than 100%) the blocking probability is reduced. However, in contrast with the results shown in Fig. 49, the blocking probability monotonously decreases as we move towards lower percentages of “gold” connections (without observing that sweet spot at an intermediate percentage). This is due to the fact of using the hybrid protection method in the “silver plus” category. The hybrid strategy includes a second phase (see Table 13) that enables backup connections for low priority requests (“silver plus”) to utilize the L-band if needed (unlike the previous strategy, “silver”).

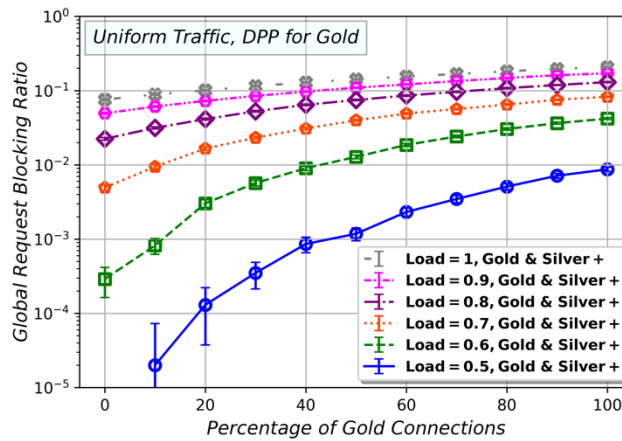


**Figure 51.** Global request blocking ratio with respect to the network load and the percentage of “gold” connections, when considering “gold” and “silver plus” clients.

Fig. 52 shows the blocking ratio of “gold” and “silver plus” requests separately for 0.5 network load (which corresponds to the blue line in Fig. 51). It is now observed that when the percentage



of high priority (“gold”) requests is roughly lower than 30%, the blocking ratio for both, high priority and low priority (“silver plus”) requests is below  $10^{-3}$ . In contrast, with the previous strategy (Fig. 50) the range in which the blocking probability for both high priority and low priority requests (“silver”) was below  $10^{-3}$  was narrower.

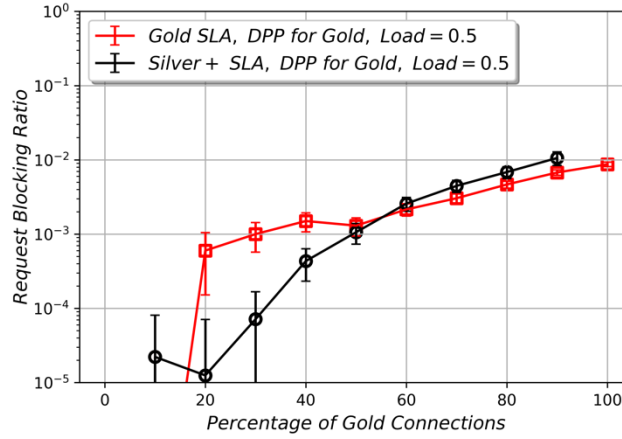


**Figure 52.** Request blocking ratio of each SLA with respect to the network load and the percentage of “gold” connections, when considering “gold (DPP)” and “silver plus” clients.

In order to facilitate the comparison of the two strategies: the use of “gold” and “silver” categories and the use of “gold” and “silver plus” categories, the previous results are presented jointly in Figs. 53 to 55. Fig. 53 demonstrates that the global request blocking probability is always lower (or at least similar) when the “gold” and “silver plus” SLA strategy is used. The reduction is particularly significant when the percentage of “gold” connections is below 20%. Similarly, Fig. 54 demonstrates that the low priority connections always obtain lower blocking with the new strategy. In fact, “silver plus” connections not only have better performance in terms of request blocking ratio, but also provide a better level of protection (as some of them will be accommodated using disjoint lightpaths and thus are also protected against single fiber failures). Fig. 55 demonstrates that both strategies lead to similar blocking ratios for the “gold” connections. Therefore, it shows that despite the additional protection level and improved blocking performance that is provided for the “silver plus” category through the employment of the hybrid protection, this protection approach does not have negative impact on the performance of “gold” connections.

In summary, it has been demonstrated that the use of “gold” and “silver plus” categories brings performance advantages compared to the use of “gold” and “silver” categories. The performance of low priority connections is improved without having noticeable impact on the high priority connections. Therefore, from now on in this chapter, the “silver plus” approach will be considered for the low priority connections.

Moreover, it has also been demonstrated that the use of SLA-differentiated protection always reduces the blocking ratio compared to a network that only implements classical dedicated path protection (100% “gold (DPP)”). This reduction becomes more noticeable as the percentage of

users requiring gold connections decreases. The reduction in the blocking ratio can be translated into an increase in the total supported load and, consequently, in operators' revenue, which is even more significant when proper pricing strategies are used for different SLAs.

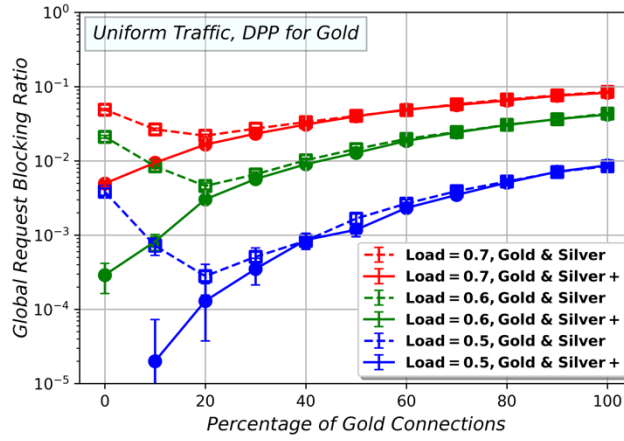


**Figure 53.** Comparison in terms of global request ratio when EDFA protection (“silver”) and hybrid protection (“silver plus”) is used for the low priority category.

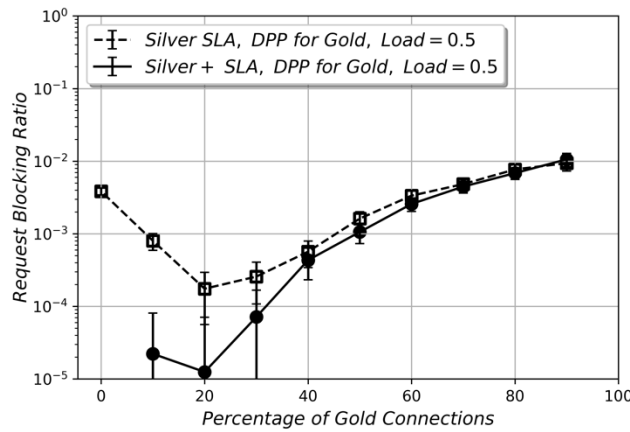


**Figure 54.** Request blocking ratio of “silver” and “silver plus” SLA categories depending on network traffic load and the percentage of “gold” connections.

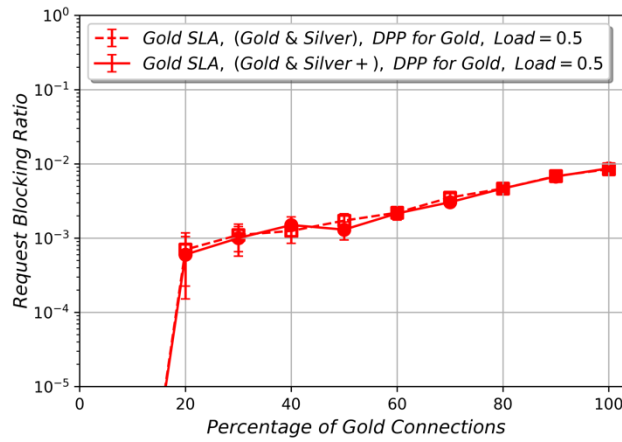


**Figure 55.** Request blocking ratio of “gold (DPP)” SLA in the presence of “silver” or “silver plus” SLA categories.

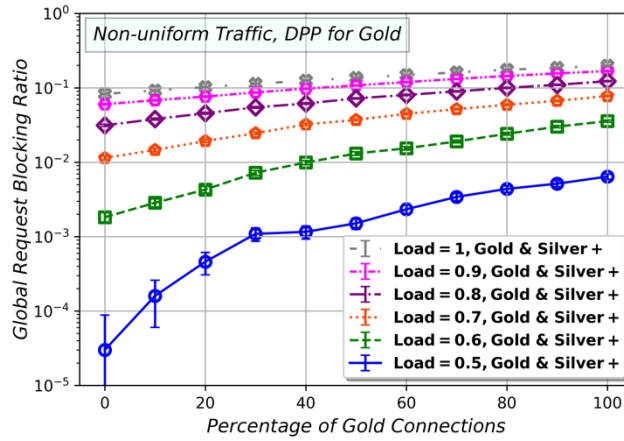
#### 6.4.3 Analysis of SLA-Differentiated Protection Techniques under Non-Uniform Traffic: “Gold (DPP)” and “Silver Plus”

After demonstrating the advantages of SLA-differentiated protection, particularly the joint use of “gold (DPP)” and “silver plus” SLA categories, we now evaluate its performance under different conditions. In this section, we extend the previous analysis by assessing the network performance using SLA-differentiated protection with “gold (DPP)” and “silver plus” categories under a non-uniform traffic model. Again, for simplicity, throughout this subsection we will simply use “gold” SLA, with the understanding that it specifically refers to “gold (DPP)”.

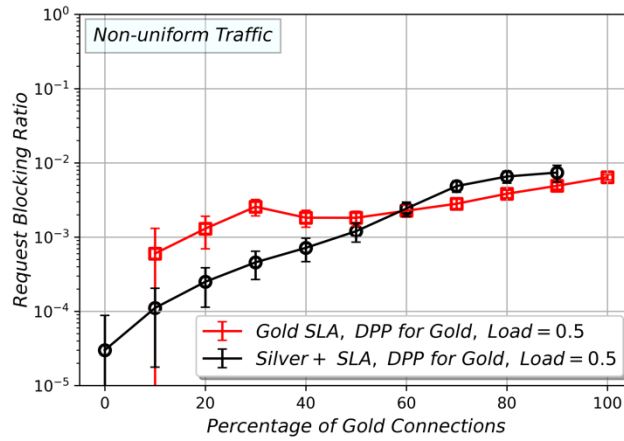
To perform this analysis, a population-based traffic matrix for the NSFNet topology has been assumed, considering the population in 2023 [88] of each U.S. state where NSFNet nodes are located. In this way, the offered traffic load between different  $s$ - $d$  pairs is not uniform, but proportional to the product of the populations of the corresponding U.S. states associated with those nodes. Without loss of generality (since traffic load is ultimately normalized) a constant of proportionality equal to one has been assumed. The traffic matrix used in this study is available on GitHub [89].

Fig. 56 shows the global request blocking ratio for different traffic loads, considering different percentages of “gold” connections when the network operates under a non-uniform traffic pattern. The results follow the same trend as those in Fig. 51. The individual request blocking ratios for the “gold” and “silver plus” SLA categories at a load of 0.5 (i.e., associated to the blue line in Fig. 56) for the non-uniform traffic are presented separately in Fig. 57. Again, similar trends are observed as in the case of uniform traffic (Fig. 52).

In summary, the analysis of non-uniform traffic does not alter our previous conclusion: SLA-differentiated protection consistently reduces the request blocking ratio compared to a network that only implements classical dedicated path protection (100% “gold (DDP)”).



**Figure 56.** Request blocking ratio of each SLA with respect to the network load and the percentage of “gold” connections, when considering “gold (DPP)” and “silver plus” clients.



**Figure 57.** Request blocking ratio of each SLA with respect to the network load and the percentage of “gold” connections, when considering “gold (DPP)” and “silver plus” clients.

#### 6.4.4 Analysis of SLA-Differentiated Protection Techniques under Uniform Traffic: “Gold (DPP)” or “Gold (SBPP)” and “Silver Plus”

Now, we turn our attention on comparing the use of the two options for the “gold” SLA: DPP and SBPP, when combined with “silver plus” for less demanding clients. SBPP makes more efficient use of network resources. However, in contrast to DPP, it does not support the 1+1 scheme (which offers zero recovery time), nor does it leverage the “extra capacity” feature. It also requires a higher computing time, as previously shown.

First, Fig. 58 demonstrates that across various traffic loads and percentages of “gold” connections, the employment of SBPP significantly decreases the global request blocking ratio compared to the use of DPP for the “gold” SLA. Following this, Fig. 59 and Fig. 60 show the request blocking ratio for each SLA category individually.

Fig. 59 focuses on the blocking probability of “silver plus” connections when DPP and SBPP are used for the “gold” category. The use of SBPP for the “gold” category allows for better utilization of network capacity by sharing backup resources, enabling the low priority (“silver

plus”) connections to benefit from additional available resources. This leads to a noticeable decrease on blocking probability compared to the case of using DPP for the gold category.

The comparison between the performance of the “gold” connections when they are protected using DPP or SBPP is represented in Fig. 60. Again, SBPP delivers better performance in terms of blocking ratio. According to Fig. 60, the reduction in blocking ratio is higher than one order of magnitude when more than 50% of the connections belong to the “gold” SLA.

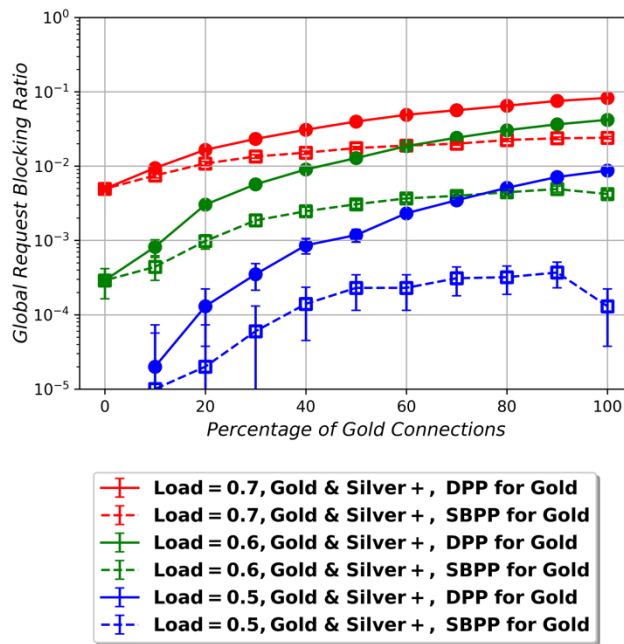


**Figure 58.** Comparison in terms of global request ratio when DPP and SBPP are used for the high priority category.

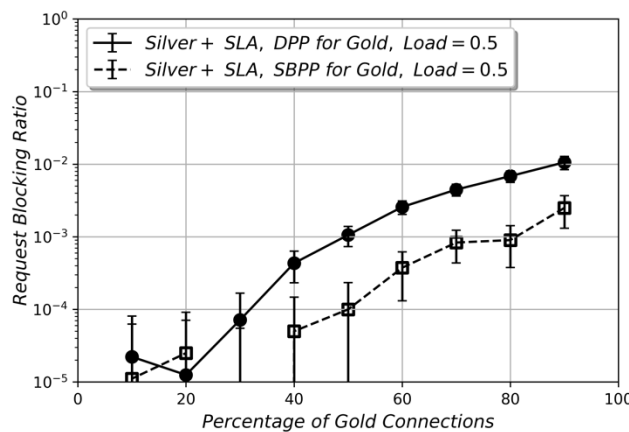


**Figure 59.** Request blocking ratio of “silver plus” SLA category depending on the percentage of “gold” connections when DPP or SBPP is used for the “gold” SLA.

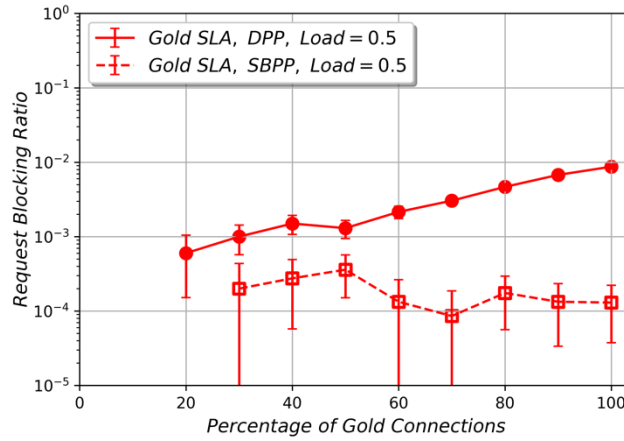


**Figure 60.** Request blocking ratio of “gold” SLA category depending on the percentage of “gold” connections when DPP or SBPP is used for the “gold” SLA.

Therefore, the combination of “gold (SBPP)” with “silver plus” is the best option for accommodating higher network loads while complying with a maximum value of blocking ratio. Coming back to Fig. 58, it is important to note that the blocking ratio is lower with SLA-differentiated protection (i.e. when splitting clients between the “gold (SBPP)” and “silver plus” categories) compared to only having “gold” clients, as long as the percentage of “gold (SBPP)” clients (and thus connections) is below 40%. This percentage is realistic, as most clients may not require “gold” level specifications.

In contrast, the use of DPP for the “gold” category is more appropriate when recovery or computing times are critical constraints, when the 1+1 protection scheme is required, or when the operator aims to utilize the “extra capacity” feature, using the backup lightpath in the absence of failure for the transmission of low priority, pre-emptable traffic. When using DPP, the blocking ratio is always lower with SLA-differentiated protection (i.e., splitting clients between the “gold (DPP)” and “silver plus” categories) compared to only having “gold (DPP)” clients (Fig. 58).

In summary, depending on the operator’s objectives, implementing SLA-differentiated protection with a well-considered choice between DPP or SBPP (as previously discussed), together with an appropriate pricing strategy, it is possible to increase the traffic carried by the network and, consequently, the revenue.

#### 6.4.5 Analysis of Admission Control Mechanism under Uniform Traffic: “Gold (DPP)” and “Silver Plus”

We now consider the use of “gold (DPP)” and “silver plus” SLA categories and investigate whether the integration of an AC mechanism consisting in ensuring that a portion of the L-band spectrum is exclusively available for “gold (DPP)” connections improves its blocking ratio without significantly degrading that of “silver plus” connections. In particular, we define a threshold for the L-band such that when a “silver plus” connection request arrives, it can only use the L-band if the percentage of available spectral slots in that band is above this threshold. If the available slots are below this threshold, the request cannot use the L-band and is therefore

not admitted (i.e., it is blocked, since the primary lightpath for silver plus should use the L-band, as shown in Table 13). Note that a threshold of 0% is equivalent to not using AC.

We first consider a situation where 50% of the total incoming connection requests are of “gold” type and the remaining 50% “silver plus”. Fig. 61 represents the global request blocking ratio for different traffic loads as a function of the threshold for AC. The figure shows that the global blocking ratio increases as the threshold is set to a higher value. However, the main interest lies in analyzing the impact on each SLA category. As shown in Fig. 62, increasing the threshold value decreases the blocking probability for “gold” connections as expected, especially for thresholds higher than 3%. Fig. 63 shows the impact on “silver plus” connections. In this case, the blocking probability significantly increases even for low threshold values. To summarize, Fig. 64 compares the blocking ratio for the “gold” and “silver plus” SLA categories with and without AC (using a 3% threshold) across different traffic loads. It shows a slight improvement for “gold connections” but a significant worsening for “silver plus” connections. Therefore, unfortunately, this AC strategy does not offer substantial advantages, although its effectiveness may depend on the operator’s pricing strategy.

We also tested different distributions of SLA categories (other than 50%-50%) and a strategy that reserves a fixed percentage of consecutive slots in the L-band for “gold” connections. Again, the improvement in blocking probability for “gold” connections does not compensate for the degradation in blocking probability for “silver plus” connections.

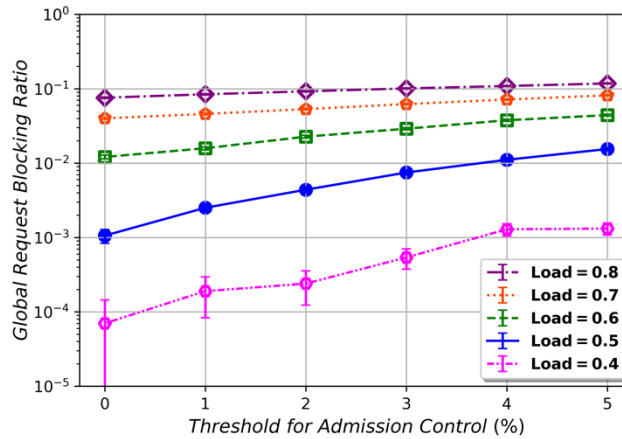


**Figure 61.** Global request blocking ratio depending on different thresholds for the AC.

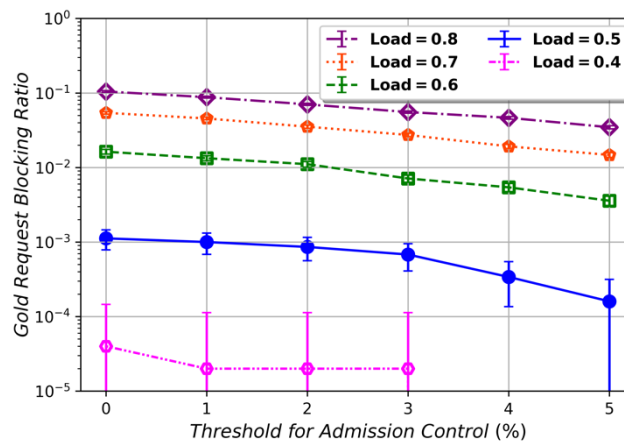


**Figure 62.** “Gold (DPP)” request blocking ratio depending on different thresholds for the AC.

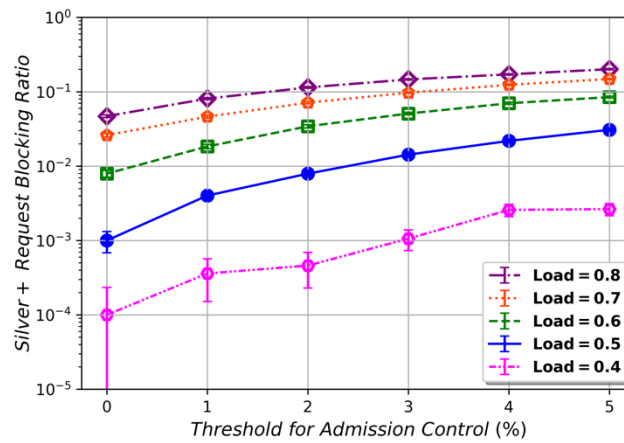


**Figure 63.** “Silver Plus” request blocking ratio depending on different thresholds for the AC.

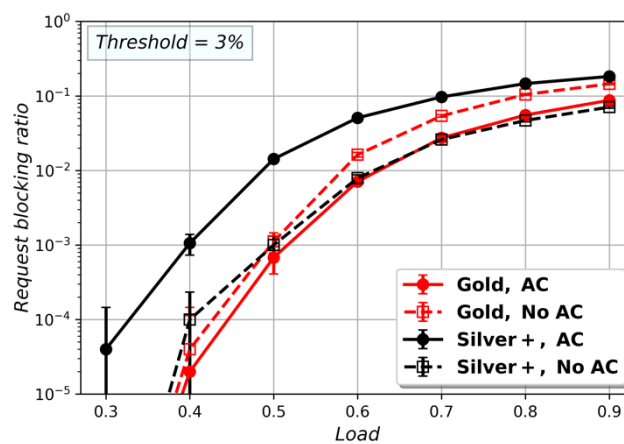


**Figure 64.** Impact of the AC procedure on request blocking ratio.

#### 6.4.6 Analysis of Enhanced SLA-Differentiation Protection

Until now, we have considered only three SLA categories available for clients: “gold” (with 100% of traffic protected by DPP or SBPP) and “silver” or “silver plus” (with 100% of traffic



protected by EDFA protection or hybrid protection). However, as discussed in Section 6.3, network operators should implement flexible mechanisms to accommodate more diverse client requirements. Clients may wish to protect a specific fraction of their traffic with DPP/SBPP, rather than choosing between 100% or 0%. In this way, we will now consider a broader selection of SLA categories. An SLA type will be denoted by the character “G” followed by a number, where the number indicates the percentage of traffic requiring DPP/SBPP, i.e. “gold” type protection. For instance, SLA type G20 means that 20% of the traffic requires DPP/SBPP (and the remaining 80% hybrid protection). Thus, a request from a client associated with this SLA category will be split into two sub-demands (as described in Section 6.3). In contrast, SLA type G100 means that all traffic requires DPP/SBPP, so there are no sub-demands. Similarly, SLA type G0 means that all traffic is provided with hybrid protection, so again, there are no sub-demands. Note that SLA types G100 and G0 correspond to the “gold” and “silver plus” SLAs analyzed in the previous subsections. The different types of SLAs that will be considered in this section are shown in Table 14.

**Table 14.** Specification of the analyzed client types.

SLA Type	% of traffic with DPP/SBPP	% of traffic with hybrid protection
<b>G100</b> (“gold” SLA)	100%	0%
<b>G50</b>	50%	50%
<b>G25</b>	25%	75%
<b>G20</b>	20%	80%
<b>G0</b> (“silver plus” SLA)	0%	100%

Note that, except for the G100 and G0 SLA categories, each connection request will be divided into two sub-requests. This implies doubling the number of lightpaths to be established in the network. The spectral requirements of each of these lightpaths will be lower (because the traffic is split between the sub-demands), making it easier to find an available spectral gap to allocate them in the network. However, since more lightpaths are established, the number of guard bands also increases, resulting in a waste of bandwidth. Therefore, it is necessary to analyze this trade-off between the ease of allocating lightpaths of smaller spectral size and the additional bandwidth consumed due to guard bands.

In this subsection, different network cases are set up to compare the previous approach, which had only two types of SLAs (i.e. only “gold” and “silver plus” clients or equivalently only G100 and G0 clients), with this new approach with more flexibility in terms of SLA types. Table 15 shows the different cases that will be evaluated during this analysis. In cases A1 to A3, 20% of the total traffic of the network requires DPP/SBPP. However, that value is obtained with different mixes of SLA types:

- In case A1, there is only one type of client (G20), so each request will be split in two sub-demands of different sizes (data rates).
- In case A2, there are two types of clients: 20% of the clients are G100 and the remaining G0. This case corresponds to the scenario we have analyzed so far, where we have “gold” and “silver plus” clients, and requests are not split).
- In case A3, there is a mix of three SLA types (G100, G50, G0), with one of them (G50) employing splitting.

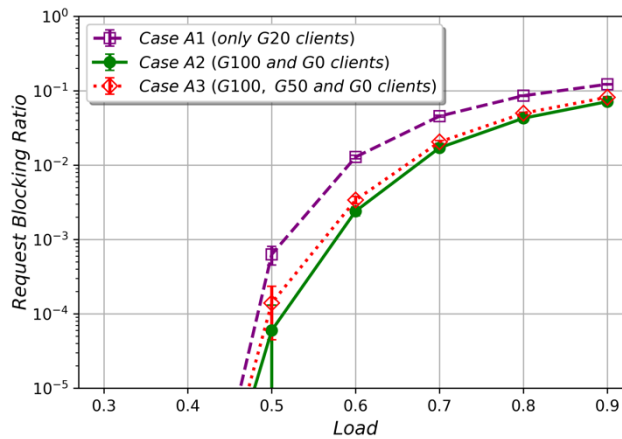
On the other hand, cases B1 to B3 consider different mixes of SLA types but all of them lead to 50% of the traffic employing DPP/SBPP.

**Table 15.** The analyzed network cases.

Cases	Distribution of client types	% of traffic with DPP in the network
A1	100% of G20 clients	20%
A2	20% of G100 clients + 80% of G0 clients	
A3	10% of G100 clients + 20% of G50 clients + 70% of G0 clients	
B1	100% of G50 clients	50%
B2	50% of G100 clients + 50% of G0 clients	
B3	30% of G100 clients + 30% of G50 clients + 20% of G25 clients + 20% of G0 clients	

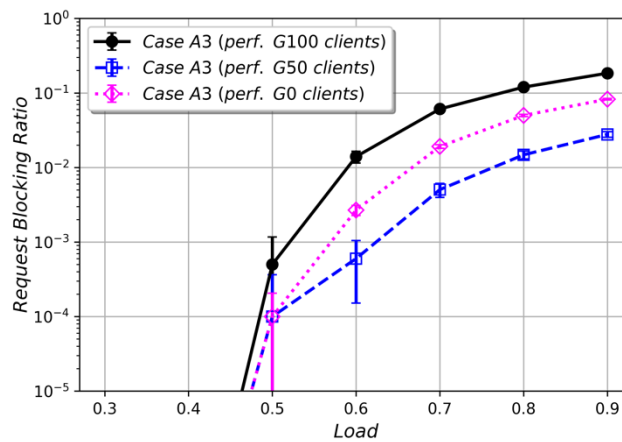
As in the previous subsections, the analysis will begin by evaluating the use of DPP to protect “gold” traffic. Following this, the results of using SBPP for “gold” traffic protection will be presented.

Thus, Fig. 65 shows a comparison of cases A1 to A3 when DPP is used for “gold” traffic. The lowest global blocking probability is obtained when there is only G100 (“gold”) and G0 (“silver plus”) clients (case A2), i.e., when requests are not split. When we have only G20 clients and all requests are split, the blocking probability increases, which is due to the waste of bandwidth caused by the increased number of guard bands in the spectrum due to splitting each requested connection into two (and note that this split is done for both the primary and the backup connections). The figure also shows the results for case A3, where a mix of G100, G50 and G0 clients is considered. This case achieves similar performance to case A2 (the best one), as only a small part of the client requests (20%) involves request splitting (those generated by G50 clients).



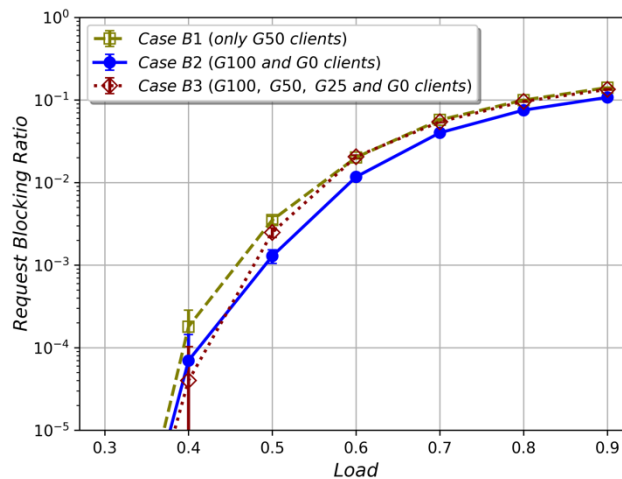
**Figure 65.** Comparison of the global request blocking ratios for cases A1 to A3, when DPP is used for “gold” traffic.

Fig. 65 represented the global request blocking ratio in the network. Next, Fig. 66 focuses on case A3 and compares the blocking probability associated with each SLA client. SLA type G50 is the only one that involves splitting. This means that additional spectral guard bands are required, but this drawback affects all clients which are using the network concurrently, regardless of their SLA type. However, since splitting reduces the spectrum demand of the lightpaths associated with SLA G50, it is easier to find available spectral gaps for these sub-requests. For this reason, the blocking probability for this SLA type is lower.



**Figure 66.** Comparison of the request blocking ratios for each client type in the case A3, when DPP is used for “gold” traffic.

Figure 67 shows the global blocking probability for cases B1 to B3. These cases consider different mixes of SLA types, but all lead to 50% of the traffic employing DPP. Again, the case with no request splitting has the lower blocking probability, which is case B2, where 50% of requests are G100 (“gold”) and 50% are G0 (“silver plus”). Case B1, where all requests are split (since they all come from G50 clients), results in a slightly higher blocking probability. Finally, case B3, which includes a mixture of clients from four different SLAs (50% requiring splitting and 50% not), generally yields similar results to case B1. The blocking ratio of each different SLA client considered in case B3 is shown in Fig. 68.



**Figure 67.** Comparison of the global request blocking ratios for cases B1 to B3, when DPP is used for “gold” traffic.

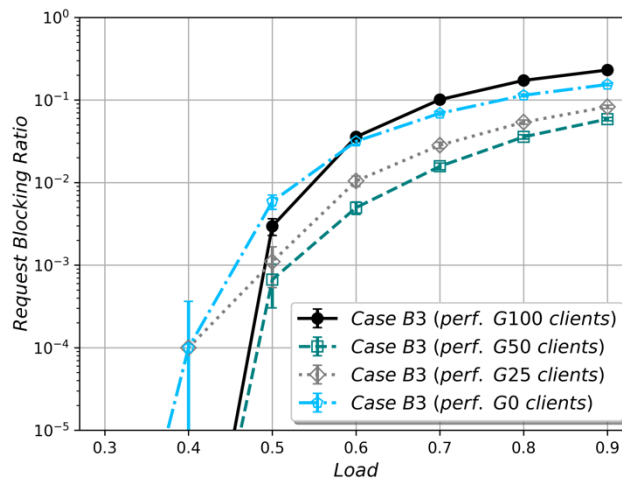


**Figure 68.** Comparison of the request blocking ratios for each client type in the case B3, when DPP is used for “gold” traffic.

Finally, the impact of using SBPP to protect “gold” traffic, as opposed to DPP, is analyzed in the same scenarios as before. This includes cases A1 to A3, where 20% of network traffic is protected by SBPP, and cases B1 to B3, where 50% of network traffic is protected by SBPP. The results are presented in Figs. 69 to 72. As these figures illustrate, the use of SBPP results in a reduction of the blocking ratio for each case compared to the DPP method (Figs. 65 to 68). Notably, the trends in Figs. 69 to 72 generally align with those observed in Figs. 65 to 68, so that the conclusions drawn from the earlier figures are also applicable when employing SBPP.

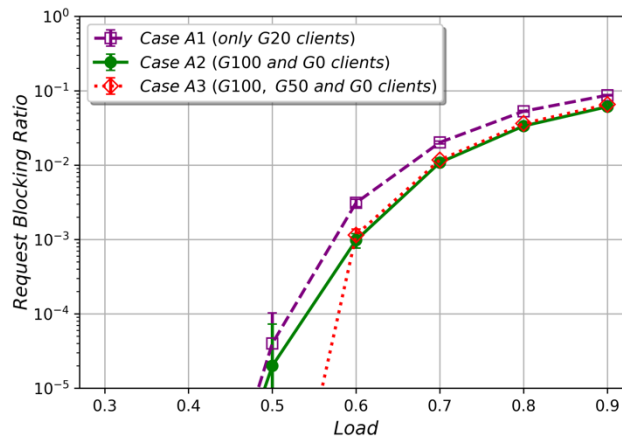


**Figure 69.** Comparison of the global request blocking ratios for cases A1 to A3, when SBPP is used for “gold” traffic.

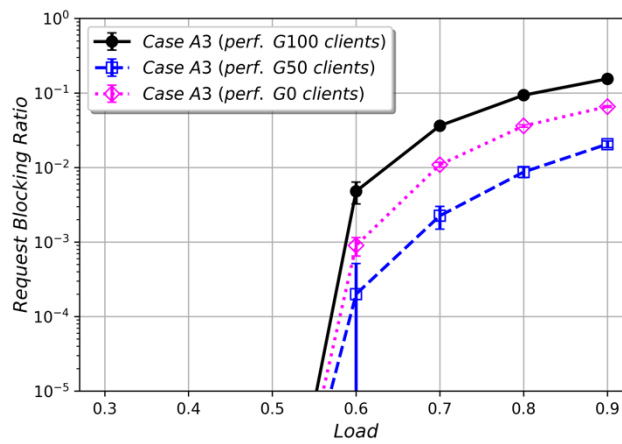


**Figure 70.** Comparison of the global request blocking ratios for cases A1 to A3, when SBPP is used for “gold” traffic.

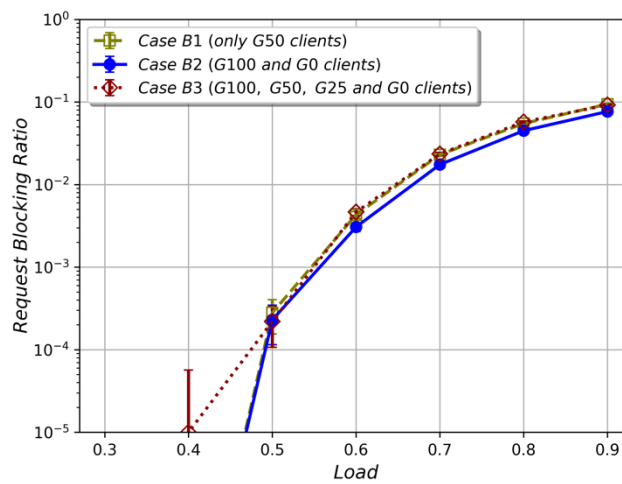


**Figure 71.** Comparison of the global request blocking ratios for cases A1 to A3, when SBPP is used for “gold” traffic.

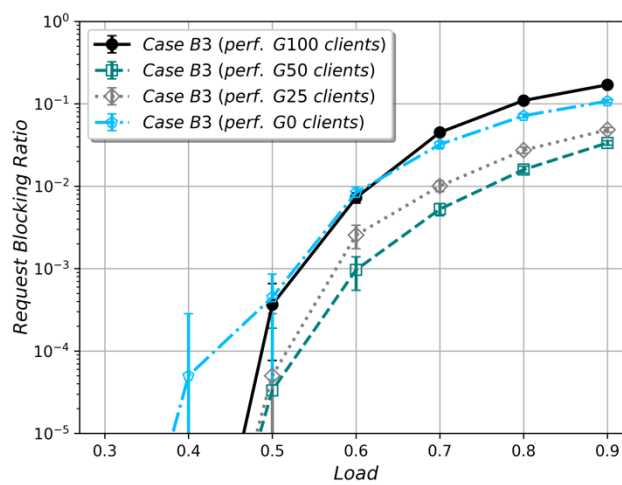


**Figure 72.** Comparison of the global request blocking ratios for cases A1 to A3, when SBPP is used for “gold” traffic.

In summary, offering a broader selection of SLA types enhances flexibility in accommodating client demands. Thus, introducing SLA types beyond the “gold” and “silver plus” categories enables tailored solutions that better meet the specific needs of clients. However, this additional SLA categories requires splitting requests, which increases the number of spectral guard bands as more lightpaths are established. The presence of guard bands leads to bandwidth inefficiencies, impacting all clients using the network concurrently, and thus affect the blocking probability. Despite these challenges, careful balancing of SLA types (like in cases A3 and B3) can achieve excellent network performance while still providing flexibility in supporting different SLA categories.

## 6.5 Conclusions

In this chapter, we have considered four different types of protection methods enabled by the use of the architecture of separate amplifiers in multiband C+L elastic optical networks: (1) DPP, which protects connections from fiber and EDFA failures, (2) SBPP, which provides similar level of protection as DPP with improved efficiency due to sharing the protection capacity between different backup lightpaths, (3) EDFA protection, which protects only against EDFA failures, and (4) hybrid protection, which guarantees protection against EDFA failures and provides some connections with fiber failure protection. The use of these methods enables the introduction of SLA-differentiated protection. Thus, clients are classified into “gold (DPP)”, “gold (SBPP)”, “silver” or “silver plus” categories according to their needs, and using the protection strategies previously described, respectively.

It has been demonstrated that the use of “gold” and “silver plus” categories within a network brings advantages compared to the use of “gold” and “silver” categories. Specifically, the blocking probability for low-priority users (those not associated with the “gold” category) decreases –in some cases significantly–, while also providing a higher level of protection in certain cases. This approach does not have a noticeable impact on the performance of high-priority (“gold”) clients. Moreover, the introduction of this SLA-differentiated protection improves network performance compared to a scenario where DPP or SBPP is applied to all connections (for the latter as long as the “gold” clients do not exceed approximately 40% in the conducted experiments).

We have also analyzed an AC mechanism aimed at increasing the probability of successfully establishing high-priority services (“gold”) by reserving a portion of the L-band spectrum exclusively for these connections. However, the improvement in blocking probability for “gold” connections when this strategy is used does not compensate for the degradation in blocking probability for “silver plus” connections.

Finally, an enhanced SLA-differentiated protection mechanism is also proposed that allows clients to choose a more flexible categorization. Instead of being limited to the “gold” category (with 100% of their traffic protected by DPP or SBPP) or the “silver plus” category (with 100% of their traffic protected by hybrid protection), the new mechanism enables more flexibility,

allowing them to protect a specific portion of their traffic with DPP/SBPP and the remaining part with hybrid protection. This functionality is implemented by splitting connection requests into sub-requests. Splitting implies a higher number of guard bands, and has an impact on performance (but it is reduced by the fact that the sub-requests have smaller size and are easier to allocate). This new enhanced SLA-differentiated protection mechanism provides more flexibility to network operators. This feature, along with suitable pricing policies for the different categories, may lead to increased operator revenues, optimizing network performance and meeting diverse client requirements.



## Chapter 7.

### Conclusions and Future Plans

The capacity crunch issue induces network operators and the research community to find alternative solutions for supporting the ever-increasing network traffic demands. Therefore, in this thesis, we have focused on two proposed solutions aimed at enhancing the capacity of optical transport networks: 1) space division multiplexing (SDM) technology and 2) multi-band elastic optical networks (MB-EON). The employment of SDM technology or MB-EON, along with the efficient utilization of spectrum resources through advanced modulation formats provides network operators with additional resources to adapt optical networks to the significant growth in traffic demands in recent years.

There are different approaches for the realization of SDM networks, such as multi-core fibers (MCFs), multi-mode fibers (MMFs) and multi-fiber transmission (MFT). Since MCFs is the most commonly used architecture in the literature, it is the architecture that we have considered for the implementation of SDM-enabled EON in Chapter 3. Considering multiple cores within a single cladding transforms the traditional routing, modulation level, and spectrum assignment algorithm into a more challenging problem, known as routing, modulation level, spatial, and spectrum assignment (RMLSSA). Furthermore, multiple cores consideration introduces a new challenge to the quality of optical signals, referred to as inter-core crosstalk (XT). In order to maximize benefit from the implementation of SDM networks using MCFs, in Chapter 3, a novel multi-path RMLSSA algorithm has been proposed [74]. Our proposed algorithm in Chapter 3 employs the minimum number of cores as possible for the establishment of a certain demand in case that there are not enough resources required to serve the demand over a single core. It also allocates resources only if the accumulated XT does not have a significant negative impact on the quality of the transmitted signal. The employment of a multi-path strategy as well as keeping the number of utilized cores as low as possible improves the network performance through a reduction in blocking ratio and in energy consumption of bandwidth variable transponders (BVTs). Additionally, the realization of the multi-path strategy using different cores of the optical fibers sets the differential delay parameter to zero.

The SDM technology is an excellent solution to increase the capacity of optical networks, but leasing or rolling out new dark fibers, which is required for SDM activation, is a highly costly process for the network operators. Therefore, exploiting the L-band spectrum of the existing optical fibers is considered as a promising short-medium term practical solution for the capacity enhancement. The C+L multi-band optical networks are based on the establishment of all-optical circuits or lightpaths, and for each connection request, the routing, band, modulation level, and spectrum assignment (RBMLSA) problem must be solved.

As evolving from the C-band to the L-band requires the deployment of different components such as amplifiers, equipping all the fibers in a network with multiband devices would potentially increase the costs significantly. Accordingly, how to achieve a partially upgraded network in which the L-band of a subset of optical fibers has been lit up is the focus of Chapter 4. In Chapter 4, different planning strategies have been presented to achieve a hybrid C/C+L optical network. In that chapter, we first proposed a heuristic approach for partially upgrading a network from the C-band to C+L bands [82]. The proposed heuristic prioritizes the optical fibers based on the number of times they appear in the first precomputed shortest paths between all source-destination pairs. Then, we introduced a new integer linear programming (ILP) formulation with the objective of maximizing the number of shortest paths that can benefit from the partial migration [83]. The ILP formulation can be solved very quickly, and the network operators can be provided with a solution of the partial migration in less than 20 seconds (depending on network size). We have compared the ILP formulation with the heuristic approach based on overall network performance, considering three geographically different network topologies: the American NSFNet topology, the Asian JPN12 topology, and the European DT network. It has been demonstrated that the ILP formulation performs the partial migration of a network generally leading to better network performance in terms of bandwidth blocking ratio (BBR). However, the proposed heuristic and the ILP formulation do not consider that upgrading different fibers may involve different costs. In order to address this issue, in Chapter 4, we have presented three different heuristics taking into account that different fibers impose different upgrading costs on the network operators [84]. This is because different fibers might have different lengths, resulting in different numbers of erbium doped fiber amplifiers (EDFAs). Therefore, the proposed heuristics are subjected to the maximum number of EDFAs that can be upgraded to the L-band. In the first heuristic, MostUsed, the process of partial migration of a network is performed by prioritizing the most used optical fibers. The objective of the second heuristic, MaxPaths, is to maximize the number of shortest paths in which the L-band has been activated. The third heuristic, MaxFibers, aims to maximize the number of upgraded fibers, capable of operating over C+L bands. The network performance evaluation for three different network topologies, NSFNet, JPN12, and DT, under both uniform and non-uniform traffic patterns has demonstrated that the MaxPaths method generally provides better results in terms of BBR. Additionally, we have introduced two different metrics to quickly provide a hint of the performance of the proposed methods in different scenarios of partial migration of a network. The introduced metrics are: 1) number of precomputed paths in which all links can operate over both the C- and L-bands, and 2) number of times that the most-used fiber, which has not been upgraded to the L-band is utilized in the precomputed shortest paths. Although these metrics can assist network operators in making an initial decision regarding the employment of the best heuristic for every scenario of partial migration, launching the simulation is recommended to make the final decision.

The partial migration of a network can be realized through two different types of transceivers: multi-band transceivers or separate single-band C and single-band L transceivers. The techno-economic analysis of the potential transceivers is another focus of Chapter 4, helping network operators to achieve a cost-effective partially upgraded network through the deployment of an

economical transceiver option [85]. It has been demonstrated that performing signal transmission over the L-band through the deployment separate L-band transceiver is a more cost-effective option in a partially upgraded network.

Increasing the capacity of optical networks through the employment of C+L band systems makes the implementation of survivability strategies (i.e., the ability of the network to withstand failures) a mandatory requirement for network operators. Therefore, in Chapter 5, we have presented different methods for the realization of survivable C+L band networks in response to potential failures [72], [94]. We have proposed a protection method, *EDFA protection*, to provide survivability against the most common failures in the networks (i.e., EDFA failures) by leveraging the separate amplifiers architecture for the implementation of C+L multi-band optical networks. This architecture allows the network operators to transmit the primary and backup lightpaths over different spectral bands, ensuring a continuous transmission even if one of the EDFAs fails. Additionally, we have introduced another protection method, *hybrid approach*, in order to improve the network performance and resiliency. This approach is an extension of the EDFA protection method, and in the case that there are not enough resources to realize the EDFA protection, the second phase of the hybrid approach will be activated. In the second phase, the EDFA protection transforms into the classical dedicated path protection (DPP) method, utilizing two disjoint paths for the primary and backup connections. Therefore, survivability against a single failure in EDFAs and optical fibers is achieved for those connections that are served in the second phase of the hybrid approach. The proposed hybrid approach has been analyzed in partially and fully upgraded C+L band networks. The network performance assessment has been performed to compare the hybrid approach and the DPP method. It has been shown that although the DPP method offers higher level of resiliency, the hybrid approach usually provides better results in terms of request blocking ratio. Finally, in Chapter 5, we have evaluated the dynamic restoration method under different failure scenarios in a partially upgraded network in which the L-band activation has been performed for a subset of optical fibers [93].

Since the evaluated protection strategies, EDFA protection, hybrid approach, and DPP method, offer different levels of protection, they can be used to serve different requests depending on the protection level associated to their service level agreements (SLAs). In addition to the aforementioned protection strategies, in Chapter 6, the shared backup path protection (SBPP) method has also been considered. In that chapter, we have proposed an SLA-differentiated protection mechanism to categorize the users/services based on their required level of protection [100]. In this way, high priority connections are categorized under the “gold” SLA, while moderate priority connections are assigned to the “silver plus” SLA and low priority connections to the “silver” SLA. The connections associated to the “gold” SLA use DPP/SBPP method while connections associated to the “silver plus” SLA and “silver” SLA implement the hybrid approach and the EDFA protection method, respectively. The simulation results have shown that the employment of different SLA categories leads the network performance to be improved compared with a scenario where DPP or SBPP is used for all the services (for the latter under certain conditions). In order to enhance the performance of “gold” connections, we have also implemented an AC strategy during the resource allocation phase for C+L band

systems. In this way, we have analyzed the impact of reserving a portion of the L-band spectrum for the “gold” users on the overall network performance. Finally, in Chapter 6, we have introduced an enhanced SLA-differentiated protection mechanism that allows each client’s traffic to be divided in two portions: one requiring a high level of protection (“gold” SLA) and the other a moderate level of protection (“silver plus” SLA). Connection requests for these clients are handled by splitting them into two sub-demands. Although the additional spectral guard-bands required due to this splitting impact overall network performance, it has been shown that a careful balance of SLA types can minimize the impact. Ultimately, this flexibility enhances the protection options available to network clients, and thus can be an attractive option for network operators.

This thesis opens several future research lines. One key direction is the evaluation of the proposed multi-path routing algorithm for the SDM technology, enabled through other structures like MMFs and MFT. Additionally, conducting a sensitivity analysis is another potential area for future research. This analysis would assess how changes in the parameters used to calculate inter-core XT affect the performance of the proposed algorithm in SDM networks. Regarding the partial migration of a network from the C-band to C+L bands, we have shown that there is trade-off between the congestion and the number of precomputed paths that benefit from the upgrade. Therefore, it would be worthy to explore whether the combination of these two metrics in a single objective function brings advantages compared to the individual use of the proposed methods of MaxPaths or MostUsed to achieve a partially upgraded network. Another research line to be studied is incorporating the cost of upgrading not only EDFAs but also reconfigurable optical add-drop multiplexers (ROADMs) and transceivers into the process of partial migration. Future work will also include analyzing the performance of the proposed partial migration methods in bigger topologies and studying different configuration options. Furthermore, again, a sensitivity analysis could be a key area for future research, investigating how changes in factors like cost affect the conclusions about the cost-effectiveness of separate single-band transceivers.

The proposed enhanced SLA-differentiated protection, along with suitable pricing policies for different SLA categories, may lead to increased operator revenues, optimizing network performance and meeting diverse client requirements. The study of pricing policies can be considered as an interesting direction for the future work. Furthermore, how different protection levels for the proposed SLA-differentiated mechanism may impact on the number of transceivers, required for the accommodation of each SLA category is a promising aspect to be explored.

## Chapter 8.

### List of Publications

This chapter provides a comprehensive list of journal and conference publications resulting from the research carried out in this thesis, up to the date of submission.

#### 8.1 Journals

1. **Soheil Hosseini**, Ignacio de Miguel, Noemí Merayo, Ramón de la Rosa, Rubén M. Lorenzo, Ramón J. Durán Barroso, "Energy Efficient Multipath Routing in Space Division Multiplexed Elastic Optical Networks," *Computer Networks*, 244C, 110349, May 2024.  
<https://doi.org/10.1016/j.comnet.2024.110349> [74]
2. **Soheil Hosseini**, Ignacio de Miguel, Noemí Merayo, Juan Carlos Aguado, Óscar González de Dios, Ramón J. Durán Barroso, "Migration of elastic optical networks to C+L bands subject to a partial upgrade of the number of EDFAs," *Journal of Optical Communications and Networking (JOCN)*; Multiband Special Issue, Vol. 15, No. 11, pp. F22-F35, October 2023.  
<https://doi.org/10.1364/JOCN.493231> [84]
3. **Soheil Hosseini**, Ignacio de Miguel, Noemí Merayo, Óscar González de Dios, Rubén M. Lorenzo, Ramón J. Durán Barroso, "Enabling Service Level Agreement-Differentiated Protection in C+L Multiband Optical Networks," *IEEE Open Journal of the Communications Society*, vol. 6, pp. 316-331, January 2025.  
<https://doi.org/10.1109/OJCOMS.2024.3520234> [101]

#### 8.2 Conferences

1. **Soheil Hosseini**, Ramón J. Durán Barroso, Ignacio de Miguel, Óscar González de Dios, Noemí Merayo, Juan Carlos Aguado, "Protection Methods Analysis in a Hybrid C/C+L Optical Network [Invited]," *International Conference on Transparent Optical Networks (ICTON)*, IEEE, Bari, Italy, 14-18 July 2024.  
<https://ieeexplore.ieee.org/document/10648116> [94]
2. **Soheil Hosseini**, Ignacio de Miguel, Óscar González de Dios, Juan Pedro Fernández-Palacios, Ramón J. Durán Barroso, "Dilemma for Multi-Band Network Migration: Single-Band or Multi-Band Transceivers," *International Conference on Optical Network Design and Modelling (ONDM)*, IEEE, Madrid, Spain, 6-9 May 2024.  
<https://opendl.ifip-tc6.org/db/conf/ondm2024/ondm2024/1570996414.pdf> [85]

3. **Soheil Hosseini**, Ignacio de Miguel, Óscar González de Dios, Noemí Merayo, Juan Pedro Fernández-Palacios, Ramón J. Durán Barroso, "Dynamic Restoration Assessment in Partially Upgraded Networks from the C to the C+L bands," International Conference on the Design of Reliable Communication Networks (DRCN), IEEE, Montreal, Canada, 6-9 May 2024.  
<https://doi.org/10.1109/DRCN60692.2024.10539152> [93]
4. **Soheil Hosseini**, Ignacio de Miguel, Ramón J. Durán Barroso, Noemí Merayo, Óscar González de Dios, Maryam Masoumi, Hafiza Kanwal Janjua, Juan Carlos Aguado Manzano, Patricia Fernández, "Multi-Band Elastic Optical Networks: Overview and Recent Contributions from the IoTalentum Project," International Conference on Distributed Computing and Artificial Intelligence (DCAI), Special Session, Guimaraes, Portugal, 12-14 July 2023.  
[https://doi.org/10.1007/978-3-031-38318-2\\_46](https://doi.org/10.1007/978-3-031-38318-2_46) [103]
5. **Soheil Hosseini**, Ignacio de Miguel, Ramón J. Durán Barroso, Óscar González de Dios, Noemí Merayo, Juan Carlos Aguado, "An ILP formulation for Partially Upgrading Elastic Optical Networks to Multi-Band," International Conference on Optical Network Design and Modeling (ONDM), IEEE, Coímbra, Portugal, 8-11 May 2023.  
<https://ieeexplore.ieee.org/abstract/document/10144883> [83]
6. **Soheil Hosseini**, Ramón J. Durán Barroso, Ignacio de Miguel, Óscar González de Dios, Noemí Merayo, Juan Carlos Aguado, "Migration Strategy from C-Band Elastic Optical Network to C+ L Multiband Optical Network," International Telecommunication Networks and Applications Conference (ITNAC), IEEE, Wellington, New Zealand, 30 November - 2 December 2022.  
<https://doi.org/10.1109/ITNAC55475.2022.9998374> [82]
7. **Soheil Hosseini**, Ramón J. Durán Barroso, Ignacio de Miguel, Óscar González de Dios, Noemí Merayo, Juan Carlos Aguado, "SLA-Differentiated Protection in Multi-Band Elastic Optical Networks," IEEE Photonics Conference (IPC), Vancouver, Canada, 13-17 November 2022.  
<https://doi.org/10.1109/IPC53466.2022.9975777> [100]
8. **Soheil Hosseini**, Ignacio de Miguel, Noemí Merayo, Óscar González de Dios, Ramón J. Durán Barroso, "Survivability against Amplifier Failures in Multi-band Elastic Optical Networks," Asia Communications and Photonics Conference (ACP), IEEE, Shenzhen, China, 5-8 November 2022.  
<https://doi.org/10.1109/ACP55869.2022.10088543> [72]

## References

- [1] E. Palkopoulou *et al.*, "Quantifying Spectrum, Cost, and Energy Efficiency in Fixed-Grid and Flex-Grid Networks [Invited]," *Journal of Optical Communications and Networking*, Vol. 4, Issue 11, pp. B42-B51, vol. 4, no. 11, pp. B42–B51, Nov. 2012, doi: 10.1364/JOCN.4.000B42.
- [2] O. Gerstel, M. Jinno, A. Lord, and S. J. B. Yoo, "Elastic optical networking: A new dawn for the optical layer?," *IEEE Communications Magazine*, vol. 50, no. 2, Feb. 2012, doi: 10.1109/MCOM.2012.6146481.
- [3] M. Jinno, H. Takara, B. Kozicki, Y. Tsukishima, Y. Sone, and S. Matsuoka, "Spectrum-efficient and scalable elastic optical path network: Architecture, benefits, and enabling technologies," *IEEE Communications Magazine*, vol. 47, no. 11, pp. 66–73, Nov. 2009, doi: 10.1109/MCOM.2009.5307468.
- [4] D.-S. Ly-Gagnon, K. Kikuchi, S. Tsukamoto, and K. Katoh, "Coherent Detection of Optical Quadrature Phase-Shift Keying Signals With Carrier Phase Estimation," *Journal of Lightwave Technology*, Vol. 24, Issue 1, pp. 12–, vol. 24, no. 1, pp. 12–, Jan. 2006, Accessed: Sep. 27, 2024. [Online]. Available: <https://opg.optica.org/abstract.cfm?uri=jlt-24-1-12>
- [5] A. D. Ellis, N. Mac Suibhne, D. Saad, and D. N. Payne, "Communication networks beyond the capacity crunch," *Philosophical Transactions of the Royal Society A: Mathematical, Physical and Engineering Sciences*, vol. 374, no. 2062, Mar. 2016, doi: 10.1098/RSTA.2015.0191.
- [6] M. Klinkowski, P. Lechowicz, and K. Walkowiak, "Survey of resource allocation schemes and algorithms in spectrally-spatially flexible optical networking," *Optical Switching and Networking*, vol. 27, pp. 58–78, Jan. 2018, doi: 10.1016/J.OSN.2017.08.003.
- [7] G. M. Saridis, D. Alexandropoulos, G. Zervas, and D. Simeonidou, "Survey and evaluation of space division multiplexing: From technologies to optical networks," *IEEE Communications Surveys and Tutorials*, vol. 17, no. 4, pp. 2136–2156, Oct. 2015, doi: 10.1109/COMST.2015.2466458.
- [8] A. Napoli *et al.*, "Perspectives of Multi-band Optical Communication Systems," *23rd Opto-Electronics and Communications Conference, OECC 2018*, Jul. 2018, doi: 10.1109/OECC.2018.8730026.
- [9] J. K. Fischer *et al.*, "Maximizing the Capacity of Installed Optical Fiber Infrastructure Via Wideband Transmission," *International Conference on Transparent Optical Networks*, vol. 2018-July, Sep. 2018, doi: 10.1109/ICTON.2018.8473994.
- [10] K. Nakajima, P. Sillard, D. Richardson, M. J. Li, R. J. Essiambre, and S. Matsuo, "Transmission media for an SDM-based optical communication system," *IEEE Communications Magazine*, vol. 53, no. 2, pp. 44–51, 2015, doi: 10.1109/MCOM.2015.7045390.
- [11] T. Mizuno, H. Takara, A. Sano, and Y. Miyamoto, "Dense Space-Division Multiplexed Transmission Systems Using Multi-Core and Multi-Mode Fiber," *Journal of Lightwave Technology*, vol. 34, no. 2, pp. 582–592, Jan. 2016, doi: 10.1109/JLT.2015.2482901.
- [12] K. Takayuki, "1-Pb/s (32 SDM/46 WDM/768 Gb/s) C-band dense SDM transmission over 205.6-km of single-mode heterogeneous multi-core fiber using 96-Gbaud PDM-16QAM channels | IEEE Conference Publication | IEEE Xplore." Accessed: Sep. 27, 2024. [Online]. Available: <https://ieeexplore.ieee.org/abstract/document/7937146>
- [13] J. Pedro *et al.*, "Assessment on the Achievable Throughput of Multi-Band ITU-T G.652.D Fiber Transmission Systems," *Journal of Lightwave Technology*, Vol. 38, Issue 16, pp. 4279-4291, vol.

- 38, no. 16, pp. 4279–4291, Aug. 2020, Accessed: Sep. 27, 2024. [Online]. Available: <https://opg.optica.org/abstract.cfm?uri=jlt-38-16-4279>
- [14] N. Sambo *et al.*, “Provisioning in Multi-Band Optical Networks,” *Journal of Lightwave Technology*, vol. 38, no. 9, pp. 2598–2605, May 2020, doi: 10.1109/JLT.2020.2983227.
  - [15] B. Correia *et al.*, “Power control strategies and network performance assessment for C+L+S multiband optical transport,” *Journal of Optical Communications and Networking*, vol. 13, no. 7, pp. 147–157, Jul. 2021, doi: 10.1364/JOCN.419293.
  - [16] C. Politi, V. Anagnostopoulos, C. Matrakidis, and A. Stavdas, “Routing in dynamic future flexi-grid optical networks,” *2012 16th International Conference on Optical Networking Design and Modelling, ONDM 2012*, 2012, doi: 10.1109/ONDM.2012.6210199.
  - [17] F. Shirin Abkenar and A. Ghaffarpour Rahbar, “Study and Analysis of Routing and Spectrum Allocation (RSA) and Routing, Modulation and Spectrum Allocation (RMSA) Algorithms in Elastic Optical Networks (EONs),” *Optical Switching and Networking*, vol. 23, pp. 5–39, Jan. 2017, doi: 10.1016/J.OSN.2016.08.003.
  - [18] B. C. Chatterjee, N. Sarma, and E. Oki, “Routing and Spectrum Allocation in Elastic Optical Networks: A Tutorial,” *IEEE Communications Surveys and Tutorials*, vol. 17, no. 3, pp. 1776–1800, Jul. 2015, doi: 10.1109/COMST.2015.2431731.
  - [19] N. Hara and T. Takahashi, “A study on dynamic spectrum assignment for fairness in elastic optical path networks,” *2014, 8th International Conference on Signal Processing and Communication Systems, ICSPCS 2014 - Proceedings*, Jan. 2014, doi: 10.1109/ICSPCS.2014.7021053.
  - [20] K. Christodouloupoulos, I. Tomkos, and E. A. Varvarigos, “Elastic bandwidth allocation in flexible OFDM-based optical networks,” *Journal of Lightwave Technology*, vol. 29, no. 9, pp. 1354–1366, 2011, doi: 10.1109/JLT.2011.2125777.
  - [21] M. Jinno *et al.*, “Distance-adaptive spectrum resource allocation in spectrum-sliced elastic optical path network,” *IEEE Communications Magazine*, vol. 48, no. 8, pp. 138–145, Aug. 2010, doi: 10.1109/MCOM.2010.5534599.
  - [22] B. C. Chatterjee and E. Oki, “Performance evaluation of spectrum allocation policies for elastic optical networks,” *International Conference on Transparent Optical Networks*, vol. 2015-August, Aug. 2015, doi: 10.1109/ICTON.2015.7193485.
  - [23] F. S. Abkenar, A. Ghaffarpour Rahbar, and A. Ebrahimzadeh, “Best fit (BF): A new Spectrum Allocation mechanism in Elastic Optical Networks (EONs),” *2016 8th International Symposium on Telecommunications, IST 2016*, pp. 24–29, Mar. 2017, doi: 10.1109/ISTEL.2016.7881775.
  - [24] R. Ahumada, A. Leiva, F. Alonso, S. Fingerhuth, and G. Farías, “Spectrum Allocation Algorithms for Elastic DWDM Networks on Dynamic Operation,” *IEEE Latin America Transactions*, vol. 12, no. 6, pp. 1012–1018, Sep. 2014, doi: 10.1109/TLA.2014.6893994.
  - [25] G. Shen, H. Guo, and S. K. Bose, “Survivable elastic optical networks: survey and perspective (invited),” *Photonic Network Communications*, vol. 31, no. 1, pp. 71–87, Feb. 2016, doi: 10.1007/S11107-015-0532-0/FIGURES/12.
  - [26] R. Goścień, K. Walkowiak, and M. Tornatore, “Survivable multipath routing of anycast and unicast traffic in elastic optical networks,” *Journal of Optical Communications and Networking*, vol. 8, no. 6, pp. 343–355, Jun. 2016, doi: 10.1364/JOCN.8.000343.



- 
- [27] K. D. R. Assis, R. C. Almeida, L. P. Dias, and H. Waldman, "Squeezed Protection in Elastic Optical Networks Subject to Multiple Link Failures," *IEEE Transactions on Network and Service Management*, vol. 18, no. 3, pp. 2612–2626, Sep. 2021, doi: 10.1109/TNSM.2021.3087010.
  - [28] K. Walkowiak, M. Klinkowski, B. Rabiega, and R. Goścień, "Routing and spectrum allocation algorithms for elastic optical networks with dedicated path protection," *Optical Switching and Networking*, vol. 13, pp. 63–75, Jul. 2014, doi: 10.1016/J.OSN.2014.02.002.
  - [29] S. K. Bose, G. Shen, and Y. Wei, "Optimal Design for Shared Backup Path Protected Elastic Optical Networks Under Single-Link Failure," *Journal of Optical Communications and Networking*, Vol. 6, Issue 7, pp. 649–659, vol. 6, no. 7, pp. 649–659, Jul. 2014, doi: 10.1364/JOCN.6.000649.
  - [30] G. Shen, Q. Yang, and Y. Wei, "Shared Backup Path Protection (SBPP) in Elastic Optical Transport Networks," *Asia Communications and Photonics Conference (2012)*, paper PAF4C.6, p. PAF4C.6, Nov. 2012, doi: 10.1364/ACPC.2012.PAF4C.6.
  - [31] "Shared backup path protection in elastic optical networks: Modeling and optimization | IEEE Conference Publication | IEEE Xplore." Accessed: Sep. 28, 2024. [Online]. Available: <https://ieeexplore.ieee.org/abstract/document/6529859>
  - [32] R. Wang and B. Mukherjee, "Spectrum management in heterogeneous bandwidth networks," *Proceedings - IEEE Global Communications Conference, GLOBECOM*, pp. 2907–2911, 2012, doi: 10.1109/GLOCOM.2012.6503558.
  - [33] A. de Sousa, P. Monteiro, and C. B. Lopes, "Lightpath admission control and rerouting in dynamic flex-grid optical transport networks," *Networks*, vol. 69, no. 1, pp. 151–163, Jan. 2017, doi: 10.1002/NET.21715.
  - [34] R. R. Reyes and T. Bauschert, "Reward-based connection admission control in flex-grid optical networks," *2016 20th International Conference on Optical Network Design and Modeling, ONDM 2016*, Jun. 2016, doi: 10.1109/ONDM.2016.7494086.
  - [35] R. J. Essiambre, R. Ryf, N. K. Fontaine, and S. Randel, "Breakthroughs in photonics 2012: Space-division multiplexing in multimode and multicore fibers for high-capacity optical communication," *IEEE Photonics J*, vol. 5, no. 2, 2013, doi: 10.1109/JPHOT.2013.2253091.
  - [36] T. J. Xia, H. Fevrier, T. Wang, and T. Morioka, "Introduction of spectrally and spatially flexible optical networks," *IEEE Communications Magazine*, vol. 53, no. 2, pp. 24–33, 2015, doi: 10.1109/MCOM.2015.7045388.
  - [37] D. Siracusa, F. Pederzoli, D. Klonidisz, V. Lopezy, and E. Salvadori, "Resource allocation policies in SDM optical networks (Invited paper)," *Conference Proceedings - 2015 International Conference on Optical Network Design and Modeling, ONDM 2015*, pp. 168–173, Jun. 2015, doi: 10.1109/ONDM.2015.7127293.
  - [38] H. Tode and Y. Hirota, "Routing, Spectrum, and Core and/or Mode Assignment on Space-Division Multiplexing Optical Networks [Invited]," *Journal of Optical Communications and Networking*, Vol. 9, Issue 1, pp. A99–A113, vol. 9, no. 1, pp. A99–A113, Jan. 2017, doi: 10.1364/JOCN.9.000A99.
  - [39] M. Yaghubi-Namaad, A. G. Rahbar, and B. Alizadeh, "Adaptive Modulation and Flexible Resource Allocation in Space-Division-Multiplexed Elastic Optical Networks," *Journal of Optical Communications and Networking*, Vol. 10, Issue 3, pp. 240–251, vol. 10, no. 3, pp. 240–251, Mar. 2018, doi: 10.1364/JOCN.10.000240.

- 
- [40] W. Klaus *et al.*, "Advanced Space Division Multiplexing Technologies for Optical Networks [Invited]," *Journal of Optical Communications and Networking*, Vol. 9, Issue 4, pp. C1-C11, vol. 9, no. 4, pp. C1–C11, Apr. 2017, doi: 10.1364/JOCN.9.0000C1.
  - [41] S. Hosseini, A. Ghaffarpour Rahbar, and M. Jafari-Beyrami, "Survivable time-aware traffic grooming in spatial division multiplexing elastic optical networks with minimized crosstalk," *Computers & Electrical Engineering*, vol. 83, p. 106579, May 2020, doi: 10.1016/J.COMPELECENG.2020.106579.
  - [42] M. Klinkowski and G. Zalewski, "Dynamic Crosstalk-Aware Lightpath Provisioning in Spectrally&#x2013;Spatially Flexible Optical Networks," *Journal of Optical Communications and Networking*, Vol. 11, Issue 5, pp. 213-225, vol. 11, no. 5, pp. 213–225, May 2019, doi: 10.1364/JOCN.11.000213.
  - [43] B. C. Chatterjee, A. Wadud, I. Ahmed, and E. Oki, "Priority-Based Inter-Core and Inter-Mode Crosstalk-Avoided Resource Allocation for Spectrally-Spatially Elastic Optical Networks," *IEEE/ACM Transactions on Networking*, vol. 29, no. 4, pp. 1634–1647, Aug. 2021, doi: 10.1109/TNET.2021.3068212.
  - [44] B. C. Chatterjee, I. Ahmed, A. Wadud, M. Maity, and E. Oki, "BPRIA: Crosstalk-Avoided Bi-Partitioning-Based Counter-Propagation Resource Identification and Allocation for Spectrally-Spatially Elastic Optical Networks," *IEEE Transactions on Network and Service Management*, vol. 19, no. 4, pp. 4369–4383, Dec. 2022, doi: 10.1109/TNSM.2022.3158962.
  - [45] M. Jafari-Beyrami, A. Ghaffarpour Rahbar, and S. Hosseini, "On-demand fragmentation-aware spectrum allocation in space division multiplexed elastic optical networks with minimized crosstalk and multipath routing," *Computer Networks*, vol. 181, p. 107531, Nov. 2020, doi: 10.1016/J.COMNET.2020.107531.
  - [46] S. Trindade and N. L. S. Da Fonseca, "Split-Demand and Multipath Routing in Space-Division Multiplexing Optical Networks," *2022 IEEE Latin-American Conference on Communications, LATINCOM 2022*, 2022, doi: 10.1109/LATINCOM56090.2022.10000522.
  - [47] F. Yousefi and A. G. Rahbar, "Novel fragmentation-aware algorithms for multipath routing and spectrum assignment in elastic optical networks-space division multiplexing (EON-SDM)," *Optical Fiber Technology*, vol. 46, pp. 287–296, Dec. 2018, doi: 10.1016/J.YOFTE.2018.11.002.
  - [48] S. Paira, J. Halder, M. Chatterjee, and U. Bhattacharya, "On Energy Efficient Survivable Multipath Based Approaches in Space Division Multiplexing Elastic Optical Network: Crosstalk-Aware and Fragmentation-Aware," *IEEE Access*, vol. 8, pp. 47344–47356, 2020, doi: 10.1109/ACCESS.2020.2979487.
  - [49] R. Zhu *et al.*, "Survival Multipath Energy-Aware Resource Allocation in SDM-EONs during Fluctuating Traffic," *Journal of Lightwave Technology*, vol. 39, no. 7, pp. 1900–1912, Apr. 2021, doi: 10.1109/JLT.2020.3043271.
  - [50] J. Halder, T. Acharya, and U. Bhattacharya, "A Novel RSCA Scheme for Offline Survivable SDM-EON With Advance Reservation," *IEEE Transactions on Network and Service Management*, vol. 19, no. 2, pp. 804–817, Jun. 2022, doi: 10.1109/TNSM.2022.3142857.
  - [51] H. M. N. S. Oliveira and N. L. S. Da Fonseca, "Multipath routing, spectrum and core allocation in protected sdm elastic optical networks," *Proceedings - IEEE Global Communications Conference, GLOBECOM*, 2019, doi: 10.1109/GLOBECOM38437.2019.9013523.
  - [52] P. M. Moura and N. L. S. Da Fonseca, "Multipath Routing in Elastic Optical Networks with Space-Division Multiplexing," *IEEE Communications Magazine*, vol. 59, no. 10, pp. 64–69, Oct. 2021, doi: 10.1109/MCOM.111.2100331.

- 
- [53] R. Rumipamba-Zambrano, F. J. Moreno-Muro, J. Perelló, P. Pavón-Mariño, and S. Spadaro, "Space continuity constraint in dynamic Flex-Grid/SDM optical core networks: An evaluation with spatial and spectral super-channels," *Comput Commun*, vol. 126, pp. 38–49, Aug. 2018, doi: 10.1016/J.COMCOM.2018.05.013.
  - [54] M. Cantono, V. Vusirikala, T. Hofmeister, M. Newland, and R. Schmogrow, "Opportunities and Challenges of C+L Transmission Systems," *Journal of Lightwave Technology*, Vol. 38, Issue 5, pp. 1050–1060, vol. 38, no. 5, pp. 1050–1060, Mar. 2020, Accessed: Sep. 28, 2024. [Online]. Available: <https://opg.optica.org/abstract.cfm?uri=jlt-38-5-1050>
  - [55] F. Calderon *et al.*, "Heuristic Approaches for Dynamic Provisioning in Multi-Band Elastic Optical Networks," *IEEE Communications Letters*, vol. 26, no. 2, pp. 379–383, Feb. 2022, doi: 10.1109/LCOMM.2021.3132054.
  - [56] Q. Yao *et al.*, "SNR Re-Verification-Based Routing, Band, Modulation, and Spectrum Assignment in Hybrid C-C+L Optical Networks," *Journal of Lightwave Technology*, vol. 40, no. 11, pp. 3456–3469, Jun. 2022, doi: 10.1109/JLT.2022.3170332.
  - [57] "Investigation of mid-term network migration scenarios comparing multi-band and multi-fiber deployments | IEEE Conference Publication | IEEE Xplore." Accessed: Sep. 28, 2024. [Online]. Available: <https://ieeexplore.ieee.org/abstract/document/7537304>
  - [58] A. Ferrari, V. Curri, and E. Virgillito, "Band-Division vs. Space-Division Multiplexing: A Network Performance Statistical Assessment," *Journal of Lightwave Technology*, Vol. 38, Issue 5, pp. 1041–1049, vol. 38, no. 5, pp. 1041–1049, Mar. 2020, Accessed: Sep. 28, 2024. [Online]. Available: <https://opg.optica.org/abstract.cfm?uri=jlt-38-5-1041>
  - [59] E. Virgillito, R. Sadeghi, A. Ferrari, G. Borraccini, A. Napoli, and V. Curri, "Network Performance Assessment of C+L Upgrades vs. Fiber Doubling SDM Solutions," *Optical Fiber Communication Conference (OFC) 2020 (2020)*, paper M2G.4, vol. Part F174-OFC 2020, p. M2G.4, Mar. 2020, doi: 10.1364/OFC.2020.M2G.4.
  - [60] R. K. Jana *et al.*, "When Is Operation over  $\text{C}+\text{L}$  Bands More Economical than Multifiber for Capacity Upgrade of an Optical Backbone Network?," *2020 European Conference on Optical Communications, ECOC 2020*, Dec. 2020, doi: 10.1109/ECOC48923.2020.9333276.
  - [61] A. D'Amico, E. London, E. Virgillito, A. Napoli, and V. Curri, "Inter-Band GSNR Degradations and Leading Impairments in C+L Band 400G Transmission," *25th International Conference on Optical Network Design and Modelling, ONDM 2021*, Jun. 2021, doi: 10.23919/ONDM51796.2021.9492485.
  - [62] A. D. ' Amico, G. Borraccini, and V. Curri, "Introducing the Perturbative Solution of the Inter-Channel Stimulated Raman Scattering in Single-Mode Optical Fibers," Apr. 2023, Accessed: Sep. 28, 2024. [Online]. Available: <https://arxiv.org/abs/2304.11756v1>
  - [63] A. Mitra, D. Semrau, N. Gahlawat, A. Srivastava, P. Bayvel, and A. Lord, "Effect of reduced link margins on C + L band elastic optical networks," *Journal of Optical Communications and Networking*, vol. 11, no. 10, pp. C86–C93, Oct. 2019, doi: 10.1364/JOCN.11.000C86.
  - [64] M. Cantono, A. Ferrari, D. Pileri, E. Virgillito, J. L. Auge, and V. Curri, "Physical Layer Performance of Multi-Band Optical Line Systems Using Raman Amplification," *Journal of Optical Communications and Networking*, Vol. 11, Issue 1, pp. A103–A110, vol. 11, no. 1, pp. A103–A110, Jan. 2019, doi: 10.1364/JOCN.11.00A103.
  - [65] B. Bao *et al.*, "LoRB: Link-oriented resource balancing scheme for hybrid C/C+L band elastic optical networks," *Optical Fiber Technology*, vol. 74, p. 103071, Dec. 2022, doi: 10.1016/J.YOFTE.2022.103071.

- 
- [66] D. Uzunidis, E. Kosmatos, C. Matrakidis, A. Stavdas, A. Lord, and D. Uzunidis, "Strategies for Upgrading an Operator's Backbone Network beyond the C-Band: Towards Multi-Band Optical Networks," *IEEE Photonics J*, vol. 13, no. 2, Apr. 2021, doi: 10.1109/JPHOT.2021.3054849.
  - [67] D. Moniz, V. Lopez, and J. Pedro, "Design Strategies Exploiting C+L-band in Networks with Geographically-dependent Fiber Upgrade Expenditures," *Optical Fiber Communication Conference (OFC) 2020 (2020)*, paper M2G.3, vol. Part F174-OFC 2020, p. M2G.3, Mar. 2020, doi: 10.1364/OFC.2020.M2G.3.
  - [68] T. Ahmed, A. Mitra, S. Rahman, M. Tornatore, A. Lord, and B. Mukherjee, "C+L-band upgrade strategies to sustain traffic growth in optical backbone networks," *Journal of Optical Communications and Networking*, vol. 13, no. 7, pp. 193–203, Jul. 2021, doi: 10.1364/JOCN.427097.
  - [69] T. Ahmed *et al.*, "C to C+L Bands Upgrade with Resource Re-provisioning in Optical Backbone Networks," *Optical Fiber Communication Conference (OFC) 2021 (2021)*, paper W1F.7, p. W1F.7, Jun. 2021, doi: 10.1364/OFC.2021.W1F.7.
  - [70] Z. Luo *et al.*, "Survivable Routing, Spectrum, Core and Band Assignment in Multi-Band Space Division Multiplexing Elastic Optical Networks," *Journal of Lightwave Technology*, Vol. 40, Issue 11, pp. 3442–3455, vol. 40, no. 11, pp. 3442–3455, Jun. 2022, Accessed: Sep. 28, 2024. [Online]. Available: <https://opg.optica.org/abstract.cfm?uri=jlt-40-11-3442>
  - [71] R. K. Jana, A. Srivastava, A. Lord, and A. Mitra, "Effect of Fill Margin on Network Survivability for C+L Band Optical Networks," *IET Conference Proceedings*, vol. 2023, no. 34, pp. 1453–1456, 2023, doi: 10.1049/ICP.2023.2589.
  - [72] S. Hosseini, I. De Miguel, N. Merayo, Ó. G. De Dios, and R. J. D. Barroso, "Survivability against Amplifier Failures in Multi-band Elastic Optical Networks," *Asia Communications and Photonics Conference, ACP*, vol. 2022–November, pp. 1299–1302, 2022, doi: 10.1109/ACP55869.2022.10088543.
  - [73] A. Eira, A. Souza, and J. Pedro, "Flexible Survivability in Next-Generation Multi-Band Optical Transport Networks," p. M1G.1, May 2023, doi: 10.1364/OFC.2023.M1G.1.
  - [74] S. Hosseini, I. de Miguel, N. Merayo, R. de la Rosa, R. M. Lorenzo, and R. J. Durán Barroso, "Energy efficient multipath routing in space division multiplexed elastic optical networks," *Computer Networks*, vol. 244, p. 110349, May 2024, doi: 10.1016/J.COMNET.2024.110349.
  - [75] X. Wan, N. Hua, and X. Zheng, "Dynamic routing and spectrum assignment in spectrum-flexible transparent optical networks," *Journal of Optical Communications and Networking*, vol. 4, no. 8, pp. 603–613, 2012, doi: 10.1364/JOCN.4.000603.
  - [76] A. Muhammad, G. Zervas, and R. Forchheimer, "Resource Allocation for Space-Division Multiplexing: Optical White Box Versus Optical Black Box Networking," *Journal of Lightwave Technology*, Vol. 33, Issue 23, pp. 4928–4941, vol. 33, no. 23, pp. 4928–4941, Dec. 2015, Accessed: Sep. 28, 2024. [Online]. Available: <https://opg.optica.org/abstract.cfm?uri=jlt-33-23-4928>
  - [77] H. Huang, S. Huang, S. Yin, M. Zhang, J. Zhang, and W. Gu, "Virtual Network Provisioning Over Space Division Multiplexed Optical Networks Using Few-Mode Fibers," *Journal of Optical Communications and Networking*, Vol. 8, Issue 10, pp. 726–733, vol. 8, no. 10, pp. 726–733, Oct. 2016, doi: 10.1364/JOCN.8.000726.
  - [78] L. Ruiz, R. J. Duran Barroso, I. De Miguel, N. Merayo, J. C. Aguado, and E. J. Abril, "Routing, Modulation and Spectrum Assignment Algorithm Using Multi-Path Routing and Best-Fit," *IEEE Access*, vol. 9, pp. 111633–111650, 2021, doi: 10.1109/ACCESS.2021.3101998.

- 
- [79] J. López, Y. Ye, V. López, F. Jiménez, R. Duque, and P. M. Krummrich, "On the Energy Efficiency of Survivable Optical Transport Networks with Flexible-grid," *European Conference and Exhibition on Optical Communication (2012)*, paper P5.05, p. P5.05, Sep. 2012, doi: 10.1364/ECEOC.2012.P5.05.
  - [80] Y. Li, H. Dai, G. Shen, and S. K. Bose, "Adaptive FEC-based lightpath routing and wavelength assignment in WDM optical networks," *Optical Switching and Networking*, vol. 14, no. PART 3, pp. 241–249, Aug. 2014, doi: 10.1016/J.OSN.2014.05.021.
  - [81] I. Tomkos *et al.*, "Experimental Demonstration of an Impairment Aware Network Planning and Operation Tool for Transparent/Translucent Optical Networks," *Journal of Lightwave Technology*, Vol. 29, Issue 4, pp. 439–448, vol. 29, no. 4, pp. 439–448, Feb. 2011, Accessed: Sep. 28, 2024. [Online]. Available: <https://opg.optica.org/abstract.cfm?uri=jlt-29-4-439>
  - [82] S. Hosseini *et al.*, "Migration Strategy from C-Band Elastic Optical Network to C+L Multiband Optical Network," *2022 32nd International Telecommunication Networks and Applications Conference, ITNAC 2022*, pp. 204–206, 2022, doi: 10.1109/ITNAC55475.2022.9998374.
  - [83] S. Hosseini *et al.*, "An ILP Formulation for Partially Upgrading Elastic Optical Networks to Multi-Band," *2023 International Conference on Optical Network Design and Modeling (ONDM)*, pp. 1–5, May 2023, doi: 10.23919/ONDM57372.2023.10144883.
  - [84] S. Hosseini, I. De Miguel, N. Merayo, J. C. Aguado, Ó. G. De Dios, and R. J. D. Barroso, "Migration of elastic optical networks to the C+L-bands subject to a partial upgrade of the number of erbium-doped fiber amplifiers," *Journal of Optical Communications and Networking*, Vol. 15, Issue 11, pp. F22–F35, vol. 15, no. 11, pp. F22–F35, Nov. 2023, doi: 10.1364/JOCN.493231.
  - [85] S. Hosseini, I. de Miguel, Ó. González de Dios, J. P. Fernández-Palacios, and R. J. Durán Barroso, "Dilemma for Multi-Band Network Migration: Single-Band or Multi-Band Transceivers," *28th International Conference on Optical Network Design and Modelling (ONDM 2024)*, 2024.
  - [86] M. Nakagawa, H. Kawahara, K. Masumoto, T. Matsuda, and K. Matsumura, "Performance Evaluation of Multi-Band Optical Networks Employing Distance-Adaptive Resource Allocation," *25th Opto-Electronics and Communications Conference, OECC 2020*, Oct. 2020, doi: 10.1109/OECC48412.2020.9273660.
  - [87] "Mathematical program solvers - IBM CPLEX." Accessed: Oct. 04, 2024. [Online]. Available: <https://www.ibm.com/products/ilog-cplex-optimization-studio/cplex-optimizer>
  - [88] "World Population by Country 2024 (Live)." Accessed: Sep. 28, 2024. [Online]. Available: <https://worldpopulationreview.com/>
  - [89] "GitHub - soheilhsini/population-based\_traffic\_matrixes." Accessed: Sep. 28, 2024. [Online]. Available: [https://github.com/soheilhsini/population-based\\_traffic\\_matrixes](https://github.com/soheilhsini/population-based_traffic_matrixes)
  - [90] M. Nakagawa, T. Seki, and T. Miyamura, "Techno-Economic Potential of Wavelength-Selective Band- Switchable OXC in S+C+L Band Optical Networks," *Optical Fiber Communication Conference (OFC) 2022 (2022)*, paper W2A.24, p. W2A.24, Mar. 2022, doi: 10.1364/OFC.2022.W2A.24.
  - [91] R. Goścień and K. Walkowiak, "On the Efficiency of Survivable Flex-Grid SDM Networks," *Journal of Lightwave Technology*, Vol. 36, Issue 10, pp. 1815–1823, vol. 36, no. 10, pp. 1815–1823, May 2018, Accessed: Sep. 28, 2024. [Online]. Available: <https://opg.optica.org/abstract.cfm?uri=jlt-36-10-1815>
  - [92] H. M. N. S. Oliveira and N. L. S. da Fonseca, "Routing, spectrum and core assignment algorithms for protection of space division multiplexing elastic optical networks," *Journal of Network and Computer Applications*, vol. 128, pp. 78–89, Feb. 2019, doi: 10.1016/J.JNCA.2018.12.009.

- 
- [93] S. Hosseini, I. De Miguel, O. G. De Dios, N. Merayo, J. P. Fernandez-Palacios, and R. J. Duran Barroso, "Dynamic Restoration Assessment in Partially Upgraded Networks from the C to the C+L bands," *20th International Conference on the Design of Reliable Communication Networks, DRCN 2024*, pp. 123–128, 2024, doi: 10.1109/DRCN60692.2024.10539152.
  - [94] S. Hosseini *et al.*, "Protection Methods Analysis in a Hybrid C/C+L Optical Network," pp. 1–4, Sep. 2024, doi: 10.1109/ICTON62926.2024.10648116.
  - [95] P. Wiatr, J. Chen, P. Monti, L. Wosinska, and D. Yuan, "Device reliability performance awareness: Impact of RWA on EDFA failure reparation cost in optical networks," *Proceedings of 2017 9th International Workshop on Resilient Networks Design and Modeling, RNDM 2017*, Oct. 2017, doi: 10.1109/RNDM.2017.8093029.
  - [96] H. S. Lee, C. L. Yang, and C. H. Chou, "Protection Scheme for a Wavelength-Division-Multiplexed Passive Optical Network Based on Reconfigurable Optical Amplifiers," *Applied Sciences* 2022, Vol. 12, Page 365, vol. 12, no. 1, p. 365, Dec. 2021, doi: 10.3390/APP12010365.
  - [97] K. Murakami, Y. Hirota, H. Tode, and S. Fujii, "On-Demand Spectrum and Core Allocation for Reducing Crosstalk in Multicore Fibers in Elastic Optical Networks," *Journal of Optical Communications and Networking*, Vol. 6, Issue 12, pp. 1059–1071, vol. 6, no. 12, pp. 1059–1071, Dec. 2014, doi: 10.1364/JOCN.6.001059.
  - [98] F. S. Abkenar, A. G. Rahbar, and A. Ebrahimzadeh, "Providing Quality of Service (QoS) for Data Traffic in Elastic Optical Networks (EONs)," *Arab J Sci Eng*, vol. 41, no. 3, pp. 797–806, Mar. 2016, doi: 10.1007/S13369-015-1886-4/METRICS.
  - [99] A. Agrawal, U. Vyas, V. Bhatia, and S. Prakash, "SLA-aware differentiated QoS in elastic optical networks," *Optical Fiber Technology*, vol. 36, pp. 41–50, Jul. 2017, doi: 10.1016/J.YOFTE.2017.01.012.
  - [100] S. Hosseini *et al.*, "SLA-Differentiated Protection in Multi-Band Elastic Optical Networks," *2022 IEEE Photonics Conference, IPC 2022 - Proceedings*, 2022, doi: 10.1109/IPC53466.2022.9975777.
  - [101] S. Hosseini, I. De Miguel, N. Merayo, Ó. G. De Dios, R. M. Lorenzo, and R. J. D. Barroso, "Enabling Service Level Agreement-Differentiated Protection in C+L Multiband Optical Networks," *IEEE Open Journal of the Communications Society*, vol. 6, pp. 316–331, 2025, doi: 10.1109/OJCOMS.2024.3520234.
  - [102] D. Kumar, R. Kumar, and N. Sharma, "Proactive connection recovery strategy with recovery time constraint for survivable elastic optical networks," *China Communications*, vol. 18, no. 9, pp. 236–248, Sep. 2021, doi: 10.23919/JCC.2021.09.018.
  - [103] S. Hosseini *et al.*, "Multi-band Elastic Optical Networks: Overview and Recent Contributions from the IoTalentum Project," *Lecture Notes in Networks and Systems*, vol. 741 LNNS, pp. 467–472, 2023, doi: 10.1007/978-3-031-38318-2\_46/FIGURES/1.